Development of Neutralizing Monoclonal Antibodies (mAbs) Against Marburg Virus

By

Zirui Zhang

A Thesis Submitted to Faculty of Graduate Studies of
the University of Manitoba
in Partial Fulfillment of the Requirements for the Degree of

MASTER OF SCIENCE

Department of Medical Microbiology and Infectious Disease
University of Manitoba
Winnipeg

ABSTRACT

Marburg virus (MARV) causes Marburg virus disease (MVD) in humans and non-human primates. Outbreaks of MVD are intermittent and have mostly happened in Central Africa. The mortality rates of these outbreaks are normally more than 50%. It is generally considered that MARV is not a major public health concern. The biggest outbreak of MVD happened in Angola in 2005, which caused 374 cases and 329 deaths. However, the outbreak of Ebola virus (EBOV) between 2013 and 2016 highlighted the need for more treatment and vaccine candidates against the unpredictable outbreaks of MVD in the future.

Neutralizing antibodies are thought to be one of the best treatment candidates against filoviruses. Nevertheless, neutralizing antibodies against MARV have not yet been generated from vaccinated animals, which is different from anti-EBOV neutralizing antibodies. All the neutralizing anti-MARV mAbs are derived from human survivors. In this case, the differences between MARV and EBOV viral antigens could be the key. In this study, I focus on the differences of the mucin-like domain (MLD) on the glycoprotein (GP) between MARV and EBOV.

The efficacy of Vesicular Stomatitis Virus (VSV)-based vaccines expressing MARV-GP or MARV mucin-deleted (ΔMuc) GP were evaluated in BALB/c mice. The results showed deleting the MLD on the vaccine will decrease vaccine efficacy. On the other hand, the VSV-MARV-ΔMuc GP vaccine leads to an earlier IgG response than the VSV-MARV-GP. A low level of neutralizing antibodies was observed in some of the MARV infected mice. All the survivors in two vaccine groups had a high level of anti-MARV GP IgG. Monoclonal antibodies (mAbs) against MARV were also generated. No neutralization was detected from the hybridoma supernatant and serum from immunized mice, despite high levels of IgG antibodies detected by ELISA. Deletion of the MLD did not enhance anti-MARV neutralizing antibody generation compared to the native form.

Overall, the results from evaluating vaccine efficacy as well as mAbs development do not support the hypothesis that a vaccine expressing the ΔMuc GP of Marburg virus will yield more and better neutralizing mAbs than a vaccine expressing the full GP.

ACKNOWLEDGMENTS

First, I would like to thank my supervisor Dr Xiangguo Qiu for giving me the opportunity to be a master student and supporting me all the time with a great deal of patience. Your indoctrination helped me to build up my confidence and guided me to be a qualified student. Your advice will no doubt play an important role in my future career.

I would like to thank my co-supervisor Dr Michael Drebot for giving me so many suggestions and assistances. You always encouraged me and spent so much time to guide me even though you were unbelievably busy. Without your recommendation and assistance, it was impossible to finish my study and project.

My committee members also deserve many thanks. Dr Blake Ball and Dr Shawn Babiuk provided me great guidance over the years and always supported me not only in research but also in daily life. I really appreciated your advice during those three years.

I would like to thank Dr Shihua He for the assistance in the BSL4 and the design of experiments. As an international student, I could not get the access to enter in BSL4 lab, but you showed me your great kindness and helped me so much in my projects. It was my honor to work with you over the years, and you are really a great example for me to follow.

I would like to express gratitude to Dr Jonathan Audet for your great help. You gave me so many suggestions on my project and guided me a lot from when I first came to Canada to now. You are more like my second co-supervisor rather than a senior PhD student in the lab. Wish you a successful career in the NML!

I would like to thank Dr Guodong Liu, Dr Md Niaz Rahim and Dr Wenjun Zhu for all of your guidance on technique and daily studies. Your assistance and suggestions helped me to improve myself from an ignorant fresher to a qualified master student. I cannot imagine what would happen if not for all your great help.

The work presented in this thesis could not be performed without the help and assistance of a big number of people. Dr Mable Hagan has made storage of the VSV-based vaccines in previous studies, it was impossible to set up my project without your work. Kevin Tierney helped a lot for the animal care in BSL4 lab; also all members of Veterinary Technical Services helped me to

take care of all the mice in BSL2 lab. Anders Leung taught me how to build up the standard for real-time quantitative PCR and also assisted to monitor the animals in BSL4. Kaylie Tran gave me the training about vesicular stomatitis virus, which helped me a lot in the GFP-based neutralization assay. Dr Logan Banadyga also gave me many helpful suggestions and assisted with some of the work in BSL4. Micheal Chan helped a lot on the mycoplasma test to confirm the state of cells.

In addition, a big thank you to all the people in Special Pathogen groups, especially everyone in Dr Qiu's lab. I am a person who is not good at communication, but all of you gave me your best understanding and were always helpful. It is my pleasure to work with all of you, and I hope we could still have opportunities to operate in the future. The winter and all of you are the two most memorable memories for me in Winnipeg.

Last but not least, I would like to thank my family members, my mother Weidong Fu and my father Zhiyong Zhang, who always support and encourage me from the other side of the earth. I hope to make both of you proud of me one day.

TABLE OF CONTENTS

TABLE OF TABLES

TABLE OF FIGURES

LIST OF ABBREVIATIONS

ΔMuc	Mucin-like domain deleted
Ad	Adenovirus
Ad5	Adenovirus serotype 5
ADCC	Antibody-dependent cell-mediated cytotoxicity
ADCP	Antibody-dependent cellular phagocytosis
ADE	Antibody-dependent enhancement
APC	Antigen-presenting cell
bp	Base pairs
BSC	Biosafety cabinet
BSL4	Biosafety Level 4
CatB	Cathepsin B
CatL	Cathepsin L
CDC	Center for Disease Control and Prevention
CL4	Containment Level 4
CMT	Complement-mediated toxicity
CPE	Cytopathic effect
CSCHAH	Canadian Science Center for Human and Animal Health
DC	Dendritic cell
DMEM	Dulbecco's Modified Eagle Medium
DMSO	Dimethyl sulfoxide

DNA	Deoxyribonucleic acid
dpi	Day(s) post infection
DRC	Democratic Republic of the Congo
dsRNA	Double-stranded ribonucleic acid
EBOV	Ebola virus
ELISA	Enzyme-linked immunosorbent assay
ER	Endoplasmic reticulum
EVD	Ebola virus disease
Fab	Fragment, antigen-binding
FBS	Fetal Bovine Serum
Fc	Fragment, crystallizable
GEQ	Genome equivalent
GFP	Green fluorescent protein
GP	Glycoprotein
HIV	Human Immunodeficiency Virus
HRP	Horseradish peroxidase
hpi	Hour(s) post infection
IFN	Interferon
Ig	Immunoglobulin
IgG	Immunoglobulin G
i.p.	Intraperitoneal
LD_{50}	Median lethal dose

mAb	Monoclonal Antibody
MARV	Marburg virus
MA-MARV	Mouse-adapted MARV
MLD	Mucin-like domain
MLK	Murine leukemia virus
MOI	Multiplicity of infection
MVD	Marburg virus disease
NML	National Microbiology Laboratory
NCID	National Institute for Communicable Diseases
NCL	Micro-Chem plus
NHP	Non-human primate
NK cell	Natural Killer cell
NNS	Non-segmented negative sense
NP	Nucleoprotein
NPC1	Niemann-Pick C1
nts	Nucleotides
OD	Optical density
ORF	Open reading frame
P/S	Penicillin-Streptomycin
PBS	Phosphate-buffered saline
PCR	Polymerase chain reaction
PDA	Parenteral Drug Association

PFU	Plaque-forming units
PHAC	Public Health Agency of Canada
RT qPCR	real-time quantitative PCR
RNA	Ribonucleic acid
RPMI 1640	Roswell Park Memorial Institute 1640 Medium
siRNA	Small interfering RNA
STAT	Signal transducer and activator of transcription
$TCID_{50}$	Median tissue culture infectious dose
TMB	3,3’,5,5’-tetramethylbenzidine
UTR	Untranslated region
VEEV	Venezuelan equine encephalitis virus
VLP	virus-like particle
VP	Viral protein
VSV	Vesicular stomatitis virus
VSV-WT	Wild type vesicular stomatitis virus
WHO	World Health Organisation

CHAPTER: 1 INTRODUCTION

1.1 Filovirus

Filoviruses belong to the family *Filoviridae*, under the order *Mononegavirales*. All the filoviruses have an approximately 19kb long negative-sense single-stranded RNA genome, which includes seven genes in the order 3'-UTR-NP-VP35-VP40-GP-VP30-VP24-L-5'-UTR (Sanchez, Kiley, Holloway, & Auperin, 1993). Filoviruses were first identified in August 1967 in Frankfurt and Marburg, Germany; where several laboratory workers were infected with Marburg virus, an unknown pathogen at that time. The patients showed high fever, hemorrhagic and some other pathological reactions (such as viremia and tissue damage) with a 25% fatality rate (Gordon Smith, Simpson, Bowen, & Zlotnik, 1967). Ebola virus was reported in 1976 as a new Marburg virus "strain", and in the same year was identified as a new genus of the family *Filoviridae* (World Health Organisation, 1978). From the first outbreak until 2017, there were 47 outbreaks of filoviruses which caused at least 13,200 reported deaths in around 31,500 cases (Amman, Swanepoel, T. Nichol, & Towner, 2017). To date, there are four reported genera: *Cuevavirus, Ebolavirus, Marburgvirus* and the newly reported *Dianlovirus* (Table 1).

The genus of *Cuevavirus* was discovered in 2011 from *Miniopterus schreibersii* species bats (Negredo et al., 2011). Recently, there is only one species, *Lloviu cuevavirus*, and one virus, Lloviu virus (LLOV), belonging to this genus. Within the year following its discovery, the virus was detected in dead bats displaying which had viral pneumonia in caves in Spain, France, and Portugal, although there was no evidence to support LLOV as the cause of death. To date, no human infections have been reported, which suggests LLOV is not a pathogenic virus for humans.

The genus *Ebolavirus* contains 6 different viruses, each belonging to a separate species: Reston virus (RESTV; *Reston ebolavirus*), Tai Forest virus (TAFV; *Tai Forest ebolavirus*), Sudan virus (SUDV; *Sudan ebolavirus*), Bundibugyo virus (BDBV; *Bundibugyo ebolavirus*), Zaire virus (EBOV; *Zaire ebolavirus*) and a new reported Bombali virus (BOMV; *Bombali ebolavirus*). RESTV had some outbreaks in monkeys and pigs. but there have been no human cases of disease reported. Although anti-RESTV antibodies have been detected in humans, there are no report of disease in humans exposed to RESTV (World Health Organisation, 2010). TAFV has been

described as a non-lethal disease and there is little evidence about its natural range (Kuhn et al., 2010). SUDV was first reported in 1976 (Johnston et al., 1978), when it caused 284 cases and 151 deaths (53% fatality). The biggest SUDV outbreak happened between 2000 and 2001. The outbreak included 425 cases and 151 deaths (Okware et al., 2002). BDBV was first identified in 2007, and the next year caused an outbreak with 116 confirmed/probable/suspected cases and a 34% fatality rate (World Health Organization, 2008).

Ebola virus is the most well-known filovirus because it caused the largest outbreak to date. EBOV was first identified in 1976 with 284 reported infections and 53% fatality rate, but in some epidemics, the lethality rate has reached almost 90% (Commission, 1978). The largest outbreak happened from 2014 to 2015 in West Africa. After the first report of infection in December 2013 in Guinea, the disease quickly spread to Liberia and Sierra Leone in 2014. Due to the lack of available therapies and vaccines, the outbreak was out of control at the end of 2014. By the end of this outbreak, there were 28,616 reported patients with 11,310 deaths based on the WHO records (World Health Organization, 2018).

Recently, a new species of ebolavirus, *Bombali ebolavirus*, was reported in 2018 (Goldstein et al., 2018). Only one virus, Bombali virus (BOMV), belongs to this new species. BOMV was found in two species of bats: the Angolan free-tailed bat and the Little free-tailed bat from Sierra Leone in western Africa. *In vitro* assays showed that BOMV has the ability to infect U2OS human cells, but there are no reports yet about the human pathogenicity or infections.

In January 2019, a new genus, *Dianlovirus*, was discovered in Mengla County, Yunnan Province, China (Yang et al., 2019). There is only one species, *Mengla dianlovirus*, and one virus, Mengla virus (MLAV), belonging to this genus. MLAV was detected in *Rousettus sp.* bats and the genome sequence was close to that of the marburgviruses. There is no evidence to support the infection of human cells by MLAV, but a VSV vector expressing MLAV GP can infect HEK293 cells.

Table 1. Filovirus family members

Genus name	Species name	Virus name (abbreviation)
Cuevavirus	*Lloviu cuevavirus*	Lloviu virus (LLOV)
Ebolavirus	*Bundibugyo ebolavirus*	Bundibugyo virus (BDBV; previously BEBOV)
	Reston ebolavirus	Reston virus (RESTV; previously REBOV)
	Sudan ebolavirus	Sudan virus (SUDV; previously SEBOV)
	Taï Forest ebolavirus	Taï Forest virus (TAFV; previously CIEBOV)
	Zaire ebolavirus	Ebola virus (EBOV; previously ZEBOV)
	Bombali ebolavirus (new)	Bombali virus (BOMV)
Dianlovirus (new)	*Menglavirus*	Mengla virus (MLAV)
Marburgvirus	*Marburg marburgvirus*	Marburg virus (MARV)
		Ravn virus (RAVV)

1.2 Marburg Virus

Marburg virus is one of two viruses belonging to the genus *Marburgvirus* (Table 1) that can cause Marburg virus disease (MVD) in human beings; Ravn virus (RAVV) is the other one. Both

of them are hemorrhagic fever disease pathogens, which can cause maculopapular rash, purpura, ecchymoses, hematomas and some other hemorrhagic symptoms (Brauburger et al., 2012).

1.2.1 History

As previously mentioned, MARV was first reported in 1967, when several non-human primates (NHPs; African green monkeys) were imported to laboratories in Germany and Yugoslavia. Twenty-seven primary cases and 6 secondary infections with an unknown infectious pathogen were reported with fever, vomiting, diarrhea, bleeding, shock and some other symptoms. At the end of this outbreak, there were 7 deaths from these 31 patients (Gordon Smith et al., 1967). The primary transmissions happened when the patients were collecting the kidneys from NHPs. Around three months later, the laboratories in Hamburg and Marburg identified and characterized this new agent, Marburg virus, which used the name of the city which reported the most infections (Jacob & Solcher, 1968).

Eight years after the first outbreak, an Australian was infected with Marburg virus when he traveled through Zimbabwe in 1975 (Johnston et al., 1978). The patient showed similar symptoms with those reported during the MARV outbreak in 1967 and then died at a hospital in Johannesburg, South Africa. There were also two secondary infections but both of them recovered. During the following 23 years from 1975 to 1998, there were only intermittent outbreaks which infected a limited number of individuals in Africa, which led to the limited knowledge of and attention paid to MARV (Brauburger et al., 2012).

However, after a long hiatus, a large outbreak happened in 1998-2000 in the Democratic Republic of the Congo (DRC). This outbreak happened during the DRC civil war, which delayed the detection of the MARV outbreak. The investigation team was invited to the outbreak field after a doctor died due to an unknown hemorrhagic fever in April 1999. The pathogen was confirmed as Marburg virus in the next month by National Institute for Communicable Diseases (NCID) of South Africa. Once the MVD was detected, Congo’s Ministry of Health requested assistance from the WHO and a specialists team was set up and arrived in Durba on May 8, 1999. Although the team reported that the outbreak had already subsided, and left after 3 weeks, suspected cases continued to be reported until September 2000. In total, 128 deaths from 154 patients, including 48 laboratory-confirmed and 106 suspected cases, were reported by the end of

the epidemic (Bausch et al., 2003). More than half of the cases were young male miners, and most of them worked in the same mine. After the mine flooded, this outbreak ended, which supported the hypothesis that the outbreak derived from bats in the mine (Bausch et al., 2006). This outbreak was the first large outbreak of MARV since the first report of the virus in 1967, and the outbreak lasted one and a half years, longer than the previous outbreak. The DRC outbreak attracted more attention to Marburg virus, as most of the research and discussions about filovirus were focusing on the ebolaviruses at that time.

Just 5 years later, an acute hemorrhagic fever was reported from northern Angola in January 2005. By the middle of March, 63 deaths including 3 health care workers were reported by the Angola Ministry of Health (MOH). Just a few days later on the 21st of March, the Centers for Disease Control and Prevention (CDC) identified the fever as Marburg hemorrhagic fever. The outbreak was over in July 2005. It was reported that there was a total of 374 cases with 329 deaths (88% fatality rate) from the beginning of the outbreak to August 2005, including 158 laboratory-confirmed cases (Towner et al., 2006). During this outbreak, a technique named Reverse Transcription quantitative PCR (RT-qPCR), which was more sensitive than previous assays, was beginning to be used to detect MARV RNA. The sequence of MARV Angola showed only around 7% nucleotide difference with the majority of East African MARV, which suggested that there are no substantially distinct between the reservoir species. The virus genetic lineages among MARV Angola were quite similar (0-0.07% nucleotide differences), which is probably due to one introduction into the human population and human-to-human transmission with a rare mutant. It is the largest difference between the outbreak in Angola and the previous outbreak in the DRC, where several different virus genetic lineages were reported, and the nucleotide differences were up to 21% (Towner et al., 2006).

After these two large outbreaks of MARV, several small outbreaks happened in Uganda until 2019 (World Health Organization, 2017). The largest one during this time was an outbreak in 2008, which caused 4 deaths out of 15 cases. The two cases in the Netherlands and USA in 2008 were quite similar. Both of them were diagnosed with MVD after visiting a cave in Queen Elizabeth National Park, Uganda.

Because MARV has a high lethality and there are no approved treatments or vaccines available, it was classified as a Biosafety Level 4 pathogen, and WHO also listed it as a Risk Group 4 agent.

Table 2. The outbreak of MVD

Year	Country	Cases	Deaths	Case Fatality Rate
2017	Uganda	3	3	100%
2014	Uganda	1	1	100%
2012	Uganda	15	4	27%
2008	The Netherlands (ex-Uganda)	1	1	100%
2008	The United States of America (ex-Uganda)	1	0	0%
2007	Uganda	4	2	50%
2005	Angola	374	329	88%
1998 to 2000	The Democratic Republic of the Congo	154	128	83%
1987	Kenya	1	1	100%
1980	Kenya	2	1	50%
1975	South Africa	3	1	33%
1967	Yugoslavia	2	0	0%
1967	Germany	29	7	24%

1.2.2 Genome

The genome of MARV is a single-stranded negative-sense RNA genome of around 19 kilobases

nucleotides (nts) long, similar to other filoviruses, which contains seven monocistronic structural protein genes: NP, VP35, VP40, GP, VP30, VP24 and L (Bharat et al., 2011). The genome organization is shown in Figure 1. All these genes contain conserved start and stop signals for the viral transcription, and a long silent region at the 3' and 5' end (Feldmann et al., 1992). Upstream gene or short intergenic regions separate each gene and there is downstream gene overlap with the transcription start signal which includes five conserved nucleotides. This kind of overlap also appears in all other filovirus genomes (Mühlberger, 2007).

Cis-acting signals (Whelan, Barr, & Wertz, 2004), which are required for both transcription and replication, were found at the 3' and 5' genome ends. Moreover, there are promoters for the genome transcription and replication, which are a kind of bipartite promoter, at the ends of the genome as well. Because of the bipartite promoters, the genomes would be expected to obey the "hexad rule" – the length of the genome should be divisible by six. However, no filoviruses follow this rule (Weik et al., 2005). The leader at the 3' end contains 48 nts and the first part of the promoter. The second piece accommodates a tripartite "UNNNNN" pattern with three separated conserved uridine residues (Tapparel, Maurice, & Roux, 1998). These motif hexamers overlap with the untranslated region of the NP gene, which is the first MARV gene, and there is a 12 nts long transcription start signal between the hexamers and the first promoter (Enterlein et al., 2009). Substituting the NP transcription start signal will inhibit the transcription initiation but do not disturb replication activity.

As for the extracistronic region, it is located at the end of the genome (~75 nts), which involves a counterpart for the promoter of antigenomic replication (Tapparel et al., 1998). Although the construction of the antigenomic promoter has not been described, it could be similar to the bipartite promoter because of the $(UNNNNN)_3$ hexamers. It is common that NNS RNA viruses contain leader and trailer regions with a high complementarity of 10 to 15 nucleotides at the 3' and 5' ends (Feldmann et al., 1992). Filoviruses including MARV also share this characteristic, but internal secondary structures were also found both at the leader and the trailer, and no other NNS RNA viruses contain this feature (Druar et al., 2005).

Figure 1. The genome organization of MARV. From left to right: NP (Nucleoprotein), VP35 (Viral Protein 35), VP40 (Viral Protein 40), GP (Glycoprotein), VP30 (Viral Protein 30), VP24 (Viral Protein 24), L (Large Protein).

1.2.3 Structure

As mentioned previously, there are 7 structural proteins in MARV with different functions (Table 3).

Table 3. Functions of MARV structural proteins

Protein	Amino Acids	Function(s)
NP	695	Protect RNA Genome, Nucleocapsid formation, Budding
VP35	329	Nucleocapsid formation, Polymerase cofactor, IFN antagonist
VP40	303	IFN antagonist, Budding
GP	~681	Attachment, Binding, Membrane fusion, immune evasion
VP30	281	Nucleocapsid formation
VP24	253	Nucleocapsid formation, Budding
L protein	~2330	Catalytic of RNA polymerase

1.2.3.1 Glycoprotein (GP)

GP is the only protein on the surface of the MARV viral membrane, which is responsible for the attachment and entry to the target host cells (Will et al., 1993). GP is a homotrimeric transmembrane protein, which was encoded by the open reading frame (ORF) GP gene (Bukreyev et al., 1993). After the translation, the precursor GP will be modified (including glycosylation, acylation, and phosphorylation) during the transportation from the endoplasmic reticulum (ER) to the plasma membrane.

After the combination of precursor GP, it will be divided by furin and furin-like proteases at amino acid 435 (Volchkov et al., 2000). As a result, two subunits GP1 and GP2 are produced. GP1 is an around 160 kD protein located at the surface of the viral membrane, which contains several entry factors and receptors. And there is a receptor binding region located at the GP1 amino acids 38 to 188 (Manicassamy et al., 2007). GP2 (38kD) is a transmembrane subunit, which is similar to EBOV GP2, including a fusion peptide and causing the viral and cellular membrane fusion (Koellhoffer et al., 2012). A transmembrane domain at GP2 fixes GP on the viral membrane, which is 30 amino acids long (Mittler et al., 2007).

High level of glycosylation including complex, mannose-type glycans and mucin-type glycans were found on the GP. Most of the *N*-linked oligosaccharides and *O*-linked glycans compose a MLD (75kD) which is similar to EBOV (Feldmann, Nichol, Klenk, Peters, & Sanchez, 1994). However, the position of the MARV's MLD is quite different from EBOV (Hashiguchi et al., 2015). The MARV MLD is linked with both GP1 and GP2, which shields the base of GP but make the upper surface exposed. On the other hand, The EBOV MLD is only attached to GP1, which mask the upper area of GP but exposes the base parts. The different position of the MLD of MARV and EBOV GP may lead to a different immune response. For both EBOV and MARV, the knowledge about the function of MLD is still limited; only a handful of publications suggested it might play some roles in immune evasion and the viral entry.

Aside from the functions of entry and budding, GP also has an impact on the immune evasion. Interferon (IFN)-induced anti-MARV protein (such as IFN γ) can block the release of MARV VLP, which suggests this kind of protein could be a restriction against MARV (Jouvenet et al., 2009). However, some studies suggested a co-expression of GP could inhibit this restriction with unknown mechanisms (Kaletsky et al., 2009) (Marzi, Konrad, et al., 2011). A 17-mer peptide located at P2 subunits also showed the ability to decrease the cytokine responses (Yaddanapudi et al., 2006). And as previously mentioned, the MLD could also shield the epitopes on the GP. There is some evidence to support that the EBOV MLD could reduce the antibody titer in serum (Basler et al., 2011). But the MARV MLD functions are still unknown.

1.2.3.2 Viral Protein 40 (VP40)

VP40 is similar to the M proteins of the other NNS RNA viruses such as vesicular stomatitis virus (VSV) and rabies virus (O Dolnik, Kolesnikova, & Becker, 2007). Unlike the EBOV VP40, which is organised into hexamers or octamers, knowledge about the MARV VP40 structure is quite limited. One of the major functions of the VP40 is viral particle formation. The VP40 can transfer the nucleocapsids to cellular membrane and attract GP to the budding sites (Kolesnikova et al., 2012). When the formation of the virus particle is done, the VP40 can facilitate the virus release. The VP40 also plays an essential role in both transcription and replication. Increasing VP40 expression can reduce MARV genome expression (Wenigenrath, et al., 2010). The VP40 is a peripheral membrane protein, which is located at the inner side of the viral membrane. There is some evidence suggesting that the VP40 combines with the nucleocapsid by loose interactions, which can be removed by salt dissociation (Kolesnikova, Bugany, Klenk, & Becker, 2002).

Aside from the role of matrix protein, the VP40 is also a virulence factor which can inhibit the innate immune response and influence the host tropism of MARV (Valmas et al., 2010). It can decrease the STAT proteins activity by inhibiting the phosphorylation of Janus kinases, which are responsible for several signaling pathways (Valmas & Basler, 2011). Some papers suggest that when the host cells are stimulated by cytokines (IFNα, IFNγ or IL6), the STAT proteins do not show phosphorylation nor translocation (Ramanan et al., 2011). When the MARV-infected cells receive some other exogenous stimulations, there is still no phosphorylation on Janus kinases. In this case, it is suggested the VP40 could block the IFN signaling, and the target of the VP40 is believed to be Jak1 (Valmas et al., 2010). However, there is still a knowledge gap about the mechanism of the VP40 immune evasion.

1.2.3.3 Viral Protein 24 (VP24)

The VP24 is encoded by the sixth gene of the MARV genome, and it is also a unique protein of the filovirus family (Bamberg et al., 2005). It is usually regarded as a secondary matrix protein, but there is also some evidence showing that the location of the VP24 is extremely close to the nucleocapsid protein, which suggests it could be a part of nucleocapsid proteins (Bamberg et al., 2005). But the connection between the VP24 and the nucleocapsid is really weak; it can be separated by a high salt concentration. There are also several intracellular studies suggesting that

around 10% of the VP24 will stick on the cellular membranes, and a few of filopodia were found on it, which connect it with VP40. The other 90% of the VP24 are mainly found in the cytoplasm, free nucleocapsids, and the NP inclusions (Wenigenrath et al., 2010).

As for the functions of the MARV VP24, there are several papers suggesting it does not affect the virus-like particle (VLP) morphology nor the release ability of VLP, although it plays an important role in viral release during the infection (Valmas et al., 2010). Furthermore, knockdown of the VP24 in the infected cells did not show an impression on the replication of the genome, which suggests the VP24 does not have much influence on genome replication but showed an impact on the subsequent step of nucleocapsid formation. There is still a knowledge gap for the MARV VP24 structure. Only a few papers suggested it is an oligomer and usually developed a tetramer (Warfield et al., 2007).

1.2.3.4 Nucleoprotein (NP)

The NP is one of the nucleocapsid complex proteins, which protects the viral genome and play important roles in viral replication and transcription. The NP can form a helical tubular structure when it is expressed alone without VP30, VP35, and L, which suggests that NP can guide the formation of the nucleocapsid (Kolesnikova et al., 2000). Some papers showed a 390 N-terminal remnant of the MARV NP could successfully contain a helical structure of nucleocapsid core (Bharat et al., 2011). NP is a kind of central protein, which has interplays with most of the other MARV proteins. Especially, VP35 and VP30 showed a strong connection with the NP, which are parts of an NP-derived inclusion (Becker et al., 1998). when discussing the VP24 weak interaction between the NP and VP24 has also been reported, which explains why is demonstrated by VP24 appearing in the NP inclusions. As for the relation between the NP and VP40, some studies suggest that the interaction between them is a key for the transportation of nucleocapsids to the cellular membrane (Kolesnikova et al., 2009).

Another important function of the NP is budding. There is a C-terminal domain motif named PSAP at the NP, which is required for budding. The NP could also induce a component of ESCRT I named Tsg101 which can enhance the budding function of the VP40 (Olga Dolnik et al., 2010). And there are several studies showing the phosphorylation level of NP could harmonize the viral transcription and replication activities (DiCarlo et al., 2011).

1.2.3.5 Viral Protein 35 (VP35)

The VP35 is a part of the nucleocapsid and has several functions including nucleocapsid formation, polymerase cofactor, and IFN antagonism. The VP35 constitutes an RNA polymerase complex with a catalytic subunit of the L protein (Mühlberger et al., 1998). And it is also fixedly accompanied by the NP, which makes it a connection between the L and nucleocapsid. The L cannot link to nucleocapsids and finish the viral transcription and replication without the VP35 (Becker et al., 1998). A homo-oligomer is found on the N-terminal part of the VP35 which plays an important role in the interaction between the L and VP35. There are a lot of characteristics shared between VP35 and other NNS RNA virus phosphoproteins, for example, the position of the gene in the genome, the functions of transcription and replication. But compared with the P protein, the VP35 only contains limited phosphorylation.

Another crucial function of the VP35 is IFN inhibition (Ramanan et al., 2011). Similar to EBOV VP35, the MARV VP35 can also obstruct the IFN production by cutting off the reporter gene expression. And there is also a study showing the VP35 could intercept the human dendritic cell (DC) receiving IFNα signal. On the other hand, the EBOV VP35 could also prevent PKR activity and block the RNA silencing pathways. There is still no evidence to support that the MARV VP35 has these functions.

1.2.3.6 Viral Protein 30 (VP30)

The MARV VP30 shares a similar structure with the EBOV VP30, both of them show a firm connection with the NP. And phosphorylation located at serine and threonine residues is found on both VP30s, suggesting this phosphorylation to be key for the interaction between the VP30 and NP. However, the functions of the MARV VP30 are quite different from the EBOV VP30. EBOV VP30 showed a function as a transcription start factor (Modrof, Mühlberger, Klenk, & Becker, 2002). But for the MARV VP30, a recent study suggested it showed some impact on the viral replication (Fowler et al., 2005). Knockdown of the MARV VP30 in infected cells reduces the output of other viral proteins and influence the viral release. But there is still a knowledge gap about the role of the MARV VP30 in transcription and replication.

1.2.3.7 Large Protein (L)

The L is the main component of the MARV polymerase, its molecular weight is around 267 kDa. The L protein has an effect on viral transcription and replication. The L protein is part of the polymerase complex with the VP35, and the enzymatic activity of the polymerase also depends on the L protein. Almost all the NNS RNA viral L proteins are conserved, which form in the functional area (Poch, Blumberg, Bougueleret, & Tordo, 1990). Some other NNS RNA polymerases (Such as EBOV) can perform RNA synthesis, capping, and polyadenylation of the viral RNA. But there is still no report about the similar functions of the MARV L.

1.2.4 Life cycle

1.2.4.1 Entry

The entry of MARV includes three steps: attachment, endocytosis, and fusion. It is assumed that the filovirus glycoproteins share similar functions and characteristics because of the sequence similarity among them (Feldmann et al., 1994). However, recent studies showed MARV does not infect ferrets or ferret primary cells, where EBOV can (Soule et al., 2018). This suggests that MARV might enter cells using different entry mechanism. There are only a few mechanistic studies of MARV GP, which suggest that the structure of MARV GP2 is similar to EBOV and shares a similar mechanism of fusion (Koellhoffer et al., 2012).

1.2.4.1.1 Attachment

The first step of entry is the attachment to cells, which is performed by GP. Some strong evidence showed that the beginning of viral attachment will occur via the binding of GP to target cellular C-type lectins, including several hepatocyte receptors: DC-SIGN and DC-SIGNR (Marzi et al., 2004), ASGP-R, LESCtin (Matsuno et al., 2010), and hMGL (Dominguez-Soto et al., 2007). There are also some other cellular proteins, like AM receptor proteins, which may play roles in MARV entry. However, some publications suggest MARV can still infect cells without these receptors, which demonstrates that there might be some other proteins or receptors that can facilitate the attachment step (Kondratowicz et al., 2011). Several residues (of GP1) were identified that play roles in the EBOV viral entry and incorporation. Similar residues have also been found in the MARV GP, which suggests that MARV might share part of the entry mechanism of EBOV

(Manicassamy et al., 2007).

1.2.4.1.2 Endocytosis

After attachment, MARV will undergo endocytosis through unclear mechanisms. There are some studies showing that the cholesterol of the host cell could influence the viral infectivity in caveolin-mediated endocytosis. However, no evidence suggests caveolin was involved in the endocytosis. Some studies showed a clathrin-mediated endocytosis inhibitor, which is a chlorpromazine, could inhibit the entry of a MARV GP-encoding HIV-1, which suggests clathrin might play a role in MARV endocytosis (Bhattacharyya, Hope, & Young, 2011). Nevertheless, the problem of these MARV endocytosis studies is that all of them were designed in experiments with MARV GP-expressing retroviruses, which lacked the MARV viral structure and the influence of other proteins. Although some papers suggest cholesterol plays an important role in MARV particle uptake, caveolae and clathrin might not be that important for the endocytosis as a different mechanism of entry may be used for MARV due to its size limitations of these mechanisms (Sanchez, 2007). A MARV particle size is around 800 nm long (the maximum could be as long as 14,000 nm) and 80 nm wide, which is much larger than caveolae or clathrin pits. The Murine leukemia virus (MLK; ~100 nm) and vesicular stomatitis virus (VSV; 70 nm wide, 180 nm long) are much smaller than a MARV particle (Marzi, Schnittler, et al., 2011). It is suggested the endocytosis pathways mediated by caveolae and clathrin for the virus may be due to the use of pseudotyped virion, further experiments with live MARV are required to confirm the pathways for entry.

Another step, the proteolytic cleavage of GP1 in vesicles, appears an important process during the endocytosis (Misasi et al., 2012). The most widely accepted model for the cleavage of MARV GP1 is dependent on the host endosomal cysteine-proteases. Based on the studies of EBOV, the elimination of the GP1 and the MLD will promote the exposure of receptor-binding domain (Sanchez, 2007). There are studies supporting Cathepsin B (CatB) and Cathepsin L (CatL) as playing important roles during the entry of recombinant VSV-EBOV-GP (Chandran, Sullivan, Felbor, Whelan, & Cunningham, 2005). Moreover, when inhibitors of CatB and CatL were added to cells, the entry of VSV-EBOV-GP would be interrupted. However, the results of MARV were wholly different. It is suggested that although CatB could increase the infection activity, it was not required for the entry of MARV. As for CatL, it was required when the virus

enters into mouse embryonic fibroblasts, but it was not necessary for the virus to enter Vero cells, human macrophages, or 293T cells (Gnirß et al., 2012). Although CatB and CatL were hypothesized to be required for cleavage of GP_1 in some cell types, it is most likely some other endosomal proteases might also play roles during the activation of GP_1.

1.2.4.1.3 Fusion

The last step of entry is the fusion of the MARV membrane and the cellular endosome. Several studies have confirmed that the endosomal cholesterol transporter Niemann-Pick C1 (NPC1) was the key for the entry of both EBOV and MARV (Côté et al., 2011). Nevertheless, there were also some complexes with several homotypic fusion and vacuole protein-sorting (HOPS) which were critical for EBOV entry but not quite important for MARV entry (Carette et al., 2011). Right now, the most accepted model of EBOV and MARV fusion is the NPC1 receptor model. The heavily glycosylated domains are removed by the cleavage of GP_1, the receptor binding domain is exposed and binds to NPC1 to activate the fusion. The GP2 then changes to a protracted shape, which leads to the fusion of the viral membrane and the endo-lysosomal membranes. There is a study suggesting the fusion is low pH-dependent, increase the pH of cell media could inhibit the entry of MARV (Chan, Speck, Ma, & Goldsmith, 2000). Another study showed that ammonium chloride could prevent the entry and replication of MARV. However, a vacuolar-type H+ ATPase inhibitor, Bafilomycin A1, which can block the acidification of the vacuolar system, does not have inhibitory effects (Sanchez, 2007). There is still a knowledge gap for the MARV entry mechanism.

1.2.4.2 Transcription and Replication

After the viral membrane is fused with the endosomal membrane, the nucleocapsid is released into the cytoplasm. Around 12 h after the infection, the viral proteins and RNA can be detected, which demonstrates viral replication (Ryabchikova & Price, 2004). Then, the new nucleocapsids will implant into the viral inclusions. Although it is still unclear where the MARV replication and transcription happens within the cells, some publications about EBOV have suggested the viral replication is carried out in the inclusions, and the transcription occurs before the inclusions are formed (Mühlberger, 2007).

The seven monocistronic mRNAs are produced by the transcription of the viral genome, and the infected cell will translate all of them after they are co-transcriptionally capped and polyadenylated. The viral RNA genome is also the template for the positive-sense antigenome production. The antigenomes are the complementary copies of viral genomes, so they can serve as the templates for the replication of genomes (Whelan et al., 2004). Moreover, as mentioned, the nucleocapsid proteins also play important roles in the viral transcription and replication. On the other hand, it is commonly believed that the MARV VP40 and VP24 play a negative role in transcription and replication, which is similar to EBOV (Hoenen, Jung, Herwig, Groseth, & Becker, 2010). The inhibition from these two proteins is suggested to promote the maturation of the nucleocapsids and the beginning of budding.

1.2.4.3 Budding

The following step, which is also the last stage of the viral life cycle, is budding. As mentioned, the VP40 can mediate the release of the virion by mobilizing the GP to the budding sites, which leads to the transfer of nucleocapsids from inclusions to the cellular membrane. In the VLP model, the VP40 can also generate the composition and release of the viral particles. The NP, GP, and VP24 are thought to improve the VP40-mediated budding. Several studies suggest that the COPII and ESCRT vesicular transport system in the host cell are used for the release of viral particles. The COPII pathway was shown to be the main pathway for the VP40-involved intracellular transmission to multivesicular bodies, which is where budding occurrs (Yamayoshi et al., 2008). There are some studies supporting various proteins, including Tsg101, Vps4A/B, and Nedd4.1, that to promote the virion release with the ESCRT machinery (Kolesnikova et al., 2009).

MARV budding has been observed both at internal membranes and the cellular membrane. Most of the viral particles will be released at the filopodia and filamentous cellular protrusions. One of the functions of filopodia is exploring the extracellular environment, which might be used by the virus to infect the neighboring cells once the viral particle is released. Actin might play an important role in the viral budding at filopodia, and the depolymerization of microtubules only has limited influence. Some reports showed the MARV budding was detected at the basolateral membrane of hepatocytes and polarized epithelial cells, but the release of the virus was found at the apical membrane of the endothelial cells (Schnittler, Mahner, Drenckhahn, Klenk, &

Feldmann, 1993). This phenomenon suggests the sites of virus budding are based on the specific cell types.

The most accepted model of MARV virion release was built up based on studies of electron tomography. The budding starts when the intracellular nucleocapsids are combined with the plasma membrane. Then, the nucleocapsids are covered by the cellular membrane until it sticks out vertically from the membrane. The cell will still be viable when the infectious MARV particle (filament shape) release, with the maximum release between 24-48 hours post-infection. Around 96 h post infection, vesiculation is noticed in most of the cells, the shapes of viruses became round or bent, and the viral infectivity is also limited (Welsch et al., 2010).

1.2.5 Pathogenesis

The transmission of MARV usually occurs with directly contact with infected body fluid or animals. After contact, skin barrier disruptions or entry through the mucosal membranes could allow viral entrance. In most of the experimental animal models, several innate immune system cells like monocytes, dendritic cells (DCs) and macrophages are the early targets of MARV, which could transport MARV to the early sites of viral replication: lymph nodes, liver, and spleen, where an abundance of monocytes and macrophages are present (Reed et al., 2011). The earliest replication of MARV was found in macrophages only 24 hours after the infection in guinea pig models (Ryabchikova & Price, 2004). In addition, infected monocytes could be found as early as 2 days post infection in the NHP model (Fritz, Geisbert, Geisbert, Hensley, & Reed, 2008). In human patients, *in vitro* assays have suggested that macrophages, monocytes, and DCs from humans are sensitive infection by MARV. The cell-free viruses, infected monocytes, and macrophages could move into other organs through the lymph and blood system. It is believed to be the main way to infect multiple tissues and lead to systemic infection. In this case, high titers of the virus can be detected in the blood and several tissues just a few days post infection in most of the animal models. At the later stage of the infection, several other cell types including hepatocytes, medullary cells, fibroblasts, and adrenal cortical cells are susceptible to MARV infection as well.

In the late stage of MARV infection, some studies suggest that endothelial cells are also targets of MARV, which might be the mechanism for vascular breakage (Reed et al., 2011). However,

this hypothesis is still controversial. Only a few infected endothelial cells can be detected in NHP models, some other reports suggested maybe the paracrine effects of cytokines induce the endothelium dysfunction (Alves et al., 2010). Almost all the tissues have high levels of infectious viruses at this stage, and high levels of viral genomes are also found in most organs and blood. However, limited inflammation is observed in most of the tissues, suggesting there might be dysregulation of the immune response. An abundance of liver enzymes like ALT and ALP can be detected in the blood in this stage, indicating liver damage (Reed et al., 2011). This could be the reason for bleeding during MVD, because the high level of liver enzymes in the blood will impact the production of coagulation factors. The symptoms mentioned above simultaneously with systemic virus infection may be the reasons for multiorgan system failure, which will lead to death.

1.3 Vaccine & Treatment

Because of the two large outbreaks of Marburg virus disease in Angola and Musoke, experimental therapies and vaccines are in the process of being developed. Although there are no Food and Drug Administration (FDA)-approved vaccine or treatment, some drugs and vaccines candidates showed up to 100% protection against MVD in NHP and rodent animal model.

1.3.1 Vaccine Development

The earliest MARV vaccine was developed by using whole inactivated virus, but the vaccine failed to protect NHPs (Rollin, 2009). Furthermore, some vaccines with survival rates of in rodent models cannot provide the same protection in NHPs. There is one report describing an inactivated MARV vaccine which can protect guinea pigs against a lethal MARV challenge, but the protection of NHPs was only 50% (Ignatyev, Agafonov, Streltsova, & Kashentseva, 1996). Therefore, several different vaccines have been developed.

Recombinant antigen protein and DNA vaccines are widely used for vaccine development. In some early studies, insect cells were used to produce recombinant MARV GP, but the results only showed incomplete protection in guinea pig models (Michael Hevey, Negley, Geisbert, Jahrling, & Schmaljohn, 1997). A GP-based DNA vaccine also demonstrated showed a limited survival following challenge (M Hevey et al., 2001). A few years later, a publication reported a DNA

vaccine showing 100% protection in guinea pigs, which combined EBOV, MARV, and VEEV (Venezuelan equine encephalitis virus). However, this vaccine only showed 66% protection in NHPs. After the outbreak of MARV in Angola, several codon-optimized DNA vaccines have been reported that provide complete protection in both mice without disease outcomes and NHPs with some mild clinical signs following challenge (Grant-Klein et al., 2012). Recently, several DNA vaccines in clinical trials, and two of them were demonstrated safe in phase I clinical trials and anti-MARV GP antibodies were further detected after the vaccination. Nevertheless, some studies suggest the DNA vaccines elicit a lower antibody response compared with other vaccine candidates (Geisbert et al., 2010).

Another widely used vaccine development method is VLPs. At the beginning of the 21st century, a VLP system was used in MARV vaccine development (Warfield & Aman, 2011). A VLP vaccine generated using MARV GP and VP40, demonstrated 100% protection in guinea pigs and elicited anti-MARV GP and VP40 antibodies in the serum. There are some studies suggesting the protection from MARV VLP vaccine in guinea pigs is dependent on CD4+ T cell responses, and that only limited CD8+ cell response was involved (Warfield et al., 2004). Moreover, another group introduced a MARV Musoke VLP vaccine that can fully protect both guinea pigs and NHPs from MARV wild type and RAVV challenges(Swenson et al., 2008).

Viral vectors are also commonly used in MARV vaccine development. The two vectors most widely used for development of MARV vaccines are the adenovirus- (Ad) vectored vaccines, and the vesicular stomatitis virus (VSV) vectored vaccines. It is reported that Ad-based vaccines can provide complete protection against MARV infection in guinea pigs and NHPs (Geisbert et al., 2010). Anti-MARV IgG titer was high in the serum, and a T cell response was also detected after the vaccinations. However, the immune response against Ad vector may cause some problems when it is used in humans. As for the VSV-based MARV vaccine, a VSV expressing MARV GP can provide complete protection against MARV infection in NHPs. Furthermore, some studies showed VSV-MARV-GP can also elicit partial protection as early as seven days following immunization(Feldmann & Geisbert, 2011). Some publications also showed up to 100% protection in post-exposure experiments with a low dose virus challenge (Cross, Mire, Feldmann, & Geisbert, 2018). A single dose vaccination of VSV-MARV GP (Musoke) can provide complete protection in NHPs against RAVV, MARV Musoke, and MARV Angola. A

high level of IgG titer was detected in serum, but the neutralizing antibody titer was quite limited. Unlike the Ad5 vaccines, no T cell-mediated responses can be detected in NHPs after immunization with VSV-MARV-GP. The VSV-MARV-GP can be detected in the blood for only a few days after vaccination, which suggests the replicating live VSV vaccine is safe for use. On the other hand, although the VSV-MARV-GP was well tolerated and can induce protective immunity in immunodeficient mice and NHPs, the safety of the VSV vector for immunodeficient individuals still requires more evidence (Feldmann & Geisbert, 2011).

Recently, a rabies virus vector was reported for the filovirus vaccine development as well. For safety reasons, the rabies virus vaccine needs to be attenuated or inactivated. In BALB/c mice, the rabies virus-based MARV GP vaccines can provide 92% protection with a high antibody response, but the neutralizing antibody response is undetectable (Keshwara et al., 2018). Surprisingly, an NK cell-dependent antibody-dependent cell-mediated cytotoxicity (ADCC) was observed both *in vitro* and *in vivo* assay. This suggested ADCC might play some roles in the protection by MARV vaccines, as most of the vaccines can only induce limited neutralizing antibody response.

1.3.2 Treatment Development

There are still no approved treatments against filoviruses, despite numerous treatment candidates have been reported to be in development. Recently, direct-acting antivirals and immune therapeutics are the main types of treatments against filovirus.

Several direct-acting antivirals showed up to 100% protection against both EBOV and MARV (Liu et al., 2017). For example, BCX4430, Favipiravir (T-705) and GS-5734 all showed up to 100% survival in mouse and NHP models against MARV and EBOV (Liu et al., 2017). However, the clinical trial data from the Western Africa EVD outbreak showed two antivirals, T-707 and TKM-Ebola, which only provided limited protection (46% and 25%). On the other hand, immune therapeutics against EVD showed more positive results compared with the small molecule drugs. Interferon β-1a (IFN-β-1a) showed partial protection in mouse and NHP models against EBOV exposure (Konde et al., 2017). The clinical trial showed a 66% protection during the outbreak, although only nine patients were treated. Therefore, several studies suggested IFN-β-1a was a good adjuvant in the treatment against filovirus. Another immune therapeutic, a

mAbs combination, was suggested to be one of the best treatment candidates against EBOV (Escudero-Pérez & Muñoz-Fontela, 2019). ZMapp, a cocktail of three humanized mAbs against EBOV GP, was the only antibody-based treatment that has been tested in a clinical trial (Qiu et al., 2011). ZMapp showed up to 100% protection in EBOV infected NHPs, and it could provide partial protection in NHPs when the treatment was given after the viremia was detectable (Qiu et al., 2012). During the 2013-2016 EBOV outbreak, 36 patients were treated by ZMapp and 28 of them survived (Group et al., 2016).

There are already more than 500 anti-EBOV mAbs which were isolated from vaccinated animals and rehabilitated patients (Zhao et al., 2017). Most of these mAbs showed neutralization and provided protection in animals. However, all the neutralizing mAbs against MARV were from human survivors. There is still no report about the neutralizing mAbs isolated from immunized animals, even though the methods of mAbs development and the vaccine templates were all similar to EBOV. It is still unknown why neutralizing mAbs cannot be generated through vaccination.

1.4 Rationale

Antibody-based treatments are expected to be one of the best treatment candidates against filovirus. Neutralization was suggested to be the key function of antibody protection. Development of anti-MARV neutralizing mAbs in mice could efficiently provide therapy candidates. Anti-EBOV neutralizing mAbs can be generated from immunized animals, but that is not the case for MARV. In this case, the differences between MARV and EBOV should be the keys of the anti-MARV neutralizing mAbs generation.

In this study, VSV vaccines expressing MARV GP or MLD deleted MARV GP were evaluated and used to develop anti-MARV GP mAbs. The vaccine evaluations can help to build up a better understanding of the MLD functions. Additionally, this study shows some evidence about whether the different position of the MLD between EBOV GP and MARV GP is the reason why the generation of anti-MARV neutralizing antibody is difficult.

1.5 Hypothesis

The hypothesis of this study is:

A vaccine expressing the mucin-like domain deleted GP (ΔMucGP) of Marburg virus will yield more and better neutralizing mAbs than a vaccine expressing the full GP.

To support this hypothesis, the two following objectives were performed in this study:

1. Evaluation of two vaccines. To evaluate the two VSV vaccines expressing MARV GP or MARV ΔMuc GP, several experiments were performed, such as virus growth kinetics, vaccine efficacy evaluation and the detection of viral RNA levels.

2. Development of monoclonal antibodies by using both the VSV-MARV-GP and VSV-MARV-ΔMuc GP. For each vaccine, 3 fusions were completed. All the anti-MARV GP mAbs were screened by ELISA and GFP-based neutralization assay.

CHAPTER: 2 METHOD & MATERIAL

2.1 Biosafety

Mouse-adapted MARV (Angola) used in the experiments performed in the Biosafety level 4 (BSL4) laboratory located in the Canadian Science Center for Human and Animal Health (CSCHAH) which is part of the Public Health Agency of Canada's (PHAC) National Microbiology Laboratory (NML).

2.2 Cell lines & Viruses

2.2.1 Vero-E6 Cell line

The Vero-E6 cell line was bought from the American Type Culture Collection (ATCC). Following the protocol provided by ATCC, Vero-E6 cells were grown in T-75 or T-150 cell culture flasks (Corning) with Dulbecco's Modified Eagle Medium (DMEM; Hyclone) mixed with 5% Fetal Bovine Serum (FBS; Hyclone), 1% L-Glutamine 100x solution (L-Glu; Hyclone) and 1% Penicillin-Streptomycin 100x solution (P/S; Hyclone).

The cells were split when they reached more than 80% confluence. The media was removed from the flask and the remaining medium was washed using Phosphate Buffer Saline (PBS; NML Media service) to make sure the serum was completely removed. Three milliliters of Trypsin-EDTA (0.25%; Gibco) was added to the flask which was incubated for around 3 min to let the cell layer disperse. Seven milliliters of growth medium was added and mixed to inactivate the trypsin. Approximately 10% of the volume was left in the flask and about 14 ml of fresh complete growth medium was added. The flask was returned for incubation at 37 °C with 5% CO_2.

2.2.2 Myeloma Cell line

The Myeloma cell line, P3X63Ag8U.1, was bought from the ATCC. Cells were grown in T-25 sterile tissue culture flask (Corning) with Roswell Park Memorial Institute 1640 Medium (RPMI

1640; Hyclone) mixed with 10% FBS, 1% L-Glu and 1% P/S. The cells were passaged when the medium color changed from red to orange. Gently mixing the suspension and removing around 90% of the culture. About 9 ml fresh complete growth medium was added and the flask was incubated at 37 °C with 5% CO_2.

2.2.3 Vesicular stomatitis virus (VSV)

All the VSV vaccines or viruses used in experiments were obtained from the previous works (Hagan et al., 2007). The vaccine or virus genome designs are shown in Figure 2. VSV-wild type (VSV-WT; John Rose, Yale University) was used as a vector control in the vaccine evaluation experiments, all the gray boxes in Figure 2 show the original proteins of VSV wild type. The two vaccines, VSV-MARV-Full GP and VSV-MARV-ΔMuc GP, were generated by replacing the initial VSV G protein gene with MARV GP or ΔMuc GP genes. In Figure 2, MARV GP or ΔMuc GP genes are indicated as blue and located between the M and L protein genes. These vaccines express the MARV GP or ΔMuc GP on the surface of VSV, which worked as antigens and play roles in viral attachment to and entry in cells. The VSV-MARV-GP GFP was used for the GFP-based neutralization assay, the titre of VSV-MARV-GP GFP was 5.95 x 10^6 pfu/ml. It was constructed by inserting a green fluorescent protein (GFP; marked as green in Figure 2) gene between MARV GP and original L genes.

All the viruses were grown on Vero E6 cells in T-75 cell culture flasks (Corning). Two flasks with more than 80% confluency were required. One was for the virus infection, and another one was for mock control to confirm the cell state. Stocks of VSV vaccines were thawed and diluted with DMEM (Hyclone) to a ratio of 1:100. All the culture medium in the flasks was removed, and 5 ml of diluted vaccines were added for virus adsorption (5 ml plain DMEM media to mock control). The cells were incubated for 1 hour and gently rocked every 15 min during the incubation. Growth medium (DMEM with 2% FBS, 1% L-Glu and 1% P/S) was added to each flask to make the medium reach 20 ml. All the flasks were incubated at 37°C and monitored for cytopathic effect (CPE) every 24 hours until less than 20% of the monolayer was intact. All supernatants were transferred to a 50 ml conical centrifuge tube (Falcon) and spun for 10 minutes at 2500 rpm, 4 °C. The supernatant were collected and supplemented with FBS (Hyclone) to make the final concentration of serum 10%. Then, the stock was aliquoted and stored at -80°C.

Once the storage was done, the titers of new viruses were also measured with using the median Tissue Culture Infectious Dose ($TCID_{50}$) method. Vero E6 cells were seeded in 24-well plates (Corning) with 1 ml of medium per well (DMEM with 5% FBS, 1% L-Glu and 1% P/S). The cells would be used when they reached more than 80% confluency. Different dilutions of virus stock from 1:100 to $1:10^8$ were made for the infection. All the medium was removed from the 24-well plates (Corning) and 250 µl diluted viruses or plain DMEM were added to each well, with each dilution made in quadruplicate. The plates were incubated one hour at 37 °C to allow the viruses to attach to the cells. After the incubation, the virus inoculum was removed and replaced with 1 ml of fresh medium (DMEM with 2% FBS, 1% L-Glu and 1% P/S). All the plates were incubated again at 37 °C, and all the cells were monitored for CPE every 24 hours to calculate the $TCID_{50}$ based on the Reed and Muench method.

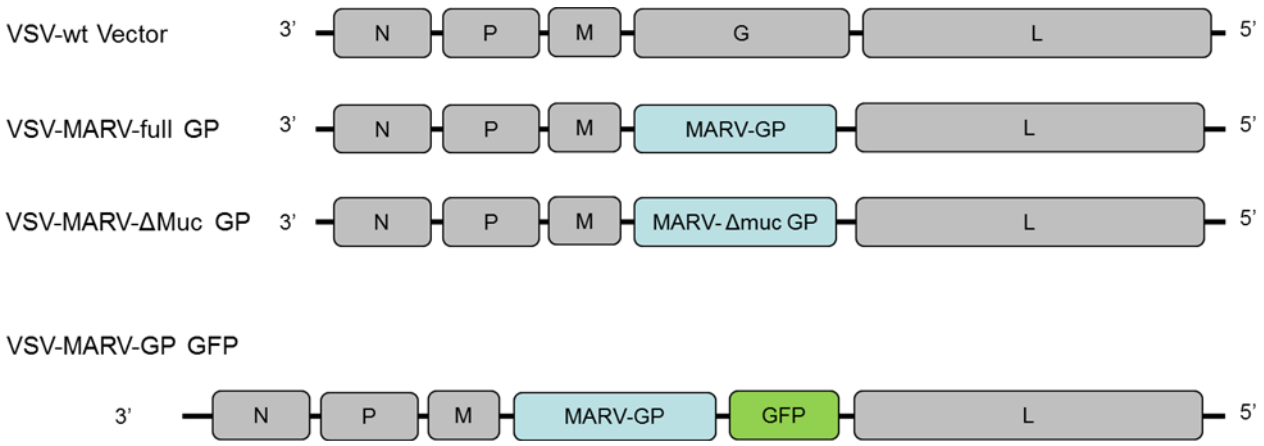

Figure 2. The VSV vaccines design. VSV-wild type (VSV-WT) was used as a vector control in the vaccine evaluation experiments, all the gray boxes showed the original proteins of VSV wild type. The two vaccines, VSV-MARV-Full GP and VSV-MARV-ΔMuc GP, were built up by replacing the initial VSV G protein gene with MARV GP or ΔMuc GP genes. MARV GP or ΔMuc GP genes were indicated as blue located between M and L protein genes. These vaccines could express the MARV GP or ΔMuc GP on the surface of VSV, which worked as antigens and play roles in viral attachment to and entry in cells. The VSV-MARV-GP GFP was used for the GFP-based neutralization assay. It was constructed by insert a Green fluorescent protein (GFP) gene between MARV GP and original L genes.

2.2.4 Marburg virus (MARV)

The virus used for the vaccine evaluation studies was the mouse-adapted Marburg virus (Marburg virus NML/M.musculus-lab/AGO/2005/Ang-MA-P2). The virus stock was from the previous study (Qiu et al., 2014), and the median Lethal dose (LD_{50}) of this stock was calculated to be 0.05 $TCID_{50}$ for BALB/c mice.

2.3 *In vitro* Assay

2.3.1 Vaccine growth curve

The three viruses, VSV-MARV-Full GP, VSV-MARV-ΔMuc GP, and VSV-MARV-GP GFP were used to make a growth curve. Vero E6 cells were seeded and grown in cell-bind surface 6-well microplates (Corning) with 2.5 ml medium (DMEM with 5% FBS, 1% L-Glu and 1% P/S). The cells were infected at 80% confluency at a multiplicity of infection (MOI) of 0.1 (Around 1.2 * 10^6 cells/well, 1.2 * 10^5 pfu/well). Each virus was diluted in triplicate compare the viruses. For the virus infections, the cells were infected with 250 µl of virus inoculum. The plates were incubated at 37°C for 1 hr with gentle rocking every 15 min. The inoculum was removed and replaced with growth medium (DMEM with 2% FBS, 1% L-Glu and 1% P/S) was added. The plates were incubated at 37°C and the supernatant was collected every 24 h for five days.

Each supernatant sample was titered using the $TCID_{50}$ method described in section 2.2.3. In this case, every virus had 9 $TCID_{50}$ data for each time point.

2.3.2 Enzyme-Linked Immunosorbent Assay (ELISA)

ELISAs were used to quantify the antibody titers in the serum of vaccinated mice and hybridoma supernatants. Half-area 96-well RIA/EIA plates (Corning) were coated with 30 µl recombinant of Marburg virus Angola glycoprotein minus the transmembrane region (MARV-Angola rGPΔTM; IBT Bioservices) at 1 μg/ml overnight at 4 °C. One hundred microliters of 5% Skim Milk (Difco) in PBS (NML Media service) was used to block the plate for 1 h at 37°C.

For the serum, dilutions the initial dilution was 1:100 with 2-fold serial dilutions in 2% skim milk (Difco). The blocking buffer was removed and 30 µl of diluted serum samples were added

to the plate, in duplicate. The plates were then incubated 1 h at 37°C. For the supernatant samples, 30 µl of supernatant from hybridomas were added after removing the blocking buffer.

The plates were washed 4 times with 0.1% PBST (PBS with 0.1% Tween-20; Fisher) using a 405 LS Microplate Washer (BioTek). Next, secondary antibodies, goat anti-mouse IgG Fab-HRP (SouthernBiotech), were diluted at the ratio of 1:2000 with 2% skim milk. The 30 µl of diluted secondary antibody was added to each well of the washed plates. All the plates were incubated at 37ºC for 1 hour. After the incubation, the plates were washed 4 times and 50 μl of pre-warmed 3,3',5,5'-tetramethylbenzidine (TMB; ThermoFisher) were added. All the plates were incubated in the dark at room temperature for 30 min. A pre-warmed VersaMax microplate reader (Molecular Devices) was used to read all the plates at 650 nm.

For serum IgG detection, the antibody titre was measured as the last dilution where the sample had an average optical density at 650 nm (OD_{650}) of more than 0.1. As for the supernatant IgG titre, the OD_{650} number was directly used as the result.

2.3.3 GFP-based neutralization assay

Vero E6 cells were seeded in 96-well clear bottom black polystyrene multicoated microplates (Corning), the cells were infected when they reached at least 80% confluency. Two-fold serial dilutions of the samples were performed in plain DMEM (HyClone) in 2 ml 96-well V-Bottom polypropylene deep well plate (Corning). A 2X virus solution in plain DMEM was prepared at the same time, 672 µl (for MOI 0.1; around 4 * 10^4 cells/well, 4000 pfu/well) of virus stock were transferred into 10 ml of DMEM (scaled up when there were too many samples), and the solution was briefly mixed by inversion several times. The samples (antibody or plain DMEM, in triplicate) and 2X virus dilution were mixed in equal volume and all the mixtures were incubated at 37 °C for 1 hour. After the incubation, 100 µl of mixture were transferred from deep blocks to cells in 96 well plates. The plates were incubated at 37 °C for 1 hour. The viral inoculum was removed and 200 µl of medium (DMEM with 2% FBS, 1% L-Glu and 1% P/S) were added to each well. All plates then were incubated at 37°C with 5% CO_2 and read 48 hours after the infection.

Synergy HTX hybrid multi-mode reader (BioTek) was used to read the plates. Before reading, blue paper towel (Scott) with 5% Micro-Chem plus (NCL) was used to clean the whole outer surface of each plate. The reading results were calculated using the equation: Infection% = 100 * (Samples - Background) / (Positive control - background).

2.4 *In vivo* Assay

All the studies were completed in consonance with Canadian laws and following guidance from the Canadian Council on Animal Care. The protocols (H15-013 and H-18-015) were approved by the Animal Care Committee of the CSCHAH. All the experiments involving live Marburg virus were accomplished in the Containment Level 4 laboratory in the National Microbiology Laboratory of the Public Health Agency of Canada.

Six to eight week-old female BALB/c mice were used in all experiments. Mice were ordered in consultation with the head of Veterinary Technical Services (VTS) and obtained from Charles River Laboratories or Jackson and shipped to Winnipeg according to the guidelines for transport of live animals. All animals were transferred to appropriate animal cages and given food, water, and environmental stimulation.

2.4.1 Vaccine evaluation

2.4.1.1 Experiment design

The purpose of this study was to evaluate the efficacy of the two vaccines: VSV-MARV-GP and VSV-MARV-ΔMuc GP.

Fifty-four mice were divided into three groups (18 mice per group). Animals in group 1 were vaccinated with VSV-MARV-GP, mice in group 2 were vaccinated with VSV-MARV-ΔMuc GP, and all animals in group 3 were immunized with VSV-wt. The vaccination plan was shown in figure 3. The challenge day was measured as day 0. All animals were vaccinated at 28 days before infection with 200 μl of vaccines (3 x 10^5 pfu) by intraperitoneal injection (i.p.) at two sites in the peritoneal cavity. All the mice were anesthetized by inhalational isoflurane with oxygen during the vaccination. All the mice were challenged with 2000 times the LD_{50} of MA-MARV Angola at

day 0 by i.p. injection in CL4. And the injection method was the same as with the vaccine injection. Four mice from each group were randomly selected and euthanized at 4 days post-infection (dpi) (12 mice total) and 6 dpi (12 mice total) to collect blood and tissues (liver, spleen, kidney, lung) to evaluate vaccine efficacy and perform virus titrations.

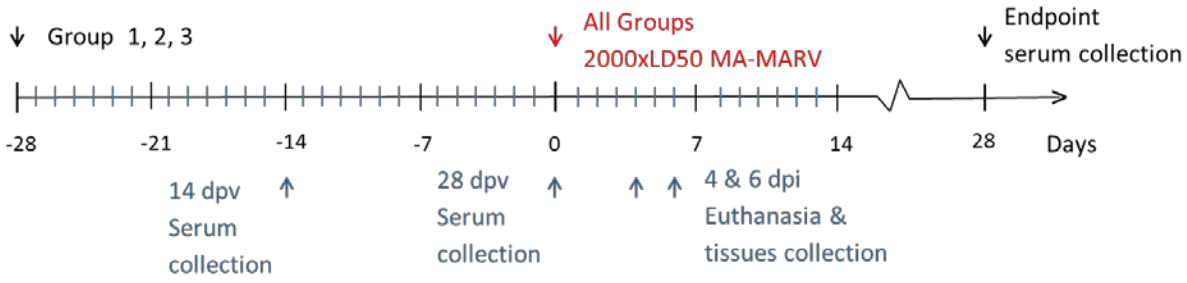

Figure 3. The timeline of vaccine immunization and samples collection. Animals in group 1 were vaccinated with VSV-MARV-GP, mice in group 2 were vaccinated with VSV-MARV-ΔMuc GP, and all animals in group 3 were immunized with VSV-wt. The vaccination plan was shown in figure 3. The challenge day was measured as day 0. All animals were vaccinated at -28 days post infection (dpi) with 200 µl vaccines (3 x 10^5 pfu) by intraperitoneal injection (i.p.) at two sites in the peritoneal cavity. All the mice were anesthetized by inhalational isoflurane with oxygen during the vaccination. All the mice were challenged with 2000 times LD50 of MA-MARV Angola at day 0 by i.p. in CL4. And the injection method was the same as the vaccine injection. Four mice from each group were randomly selected and euthanized at 4 dpi (12 mice) and 6 dpi (12 mice) to collect blood and tissues (liver, spleen, kidney, lung) to evaluate vaccine efficacy and virus titrations.

2.4.1.2 Blood collection

The blood was collected at a volume of about 0.1 ml per animal. Blood was collected in EDTA tubes to assess the viral burden (post-challenge), and in serum tubes to measure the serological response (antibody titer and neutralization). The blood and serum sampling days were marked in Figure 3. At 0 day post vaccination (dpv; “pre-serum”), 14 dpv, and 28 dpv, serum was collected from all mice. Blood was collected in serum tubes using a terminal bleed for all the animals euthanized on days 4 and 6 post-infection. All survivors were euthanized at the end of the experiments (28 dpi), and their blood and serum were collected. Serum samples were used to determine antibody titer and neutralization titers. The blood samples were used to measure the levels of viremia using RT-qPCR.

The QIAamp Viral RNA Mini Kit (Qiagen) was used for the blood sample RNA extractions. One hundred and forty microliters of blood was transferred into 560 µl of AVL, and the mixture was vortexed for around 15s. The liquid was collected to the bottom of the tube by centrifugation. After a 10 min incubation at room temperature, the blood/AVL were moved into 560 µl ethanol in fresh tubes. The same centrifuge and incubation were performed as the previous step. The tubes were removed from high containment following standard operating procedures. The next extractions were completed performed in a biosafety level 2 laboratory.

All the ethanol tubes were checked in a biosafety cabinet (BSC) before opening. The filtrate was disposed of in 5% Micro-Chem plus (NCL). The extractions were performed as described by the supplier. The samples were eluted in 60 µl of AVE buffer. After the RNA extraction, all the RNA samples were stored at -80 °C.

2.4.1.3 Tissues collection

The euthanized mice at 4 and 6 dpi were also collected tissues (liver, kidney, spleen, and lung), which were used for viremia viral genome equivalents (GEQ) test. RNeasy Mini Kit (Qiagen) was used for the tissues viral RNA extraction. 600 µl buffer RLT (provided in the kit) were prepared in 2 ml centrifuge tube in advance. Up to 30 mg tissues samples were collected, then these tissues samples were performed disruption and homogenization by using RLT buffer. A 20000 xg centrifuge was displayed and all the supernatant were collected. An equal volume of 70% ethanol was mixed with the supernatant, and then following the protocol in Containment Level 4 (CL4),

all the tubes were sterilized. The remaining RNA extraction steps were finished at biosafety level 2 laboratory.

All the tubes were checked in a biosafety cabinet (BSC) before open, 5% Micro-Chem plus (NCL) was also used for the filtrate. 700 µl samples were moved to the RNesay spin column (Qiagen) and centrifuged at 8000 x g for at least 1 min. This step was repeated until all the samples were done. 700 µl RW1 wash buffer (provided in the kit) were added into the column and centrifuge for 1 min at 8000 x g. The columns were then washed two times with 500 µl RPE Buffer (provided in the kit, 220 ml ethanol were added before use) by centrifuge at 8000 x g for 3 min. An additional centrifuge step was performed after the RPE buffer washing to confirm all the RPE was removed. At last, 50 µl RNase-free water were used for each column to elute the rival RNA. All the RNA samples were labeled and stored at -80 ^{o}C.

2.4.1.4 Daily monitoring

Animals were observed twice daily during acclimatization and convalescence by the person in CL4. In addition to observing the animals directly within the animal facility, the animals also were regularly observed by using the closed-circuit television system in the BSL4 laboratory. The survival rate was calculated until the endpoint of the experiment (28 dpi). Survival curves were compared using the Mantel-Cox log-rank test.

The weight and clinical score of every mouse were assessed every day until 13 days post infection. The clinical score for the mouse was measured in four different stages. A clinical score of 0 meant there were no clinical signs. A clinical score of 1 was given to the animals who suffered fur ruffled, low activities, more than 10% weight loss than the first day and food intake decrease. When the mouse showed Paralysis, labored breathing, hunched posture and bleeding, the clinical score 2 will be given. Clinical score 3 was given when the mouse was dead or Euthanasia. When the mouse showed clinical signs more serious than a score, for example, more than clinical score 1, but not reached the next score yet, this mouse was given a clinical score 1.5. Euthanasia was performed at the endpoint of experiment or when a mouse reaches the clinical score 2 but also had some other clinical signs like no movement or more than 20% weight loss compared with the 0 dpi.

2.4.1.5 Quantification of viral genome equivalents (GEQ)

All the viral RNA samples were tested with the method of RT qPCR. QuantStudio 3 Real-Time PCR System (Life Science) and the LightCycler 480 RNA Master Hydrolysis Probes kit (Roche) was used for the experiment, and Thermo Fisher Cloud was used for the data analyzed. The cycling conditions, MARV L gene standard, primers and probe used in this experiments was the same as the previous publication (Zhu, Zhang et al,. 2018). The results of the RT-qPCR were analyzed by the method of one-way ANOVA test with Bonferroni's multiple-comparison correction.

2.4.2 Monoclonal antibodies (mAbs) generation

2.4.2.1 Immunization of mice

Two groups of mice were immunized separately with VSV-MARV-GP and VSV-MARV-ΔMuc GP. The pre-sera were collected before the first immunization, which was used as a baseline for the antibody evaluated. For each immunization, 100 μl vaccine (dose ~3 x 10^ 6 $TCID_{50}$/ml in 10% FBS + DMEM) were injected intraperitoneally (i.p.; 50 μl per side). Vaccines were injected every three weeks, and sera were collected before the immunization.

All the collected serum samples were used to detect the anti-MARV GP IgG titer following the method of ELISA (mentioned at 2.3.2 ELISA). The sample dilution in this experiment was different, all the serum samples were diluted by the ratio of 1:400 in triplication to make the quick screen. After four- or five-times immunization, two mice in each group were chosen based on the anti-MARV GP antibody level. A final boost with purified MARV GP (100 μg in a total volume of 100μl) was performed to these chosen mice. After 3 – 5 days of the final boost, the spleens and sera were collected for the next step.

2.4.2.2 Myeloma cells for fusion

ClonaCell-HY Hybridoma Cloning Kit (STEMCELL) was used for Hybridoma development. Following the protocol of this kit, the myeloma cells were prepared at least one week in advance to confirm the cell was adapted to the hybridoma fusion media. Used the method mentioned in 2.2.2 to keep P3X cells growing before the experiments started. When the experiment started, change the growth media with 50% complete growth medium used in 2.2.2 and 50% Media A

(STEMCELL; the media for myeloma growth and Hybridoma expansion). After 1-2 passages, change the media to 100% Media A (STEMCELL) and seeded cells in T-150 flask (Corning). In Total, 2 x 10^7 myeloma cells were required for the hybridoma fusion, but more than 3.2 x 10^7 myeloma cells were prepared to avoid the shortage of cells. At the day of spleen collection, there were eight T150 flasks with the cell density of ~ 2 x 10^5 cells/ml.

2.4.2.3 Fusion

At the spleen collection day, prepared the myeloma cells at first to keep the viability of Splenocytes as high as possible. The myeloma cells were centrifuged at room temperature at 300 x g for 10 min, then the supernatant was removed, and the cells were washed three times by using 30 ml Medium B (STEMCELL; The media for cell washing and hybridoma screen). The washing step was the same with the previous centrifugation. After the washing, the cell pellets were re-suspended with 50 ml of Medium B. Cellometer Auto T4 Bright Field Cell Counter (Nexcelom) was used for the Myeloma cells counted. 10 µl cell culture was diluted with 90 µl PBS to increase the cell counting sensitive. 100 µl of 0.4 % w/v Trypan Blue (STEMCELL) was added into the diluted cell culture. After a gently mixing, 20 µl of the mixture was pipetted to a disposable hemacytometer (Nexcelom), and a repeat will be done at the same time. After the cell counting, the myeloma cells were incubated at 37 ^{0}C until the fusion.

The spleens were removed and placed in 5 ml Medium A, the fatty tissue stick on spleen was trimmed off. Two 50 ml centrifuge tubes (Falcon) with Medium B and cell strainers (Falcon) were prepared. The cell strainer was put on the centrifuge tubes and the Medium B media was added into these tubes until the screen was rinsed by the media. The spleen was moved on the cell strainer, and a plunger of a 3 ml syringe was used to grind the spleen cells out of spleen. Once all four spleens were ground, Medium B was used to wash the splenocytes at room temperature at 400 x g for 10 min. The washing step was performed three times, and for each time the cell pellets were re-suspended gently to keep the viability of splenocytes. After washing, the splenocytes were re-suspended in 25 ml Medium B, and the cell suspension was incubated at 37 ^{0}C until fusion. 10 µl of cell culture was added into 90 µl of 3% Acetic Acid with Methylene Blue (STEMCELL) to count the spleen cells. 20 µl of the mixture was pipetted disposable hemacytometer (Nexcelom) in duplicate and counted with Cellometer Auto T4 Bright Field Cell Counter (Nexcelom).

Based on the cell density calculated previously, the incubated myeloma cells and splenocytes were mixed together with the ratio of 1:5. All the splenocytes were used and a suitable volume of myeloma cells was added. The mixture was centrifuged at 400 x g for 10 min. All the supernatant was discarded and the pellets were disrupted by gently tapped the tube. Pre-warmed ClonaCell-HY PEG Solution (PEG; STEMCELL) was added slowly to the pellet by drop. The cells were then gently stirred with a pipette tip for one minute. Pre-warmed 4 ml Medium B was added by drop, and a gently stir was performed at the same time. After the mix, 10 ml Medium B were slowly added to the cells, then all the tubes were incubated at 37°C for 15 min. After the incubation, 30 ml of pre-warmed Medium A were added to each tube, then all the cells were centrifuged for 7 min at 400 x g. The supernatant was removed, and 40 ml Medium A was used to wash the cells again at 400 x g for 10 min. The cell pellets were then gently re-suspended with 10 ml Medium C (STEMCELL; media for hybridoma recovery). The cells from each group were then transferred to T-75 flasks (Corning) separately, and additional Medium C were added to make the volume of media reach 30 ml. All the flasks were then incubated at 37 ^{0}C in 5% CO_2 for 24 h.

2.4.2.4 Selection and Cloning

Medium D (STEMCELL; A semi-solid media for the hybridoma selection) was thawed one day in advance at the fridge. On the day of fusion, the Medium D was pre-warmed at room temperature. The fused cell suspension was centrifuged at 400 x g for 10 min, the pellets were then re-suspended with 10 ml Medium C. All the cell cultures were moved into 90 ml Medium D, then the bottles were inverted gently to mix. These bottles were then incubated at 37 ^{0}C for at least 15 min to make the bubbles moved to the top. 12 mL syringes (BD) with blunt-end 16-gauge needles (STEMCELL) were used to slowly move 9.5 ml of cell culture into each of ten 100 mm TC-treated cell culture dishes (Falcon). All the plates were incubated at 37 ^{0}C in 5% CO2 for 10-14 days until the colonies of hybridoma growth up. During the incubation, all the dishes were stationary to avoid the runny or hazy colonies.

2.4.2.5 Hybridoma screen

10 to 14 days after the fusion, the hybridoma colonies were available to pick. A pipettor set to 10 µl with 100 µl tips were used to transfer the colonies to 96-well plates with 200 µl Medium E (STEMCELL; media for hybridoma growth) per well. The transferred colonies were then pipetted

various times to re-suspend. All the plates were incubated at 37 ^{0}C in 5% CO_2 for 1 to 4 days. A daily monitor was performed, and 150 μl supernatant were collected from each well when the medium turned orange. Transferred 150 μl fresh Medium E to each well and the plates were incubated again.

Followed the method of 2.3.2 ELISA, all the collected supernatant was screened the anti-MARV GP antibody levels. When the OD_{650} was more than 1.0, this hybridoma was then transferred to 24-well plates for a continue growing. After a secondary screen of ELISA, the hybridoma, which contained high antibody level in the supernatant, was transferred to T-25 flasks for continue growing. The growing media in T-25 flasks was 50% Medium A with 50% Medium E. When the hybridoma cells were adaptive with the mixed media, 5-10 ml hybridoma cell suspension were transferred to T-75 flasks growth with 20 ml Medium A. When the cells density was around 4 x 10^5 cells/ml, all the supernatant was collected, and the cells were frozen with freeze solution (20% DMSO, 80% FBS) in -80^{0}C. Each freeze tube contained at least 2 x 10^6 cells. The collected supernatant was used for the neutralizing antibody test followed the method of 2.3.3 GFP-based neutralization Assay.

CHAPTER: 3 RESULTS

3.1 Vaccine evaluation

3.1.1 Virus growth kinetics

To characterize the growth kinetics of these three vaccines or viruses, recombinant VSV growth curve in Vero-E6 cells was conducted (Figure 4). The viral titers in the supernatant of three viruses increased speedily at the first 48 hours after infection. The viral titers of VSV-MARV GP and VSV-MARV-GP GFP reached the maximum, around 2 x 10^6 $TCID_{50}$/ml, at 72 hours post infection. The viral titers of VSV-MARV-ΔMuc GP were continually increasing until 96 hours reached about 4 x 10^6 $TCID_{50}$/ml. The concentration of VSV-MARV-GP GFP was jumping down almost 10 times lower at 96 hours post-infection (hpi) compared with the titer of 72 hpi, and the viral titers were continuing to reduce until the endpoint at 120 hours post-infection. As for the VSV-MARV-GP group, the number of infectious viruses showed a mild decrease from 72 h to 120 h. The viral titer of VSV-MARV-ΔMuc GP decreased to the same level as VSV-MARV-GP group at the endpoint of the experiment.

After 72 hours post infection, the viral titers of the three viruses showed some differences. The reduction of VSV-MARV-GP GFP viral titers was probably due to the cytotoxicity of the cells. By checking the wells under a microscope, more than 80% of CPE was found at 96 h. Almost all the cells were dead at the end of experiments. As for VSV-MARV-GP and VSV-MARV-ΔMuc GP, the difference between them was not significant ($p > 0.1$). Under the microscope, the percentage of CPE of each well was also similar, but one of the ΔMuc GP wells contained more cells than any other wells, which could be the reason of the continuing increase at 96 h.

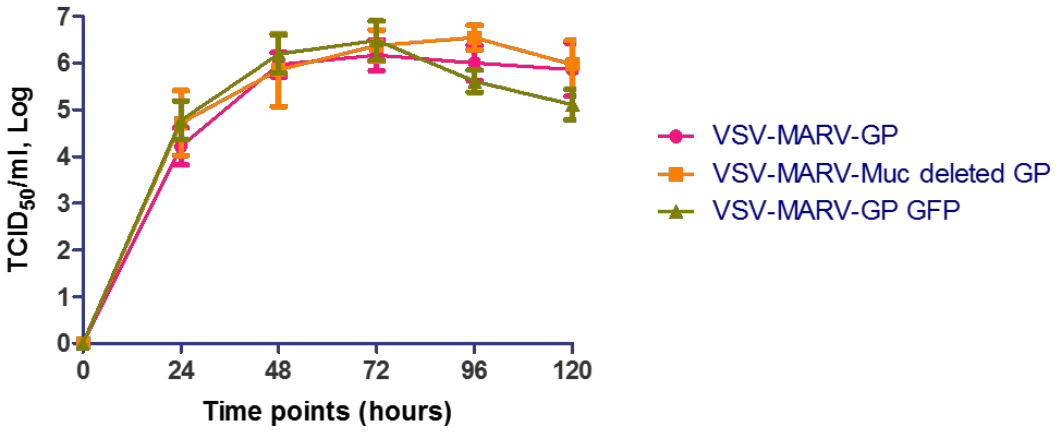

Figure 4. Vaccines growth curves in Vero-E6 cells. VSV-MARV-GP was marked with the color of pink, VSV-MARV-ΔMuc GP was marked by yellow and the VSV-MARV-GP GFP was in the color of green.

Based on the results of this experiment, the VSV-MARV-GP and VSV-MARV-ΔMuc GP were infectious, and the growth kinetics in Vero-E6 cells of two vaccines were similar. It suggested the two vaccines could be used for the vaccine evaluations. The VSV-MARV-GP GFP virus was infectious, and the best reading time point for the GFP-based neutralization assay was 48h or 72h.

3.1.2 Vaccine efficacy evaluation

To evaluate the VSV-MARV-Full GP and VSV-MARV-ΔMuc GP, the survival study of MA-MARV challenge in balb/c mice was performed. The VSV-MARV-GP group was marked as group 1, VSV-MARV-ΔMuc GP group was marked as group 2 and the vector control group was marked as group 3. All the mice in each group were numbered from 1 to 18. Based on the experiment design (Figure 3), all the mice were challenged via the intraperitoneal route (i.p.) with 2000 x LD_{50} MA-MARV at challenge day, 10 mice from each group were used for the survival study.

3.1.2.1 Survival rate and weight change

The survival rate was shown in Figure 5A. The color in pink was the survival rate change of the control group (VSV-WT), all the ten mice in this group dead before 8 dpi. One mouse was found dead a half day after the MA-MARV injection, which was dead due to the i.p. injection. At 6 dpi, one mouse reached the clinical score 2 (Figure 6C) and it could not move, so this mouse was euthanized followed the method of 2.4.1.4. There was also another individual found dead at 6 dpi in this group. Furthermore, all the other 7 mice in VSV-WT group were found dead at 7 dpi. As for the two vaccine groups, all the fatal animals were found at 7dpi. For group 1, eight mice survived until the endpoint of the experiment. 6 out of 10 mice survived in group 2. There was no statistical difference between the two vaccinated groups ($p > 0.05$). Compare with the vector control, both vaccine groups showed significance (In Figure 5A the significant star *: $p < 0.05$; **: $p < 0.01$; ***: $p < 0.001$).

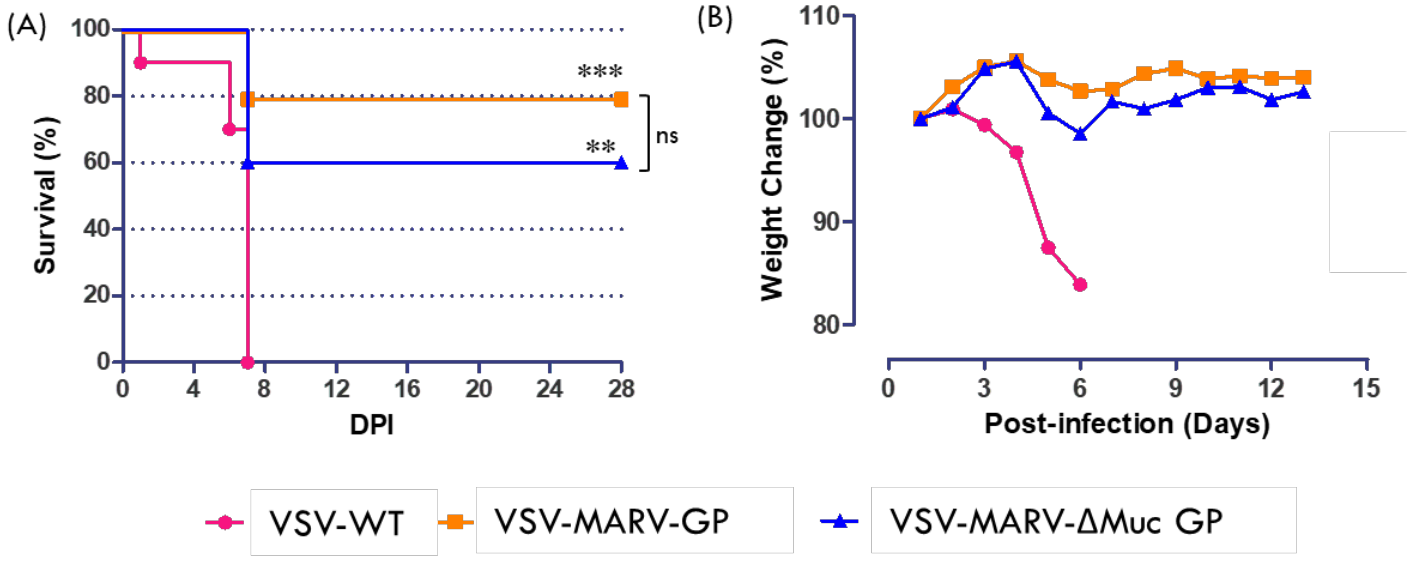

Figure 5. The survival rate and Weight change of MA-MARV infected mice. (A) The survival rate of three vaccination groups. (B) The weight change percentage of three vaccination groups. Statistical comparisons between each group were performed using the Mantel-Cox (log-rank) test: *, $p < 0.05$; **, $p < 0.01$; ***, $p < 0.001$.

The weight of each mouse was also recorded daily until 13 dpi. figure 5B showed the average weight loss percentage for each group, the baseline of each group was the 1 dpi average weight. The color of each group was the same as the survival rate graph. The average weight of group 3 increased a little bit at 2 dpi and declined from 3 dpi to 7 dpi until all the mice died. Average weight change of two vaccine groups showed similar tides. Weight increase was observed in both two vaccine groups before 4 dpi. The weight dropped at 5 and 6 dpi, then recovered at 7 dpi because the sick mice all dead at this day. From 7 dpi to 14 dpi, both groups average weight percentage remained a level with mild fluctuation. At 5 and 6 dpi, the weight decreases of group 1 were significantly more than those of group 2 ($p < 0.05$).

3.1.2.2 Clinical score

To assess the clinical signs of each mouse, the clinical scores were evaluated once the weights of mice were measured. Figure 6 showed all the 30 mice clinical scores from 1 dpi to 13 dpi. For the VSV-MARV-GP group (Figure 6A), the two dead animals #2 and #5 showed some clinical signs at 5 and 6 dpi, then were found dead at 7 dpi. All other animals in this group do not contain any clinical signs. As for the VSV-MARV-ΔMuc GP group shown at figure 6B, the four fatal mice were found more or fewer syndromes at 5 dpi, and all of them were found dead at 7 dpi. Only mouse #1 and #11 in this group did not show any clinical signs from the beginning to the endpoint. The other four survivals were observed up to 1.5 clinical scores, but all of these four sick mice recovered at 8 dpi and did not relapse until the end of the experiment. The earliest clinical signs appeared at the vector control group (Figure 6C), #1 mice in this group was observed ruffed fur and more than 5% weight loss at 4 dpi. As mentioned at 3.1.2.1, animal #18 was found dead after the injection, so the clinical score was marked three at the beginning of the experiment. All the mice were sick after 5 dpi, and there were no survivors after 7 dpi.

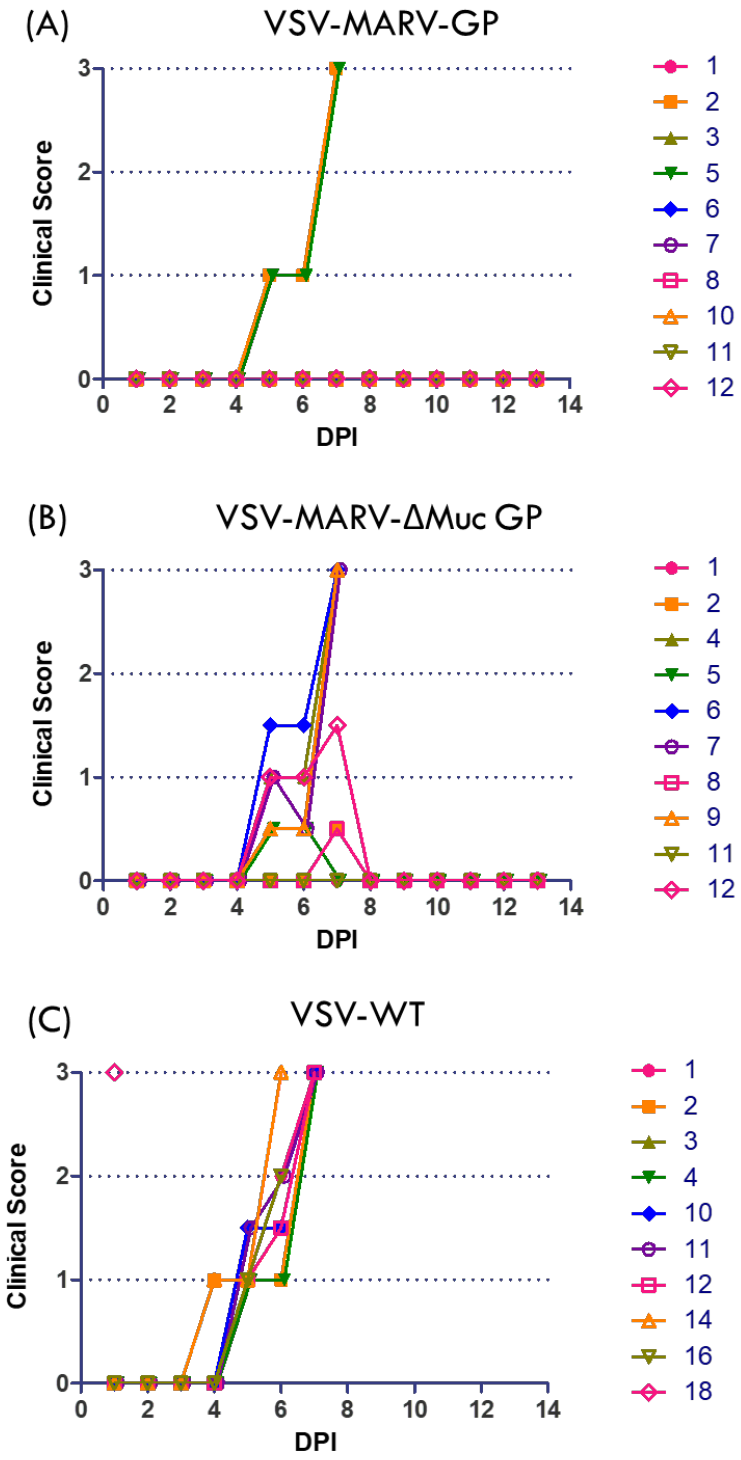

Figure 6. The clinical score for individuals in each group. Clinical score of the mice in (A) VSV-MARV-GP Group, (B) VSV-MARV-ΔMuc GP Group and (C) VSV-MARV-WT group.

The clinical score was related to the weight change, at 5 and 6 dpi, the weight decreases of group 2 were significantly more than the group 1 ($p < 0.05$). Compare with the clinical score, the reason was supported to be all the survived mice in group 1 were healthy without any clinical signs. Nevertheless, most of the animals in ΔMuc groups showed clinical signs. One-way ANOVA was used to compare the statistical difference of clinical score among these three groups. The results showed there are significant differences between the clinical score of group 1 and control group ($p < 0.01$), and between group 2 and control group ($p < 0.05$). No statistical difference was found between group 1 and group 2 ($p = 0.3762$). These results suggested the vaccine efficacy of VSV-MARV-GP is higher than those of VSV-MARV-Δmuc GP.

3.1.2.3 Pre-challenge IgG response

To analyze the antibody response after vaccinations, all the serum collected at 0, 14 and 28 dpv were used to detect the anti-MARV GP IgG titers. The pre-sera were collected at 0 dpi, which were used as a baseline for the IgG response. All the ELISA results of 14 and 28 dpv serum need to subtract the baseline before calculation. The dilution antibody titers shown in Figure 7 was the last dilution that the sample contained an average OD_{650} of more than 0.1.

The control groups did not have anti-MARV GP antibody in serum before challenge (data not shown). At 14 dpv, the anti-MARV GP antibody titer of group 1 mice was quite low (Figure 7A). The IgG was not detected in half of the serum samples. The highest IgG dilution titer was only 1/400. On the other hand, the antibody response in group 2 was much higher at 14 dpv than those in group 1 (Figure 7B). Only three mice did not contain anti-MARV GP antibodies, and high antibody response was detected in five serum samples. Mouse #9 in group 2 showed the highest anti-MARV GP antibody response, which was recognized as a 1/1600 antibody dilution titer in serum.

At 28 dpv, the antibody levels in Group 1 increased considerably compared with the 14 dpv data. Although there were three animals (#14, #15 and #16) contained a low-level antibody response, most of the other mice were observed respectable antibody levels in serum. The highest antibody response was detected as 1/3200 in the #13 mouse. For the Δmuc GP group, the average antibody titers were shown the same tide of Group 1. The mouse #18 showed the strongest antibody response with an antibody dilution titer of 1/3200, and five mice in this group involved

1/1600 antibody dilution titer in serum. However, a decrease in IgG responses was also detected in four mice. Mice #3, #8, #9 and #15 in group 2 showed a higher antibody titer in 14 dpv compared with the data of 28 dpv.

The statistical analysis (unpaired t-test) was performed to compare the antibody response between different groups at the same time point, or between different time points in the same group. In VSV-MARV-GP group, the antibody responses at 28 dpv were significantly higher than the antibody response at 14 dpv ($p < 0.0001$). The antibody titer increase of group 2 was not as much as group 1 although it was statistically significant ($p = 0.005$). At 14 dpv, the antibody titers in serum of Group 2 were significantly higher than the data of Group 1 ($p = 0.0011$). However, at 28 dpv the anti-MARV GP IgG responses in Group 1 mice were slightly higher than those in Group 2 mice although not significantly different ($p = 0.7011$).

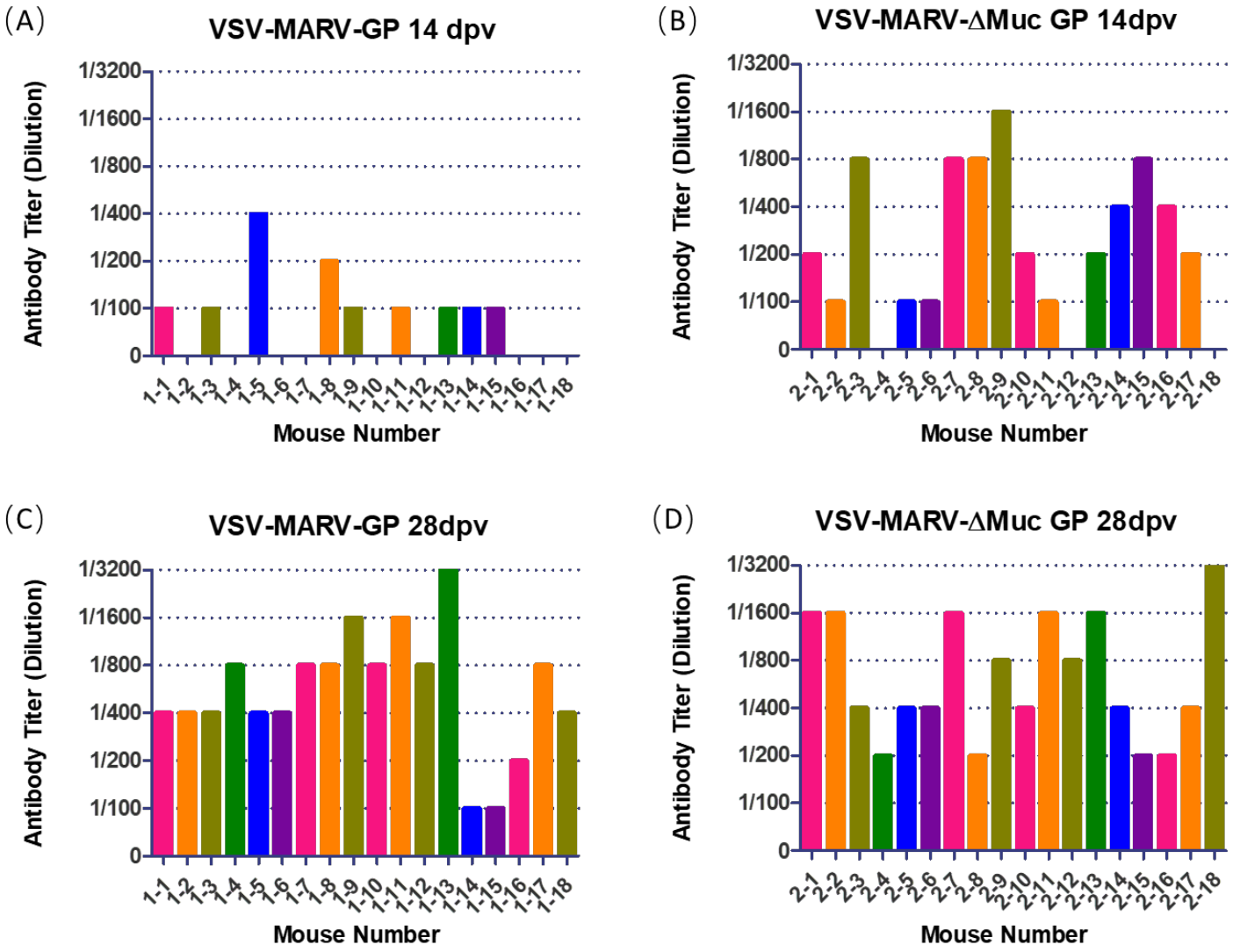

Figure 7. Pre-challenge anti-MARV GP IgG response. 14 and 28 days-post vaccination IgG titer in each group. The antibody titer (Dilution) was the last dilution that the sample contained an average OD650 of more than 0.1. Statistical comparisons between each group were performed using un-paired Student T-test.

3.1.2.4 Pre-challenge neutralizing antibody response

A GFP-based neutralization assay was also performed to analyze the pre-challenge serum. The start concentration of the serum in this experiment was 1/100 dilution. One in four dilutions with plain DMEM was implemented for all serum samples. VSV-MARV-GP GFP was used to infect cells with a ratio of MOI 0.1. The positive antibody control used in the experiments was MR191 (start concentration was 30 μg/ml). The negative antibody control was anti-EBOV GP antibody in supernatant, which did not bind to MARV GP. Mock control was used to measure the background of the experiment without any treatment or infection. The positive control, virus mixed with plain DMEM, was used as the 100% infection baseline. The data were fitted to a non-linear four-parameter variable slope logistic regression. Only the serum collected at 28 dpv were tested, as most of the serum at 14 dpv did not contain anti-MARV GP antibodies.

The infection percentages (100% - neutralization percentage) of serum from VSV-MARV-GP and VSV-MARV-ΔMuc GP groups mice were shown in Figure 8. The positive antibody control group showed a gradient with the dilution of antibodies, which suggested the method of the experiment worked. The negative antibody control group showed about 20% neutralization at the middle dilution point, which indicated that the observational error was up to 20%. No neutralization more than 20% were detected for all samples.

These results suggested both vaccines cannot induce the production of neutralizing antibody after a single dose vaccination. Because of the limited anti-MARV GP antibody titer in serum, it was not surprising that the neutralization cannot be detectable. Furthermore, based on the results showed previously in the survival study, the antibody titer in serum at the challenge day is not related to the survival rate.

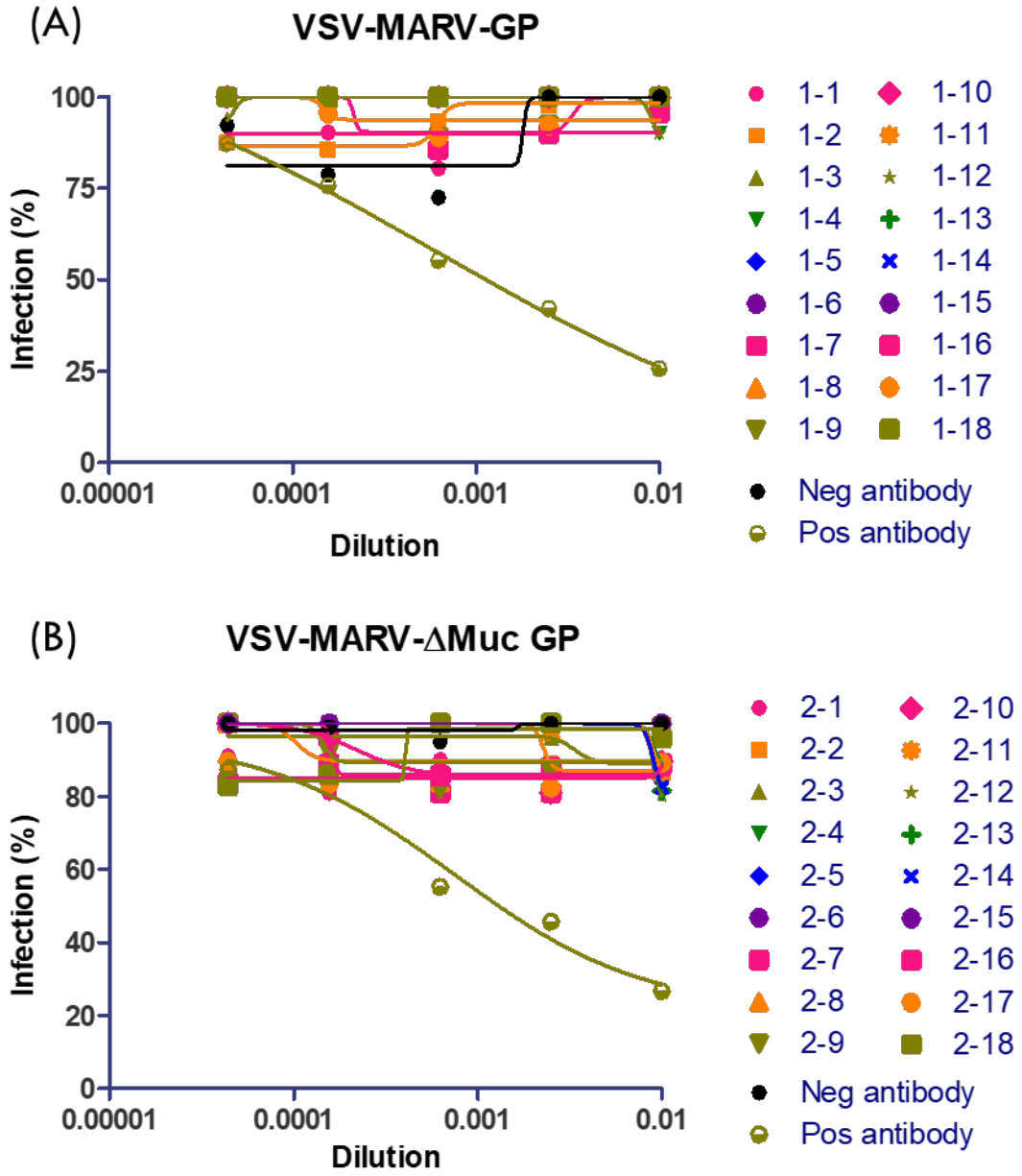

Figure 8. Neutralization of pre-challenge serum. The neutralizing antibody titer in the serum of (A) VSV-MARV-GP group and (B) VSV-MARV-ΔMuc GP Group.

3.1.2.5 Endpoint IgG response

Euthanasia of all survivors was performed at the endpoint (28 dpi) of the experiments. Serum was collected to detect the anti-MARV GP antibody titers and the neutralization levels. The method of ELISA was used to detect the antibody titer. The baseline of each serum samples was the 0 dpv serum. The dilution antibody titer shown in Figure 9 was the last dilution where the sample contained an average OD_{650} more than 0.1.

The results showed all the survivors involved a high antibody level in serum, the antibody dilution titer was as high as 1/102400. The lowest one (2-12) still contain a 1/6400 dilution titer IgG in serum. The statistic assay of unpaired student t-test was used to compare the differences between the antibody titer of two vaccine groups survivals. The results showed the average antibody titer in group 1 was mildly higher than the group 2 ($p = 0.6659$). These results suggested the antibody responses of viral exposure survivors from two vaccine groups were similar.

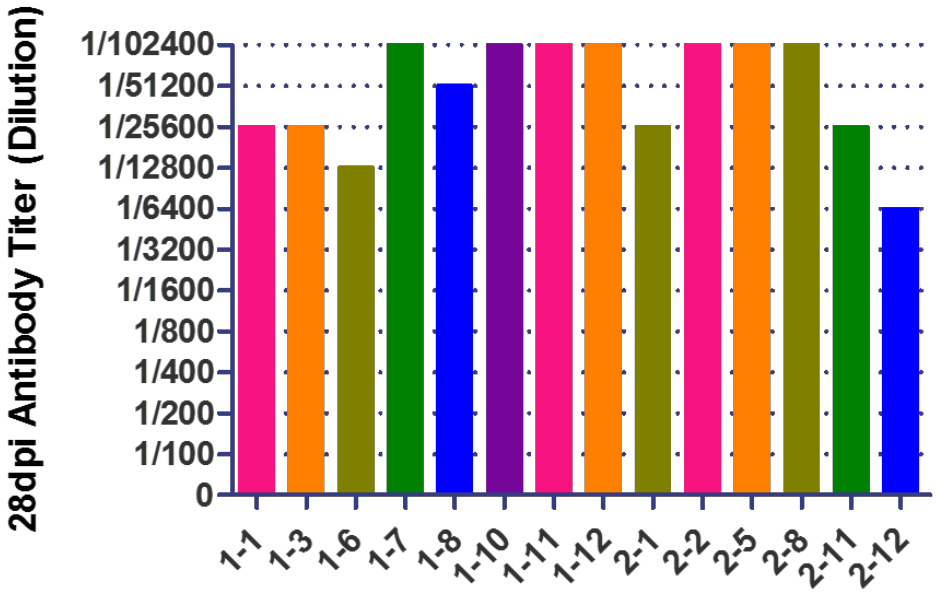

Figure 9. Endpoint anti-MARV GP IgG response. The mouse number was marked as "group number-mouse number". Group 1 is VSV-MARV-GP, group 2 is VSV-MARV-ΔMuc GP.

3.1.2.6 Endpoint serum neutralization

The endpoint sera were also used to do the neutralization assay to evaluate the relation of neutralization levels and survival rate. Because all the animals were euthanized at 28 dpi, the volumes of serum were enough to do a low dilution in the experiments. The first dilution in this experiment was 0.1, then one in three dilutions with DMEM was performed. MOI 0.1 VSV-MARV-GP GFP was used to mix with diluted serum or control solutions. After 1 h of incubation, the mixture was then used to infect the prepared cells. Plain DMEM was used as mock control at the plate to detect the background of the method. The positive control was marked as the baseline of infection. The non-linear logistic regression (four parameters) was used to draw the infection curve.

Results showed the positive mAbs control (green) and negative mAbs control (black) worked well in this experiment (Figure 10). There was one sample (1-7) showed up to 50% neutralization when the dilution was 0.1. Based on the logistic regression of 1-7 serum neutralization, the original undiluted serum should contain a ~70% neutralization. A similar logistic regression was also found for the 1-1 serum sample, but the neutralization percentage was around 30% at the dilution point 0.1. All other animals only involved limited neutralization level in serum.

These results supported that neutralizing antibodies were not essential for BALB/c mice to survive from MARV infection. All mice developed a high level of anti-MARV GP antibodies in serum, but only two animals generated limited neutralization in serum. The detected neutralization level in serum was also quite low, which suggested the neutralizing antibodies titer was low or these antibodies incorporated poor neutralization.

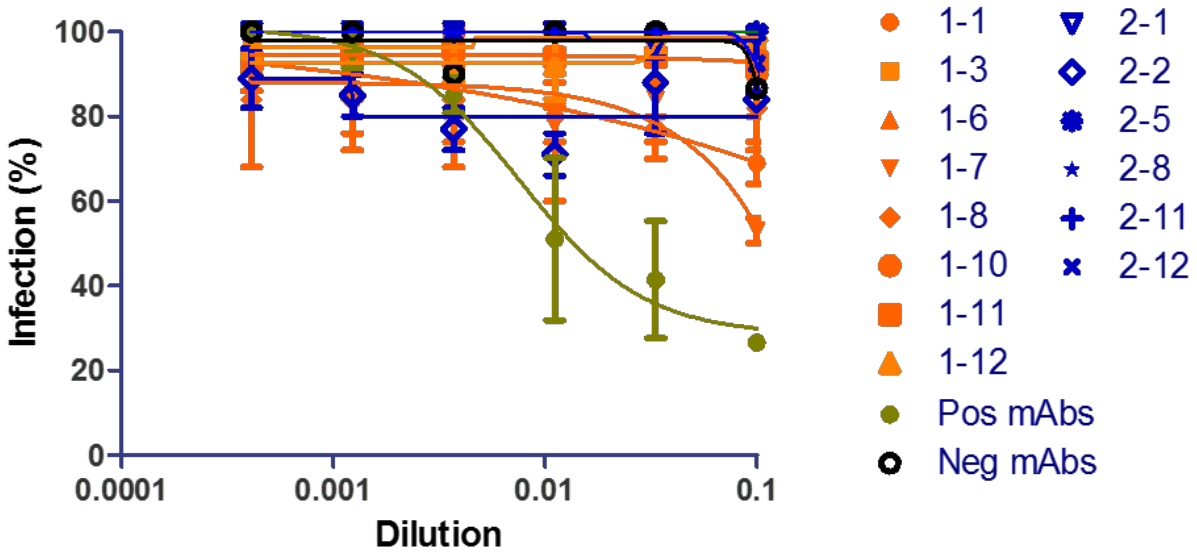

Figure 10. Neutralizing antibody level in endpoint serum. VSV-MARV-GP was marked with the color of yellow, VSV-MARV-ΔMuc GP was marked by blue, the Pos mAbs was in green and the Neg mAbs was in the color of black.

3.1.3 Viral RNA levels

To determine the systemic spread of MARV in the vaccinated mice, four animals were randomly selected to euthanize from each group at 4 and 6 dpi. Blood, liver, spleen, kidney, and lung were collected to analyze the viral RNA replication. The time point 4 days post infection was chosen because it is normally the earliest day of the clinical signs observed in BALB/c mice MA-MARV exposure experiments. The time point 6 dpi was chosen due to the fatal day of MA-MARV infection in BALB/c mice was 7 dpi.

RT qPCR was used to calculate the Quantification of viral genome equivalents (GEQ) concentration. The GEQ estimated from this method was the total copy number in the reaction mixture, which need to be calculated back to the original blood or tissues samples. The calculation for blood was: GEQ/ml = (GEQ/4 * 60)/140 * 1000. The calculation for tissues was: GEQ/gram = (GEQ/4 * 50)/30 * 1000. These calculations were based on the protocols of the viral RNA extraction kit. The numbers of group and animals followed the previous survival study. The baseline of the method was marked as around 1000 GEQ/ml or 4000 GEQ/gram, which was the Ct value 36 from the RT qPCR analysis. All the results lower than the baseline were marked as 1000 in the graph, because of the limited sensitivity. The statistic assay followed the method of one-way ANOVA test with Bonferroni's multiple-comparison correction.

3.1.3.1 Viral RNA levels at four days post infection

The viral RNA replications at 4 dpi were shown in Figure 11. The four animals in the control group contained the highest viral copy numbers in viremia among the three groups. The highest one reached 7 x 10^7 GEQ/ml. Two animals in group 1 were not detected any viral replication in blood, the other two mice in this group showed a middle level of viral copy number. Compare with the control group, the viral RNA replications in the blood of Group 1 mice were significantly lower ($p<0.05$). As for group 2, there are three mice detected a middle viral GEQ in blood, and one with a low RNA replication around 5 x 10^3 GEQ/ml. The average of viral copy number in group 2 was mildly higher than group 1 but not significant. And the differences between the control group and group 2 was also not significant.

Viral RNA replication for tissues were also described in Figure 11. The control group showed a high level of viral RNA replications in liver, which reached more than 1 x 10^7 GEQ/gram. The

average of group 1 viral GEQ was much lower than the control group, but one of the results shown the same level as group 3. Two mice in group 1 contained middle level of viral RNA replication and the last one did not show a positive result. As for group 2, the average of the GEQ was between group 1 and group 3. All viral RNA replications of group 2 were between 1 x 10^7 and 5 x 10^4 GEQ/gram. There was no statistical difference among each group.

Surprisingly, the viral copy numbers in spleen were similar among the three groups (Figure 11). There were two animals in group 1 that were not detected viral RNA in blood, but viral RNA was found in spleen. All the mice in group 3 contained around 4 x 10^6 GEQ/gram viral RNA, which was five times more than group 2. Although the average GEQ of group 1 in spleen was lowest among the three groups, there was a mouse contained a high level of viral RNA in spleen. No significant difference ($p < 0.05$) was found among the spleen viral load of three groups.

Kidney samples had lower viral RNA levels compared to other organ and blood. All kidney samples from VSV-WT group loaded a middle level of viral RNA replication (~ 5 x 10^5 GEQ/gram). The GEQ of all the mice in group 2 were around 8 x 10^4 GEQ/gram. The results of group 1 showed a polarization, which was similar to other organ data. The highest result was around 1 x 10^6 GEQ/gram, but the lowest one was undetectable. Again, there was no significant difference among each group, although the group 2 shown ten times lower GEQ than the vector control group.

Lung was also collected to analyze the viral RNA levels. The viral RNA replication level of the lung samples in control group was similar to the spleen results. However, the viral RNA levels of lung in both group 1 and 2 were extremely different from the results of spleen. In group 1, two animals showed the same viral RNA level with the control group, but the other two mice did not contain any viral RNA. Similar results were found in group 2 as well, the only difference was one animal involved an average level of viral RNA. Although the average of viral GEQ of each vaccination group was 100 times lower than the control group, the range of the data expression was too big to reach a statistical difference.

These results suggested both vaccines could provide partial protection to help host reduced or even cleared the virus in blood and tissues at 4 dpi. However, the decreased efficiency depended

on the individual difference. In general, the protection of VSV-MARV-GP was mildly higher than those of VSV-MARV-ΔMuc GP at 4 dpi.

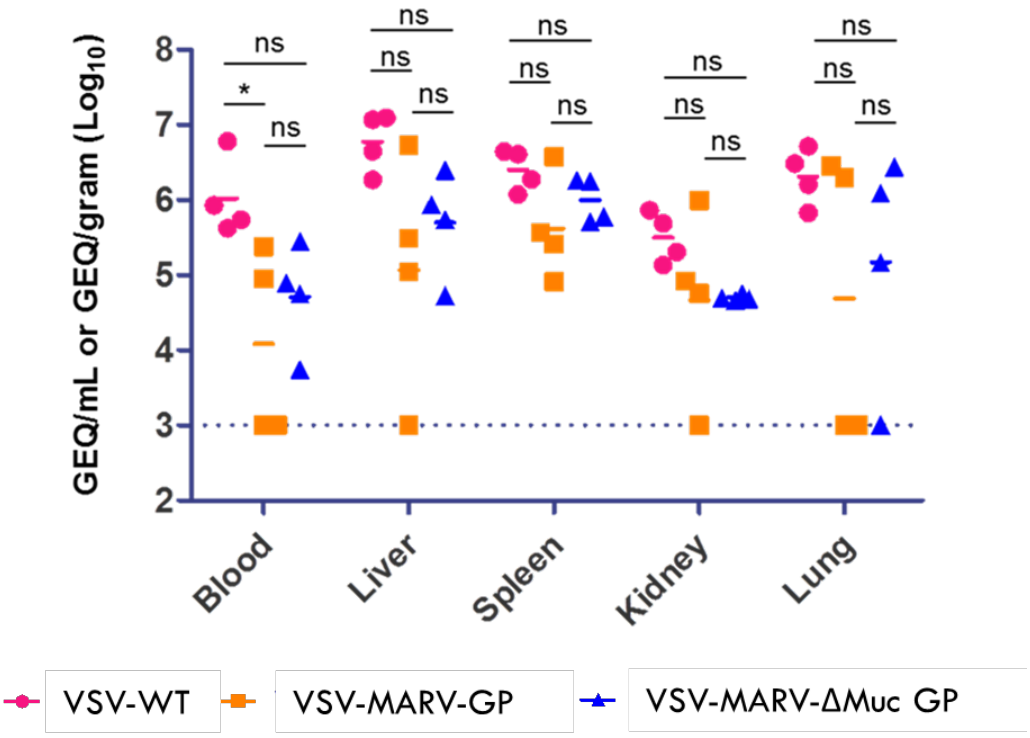

Figure 11. Viral RNA level at four days post infection. The VSV-MARV-GP group was marked as group 1 with the color of yellow; the VSV-MARV-ΔMuc GP group was group 2 in the color of blue; group 3 was VSV-WT group with pink. Statistical comparisons between each group were performed using one-way ANOVA test with Bonferroni's multiple-comparison correction: *, $p < 0.05$; **, $p < 0.01$; ***, $p < 0.001$.

3.1.3.2 Weight change, IgG response and clinical score of euthanized mice at 4dpi

To analyze the health state of the euthanized mice at 4 dpi, weight change and clinical score were monitored. The weight change data were shown in Figure 12A. All the mice in VSV-MARV-GP group did not lose weight until 4 dpi. On the other hand, the weight of all the mice in the control group decreased. Mouse 3-2 lost around 7% weight compared with the challenge day. Most mice in group 2 gained weight until 4 dpi, but mouse 2-15 lost 5% weight from 3 dpi to 4 dpi. For each group, the tides of weight change were similar to the survival study results.

The clinical score results were described in Figure 12C. All the animals in group 1 did not show any clinical signs, which related to the results of weight change. The mouse 2-15 in group 2 was observed to have some mild clinical signs at 4 dpi and all other three mice in the same group did not appear to have any clinical signs. Abnormally, two mice in the control group did not appear to have clinical signs, but the other two did.

To analyze the antibody response, ELISA was performed to detect the IgG titer in the serum of euthanized mice. The IgG levels from pre-vaccination until euthanasia were exhibited at Figure 12B. Generally, a decrease of the antibody titer in 4 dpi was observed at almost all animals in the vaccinated groups, except for 1-17 that showed a continuous increase at 4 dpi. The anti-MARV GP antibody was undetectable in the control group from the beginning to 4 dpi. Surprisingly, most of the animals only contained a limited or undetectable antibody titer in serum at 4 dpi.

Comparing the weight change, IgG response and clinical score to the viral RNA replication level in each mouse, antibody-undetectable mice (1-15, 2-15, all mice in control group) shown a higher viral RNA level in blood and most of the organs. All these mice were observed a higher weight loss compared with the other mice. Furthermore, the mouse with the highest anti-MARV-GP antibodies (1-17) was observed an increased weight until 4 dpi, undetectable RNA level in blood and most organs, and no clinical sign. These results suggested antibodies might play an important role in vaccine protection. And a possible reason for the reduction of antibody titer is all the antibodies were preoccupied with binding to the virus, as the viral titers in blood and tissues were extremely high.

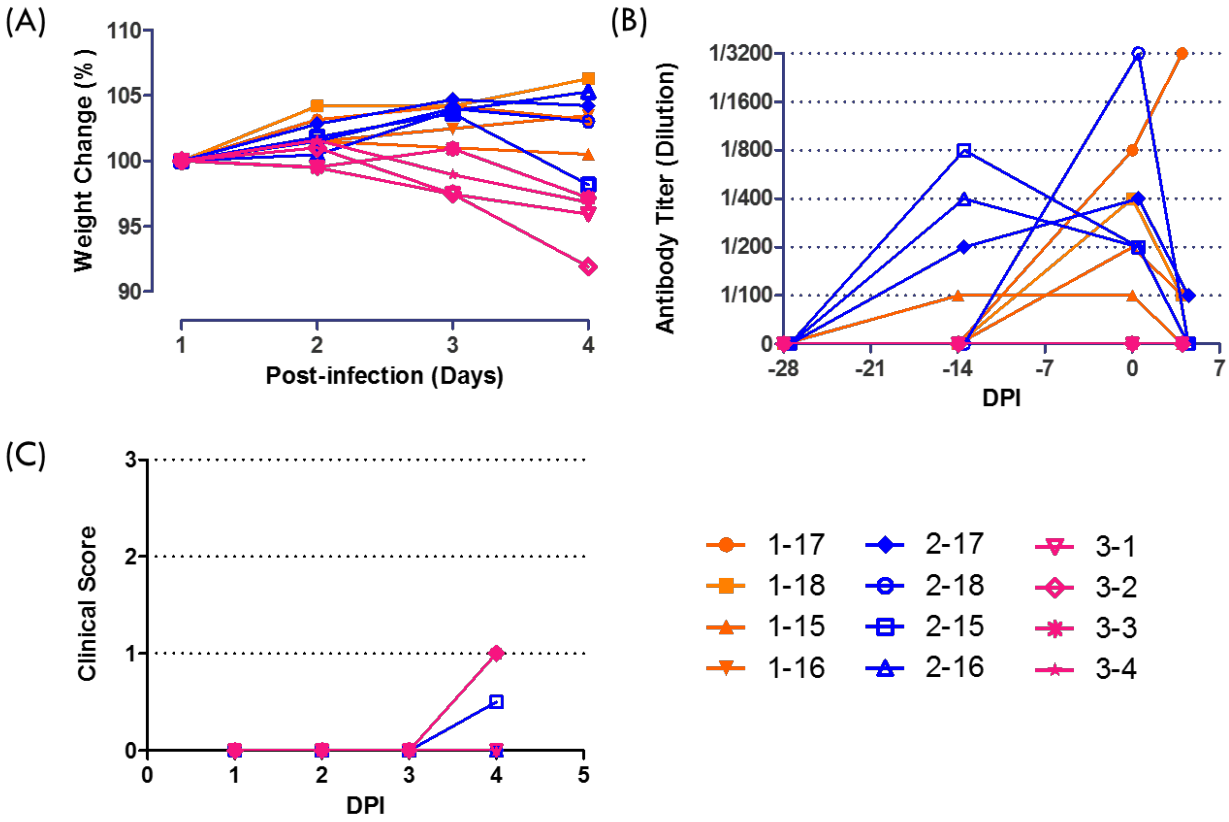

Figure 12. Weight change, IgG response and clinical score of euthanized mice at 4 dpi. The VSV-MARV-GP group was marked as group 1 with the color of yellow; the VSV-MARV-ΔMuc GP group was group 2 in the color of blue; group 3 was VSV-WT group with pink. The mouse number was marked as "group number-mouse number".

3.1.3.3 Viral RNA levels at six days post infection

The viral RNA replications at 6 dpi were shown in Figure 13. There are two animals that failed to retrieve collected blood (2-13, 3-8); the blood and serum data were missed for two mice. Two animals in each vaccine group did not contain viral RNA in all blood and tissues samples (1-4, 1-9, 2-13 and 2-14). Control group showed a middle level of viral RNA in blood, which was around 2 x 10^5 GEQ/ml. The viral copy number in blood was reduced compared with the 4 dpi results. Two mice samples from group 1 detected a low level of viral RNA, one was 5 x 10^4 GEQ/ml another one was around 5 x 10^3 GEQ/ml. As for group 2, the only detectable blood sample showed a viral titer of 2 x 10^4 GEQ/ml. The viral load in the blood of VSV-MARV-GP group was significantly lower than the control group ($p < 0.05$) but did not show a statistical difference with group 2. On the other hand, the VSV-MARV-ΔMuc GP group showed a significant difference compared with the control group as well ($p < 0.01$).

Extremely high viral copy number in liver were observed in the control group, which reached up to 9 x 10^7 GEQ/gram. The average viral load level of the control was around 4 x 10^7 GEQ/gram. As for group 1, one mouse contained a middle level of viral GEQ and another was only a limited result. The group 2 results were astonishing that high level (up to 2 x 10^7 GEQ/gram) of viral RNA replication in two mice. These results shown both two mice without blood samples all contained high viral RNA genomes in the liver. Compare with the VSV-WT group, both vaccine groups liver results showed significantly lower results ($p < 0.05$). However, although the average of group 2 viral RNA level was almost 100 times higher than group 1, there is still no statistical difference between the two vaccination groups.

In spleen, the VSV-WT still showed a high level of viral RNA level, which was around 5 x 10^6 GEQ/gram. Only a limited MARV viral RNA level was found in group 1, which showed a significant difference compared with the control group ($p < 0.01$). As for the VSV-MARV-ΔMuc GP group, high level of viral titers was detected in one of the mice (3 x 10^6 GEQ/gram), and another viral RNA detectable sample shown an average level of viral titer (2 x 10^4 GEQ/gram). No statistical difference was found between two vaccine groups, but the average viral GEQ of VSV-MARV-GP group was more than 10 times lower than VSV-MARV-ΔMuc GP group.

The viral RNA level in kidney was lower than the other three organs, which was similar to the 4 dpi results. A middle level of viral RNA replication was analyzed in the control group, which was around 1 x 10^5 GEQ/gram. Two animals in the VSV-MARV-GP group detected a low-level of viral RNA number, both of them were lower than 1 x 10^4 GEQ/gram. The two kidney samples from group 2 show a similar GEQ with the control group. No significant difference was found among the three groups, even though the group 1 viral GEQ was quite lower than the control group.

The last organ was lung, the viral RNA level of the control group was around 5 x 10^6 GEQ/gram. As for group 1, the viral RNA levels of the two animals were quite different. The higher one was around 1 x 10^5 GEQ/gram, and another one was around 50 times lower than it. The average viral RNA replications of group 2 were much higher than group 1, but more than 100 times lower than the control group. Two animals in this group contained around 2 x 10^6 GEQ/ml viral load in the lung, which was as high as control groups. The viral copy number of VSV-MARV-GP group was significantly lower than the control group ($p < 0.05$) but had no statistical difference compared with VSV-MARV-ΔMuc GP group. As for the difference between the control group and VSV-MARV-ΔMuc GP group, it was insignificant as well.

These results suggested VSV-MARV-GP vaccine could efficiently prevent the infectious mouse from viral infections in blood and tissues. Compare with the control group, the viral replications in blood and tissues were inhibited. As for VSV-MARV-ΔMuc GP vaccine, it could provide partial protection against MA-MARV infections depended on individuals.

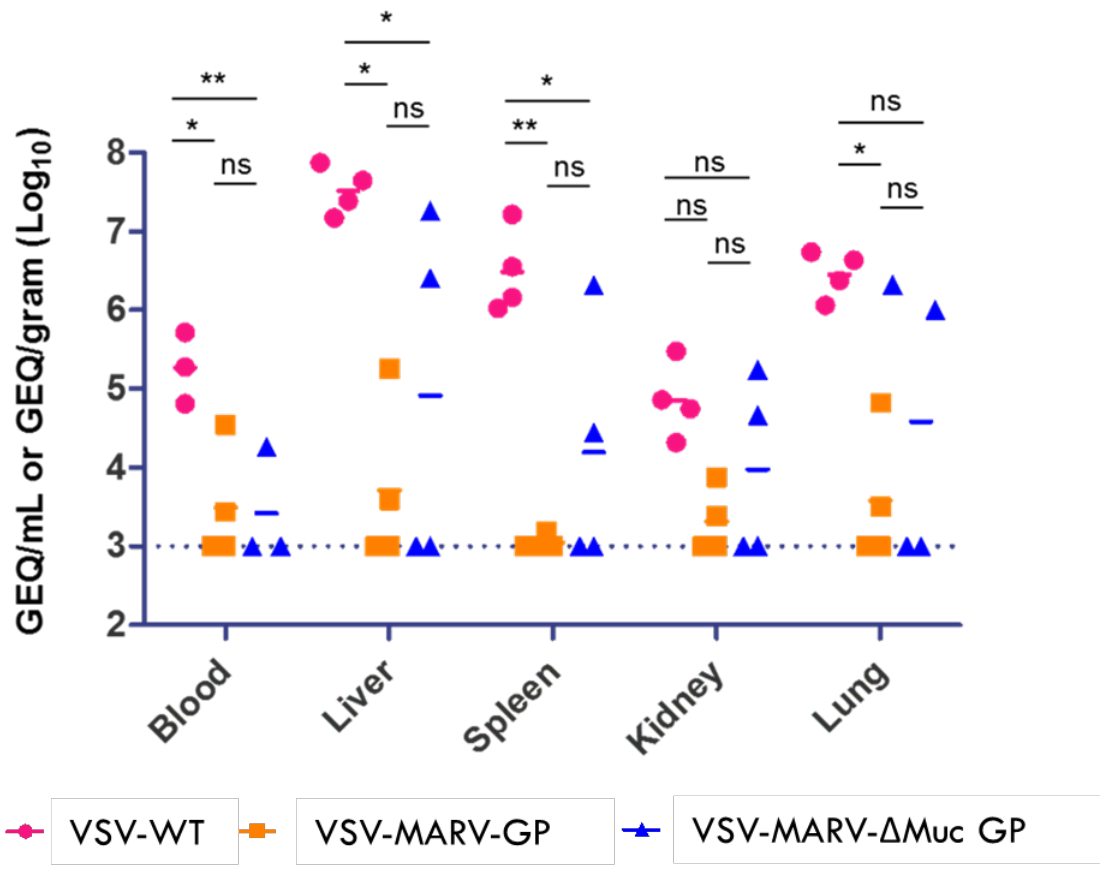

Figure 13. Viral RNA level at six days post infection. The VSV-MARV-GP group was marked as group 1 with the color of yellow; the VSV-MARV-ΔMuc GP group was group 2 in the color of blue; group 3 was VSV-WT group with pink. Statistical comparisons between each group were performed using one-way ANOVA test with Bonferroni's multiple-comparison correction: *, $p < 0.05$; **, $p < 0.01$; ***, $p < 0.001$.

3.1.3.4 Weight change, IgG response and clinical score of euthanized mice at 6 dpi

Weight change, clinical score, and antibody response were also analyzed to describe the state of the euthanized mice. The weight change data were shown in Figure 14A. All the 18 mice did not lose weight before 3 dpi. From 3 dpi to 6 dpi, all the mice in the control group show an around 10% weight loss. Three mice in group 1 observed a mild decrease after 4 dpi on weight, but there was no weight loss compared to the pre-challenge at 6 dpi. Only one animal (1-13) in group 1 showed weight loss on the euthanasia day, which continually lost weight from 4 dpi to 6 dpi. As for group 2, all mice had observed a weight reduction between 3 dpi and 5 dpi. Two animals noted an up to 10% increase at 6 dpi, on the other hand, the other two continually lost weight at 6 dpi.

The clinical score results were related to weight change (Figure 14C). During the first three days after infections, there were no clinical signs observed. At 4 dpi, although several animals showed weight loss, only animal 2-3 in group 2 was monitored some mild clinical signs. At 5 dpi, a mild level or more serious level of syndromes were detected in all the mice in group 2 and the control group. On the other hand, all the mice in group 1 still kept healthy. However, only two animals in group 1 (1-9, 1-4) did not show any clinical sign at 6 dpi, and two mice in group 2 recovered at 6 dpi (2-3, 2-14).

The IgG response in serum was described at Figure14B. As mentioned precious, two animals failed to collect blood (2-13, 3-8), so only 3 points were included for group 2 and group 3 at 6 dpi. There was no detectable anti-MARV GP antibody in the mice of the control groups. All the mice in group 1 shown a continued growth of anti-MARV GP antibody titer from the -28 dpi to 6 dpi. Based on the data shown at 4 dpi-euthanized mice, there should be a decrease at 4 dpi but there are no serum or data available for these 6 dpi-euthanized mice. On the other hand, one mice (2-3) in group 2 shown a mild decrease of antibody titer in serum at challenge day. The IgG level of the other mice in group 2 shown increase or no change. At 6 dpi, two animals had detected a continuing increase of IgG level (2-14, 2-3), but the antibody titer of 2-10 did not change.

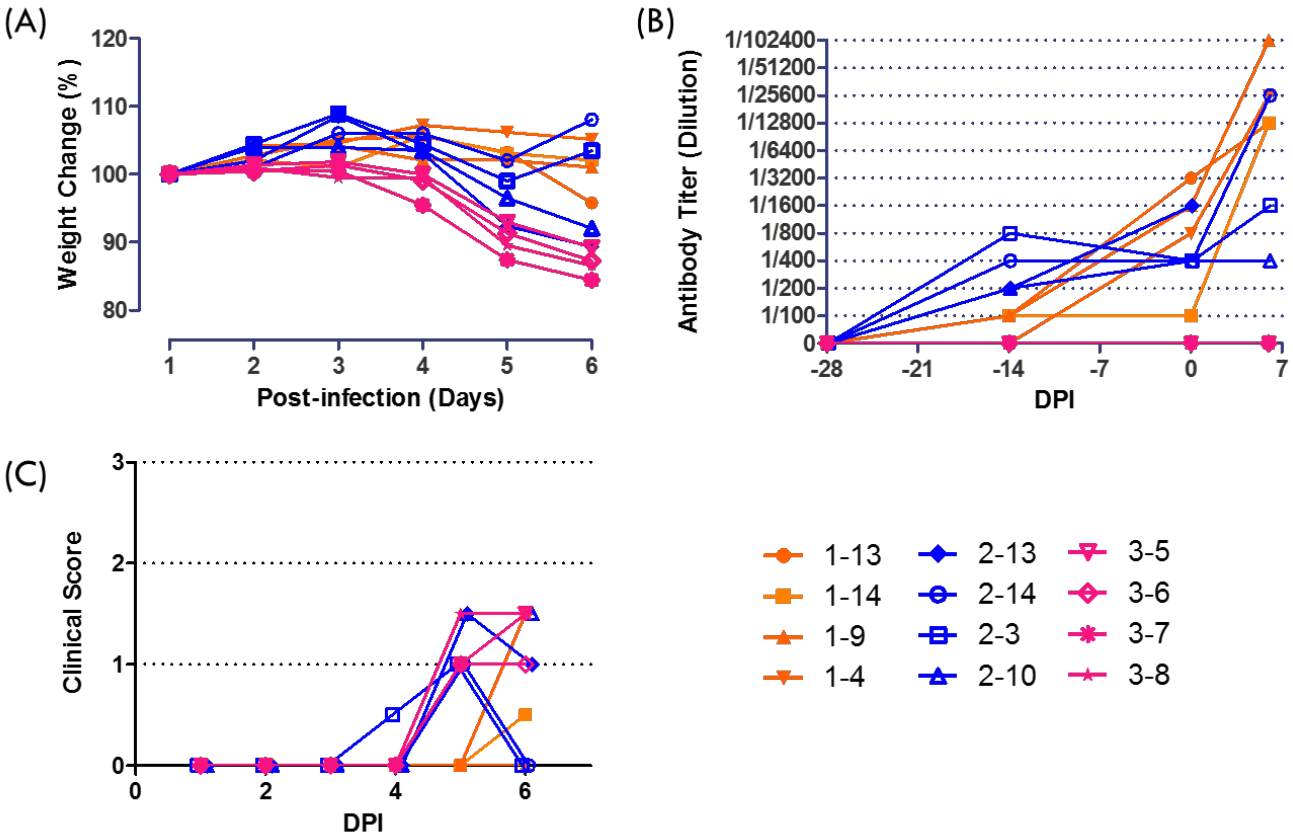

Figure 14. Weight change, IgG response and clinical score of euthanized mice at 6 dpi. The VSV-MARV-GP group was marked as group 1 with the color of yellow; the VSV-MARV-ΔMuc GP group was group 2 in the color of blue; group 3 was VSV-WT group with pink. The mouse number was marked as "group number-mouse number".

These data indicated a high relation among the antibody titer, weight change, and clinical score. Most animals contained high antibody response were observed a lower clinical score and weight loss. This tide was more obvious in VSV-MARV-ΔMuc GP. Although there was one mouse in Group 1 (1-13) did not follow this trend. Furthermore, compared to the others, lower GEQ in blood and tissues were measured in most of the animals involved a high level of anti-MARV GP antibody in serum.

3.1.3.5 Serum neutralization of euthanized mice at 6 dpi

To analyze the neutralization level of serum in 6 dpi mice, a GFP-based neutralization assay was performed to test all the serum samples from euthanized mice. The first dilution of the serum was 1/10 as the serum volume was enough. The ratio of MOI 0.1 VSV-MARV-GP GFP were used to infect Vero-E6 cells. Four control groups were used in the experiment: 1. A mock control used non-infection without any treatment on the cells; 2. Positive control used viruses mixed with plain media to infect cells; 3, Positive mAbs control with MR191 antibodies started the dilution titer at 50 μg/ml; 4. Negative mAbs control was supernatant of anti-EBOV GP antibodies. All the samples were diluted with the ratio of 1:3 with DMEM plain media. Infection percentage curves were made based on the method of non-linear logistic regression with four parameters in GraphPad Software.

The results were shown in Figure 15, both the positive control and the negative control worked well. Only three animals contained a detectable neutralization at the beginning dilution point: the serum sample from mouse 1-4 reached 50% neutralization, mouse 2-14 and mouse 1-9 were detected a 40% neutralization. All other mice were detected a limited level of neutralization even though the dilution was low.

These results suggested the neutralizing antibody in serum was not the main protection against MARV infection, as the neutralizing antibody titer was quite limited in serum. However, all the three mice shown limited neutralization in serum did not observed clinical signs or viral RNA replication at 6 dpi. Although these results were more related to the antibody titers but not the neutralization titer, the limited neutralization was supported to assist the protection against MARV infections. There was one mouse (1-13) contained a very high level of anti-MARV GP antibody, but a clinical score of 1.5 and weight loss were monitored at 6 dpi.

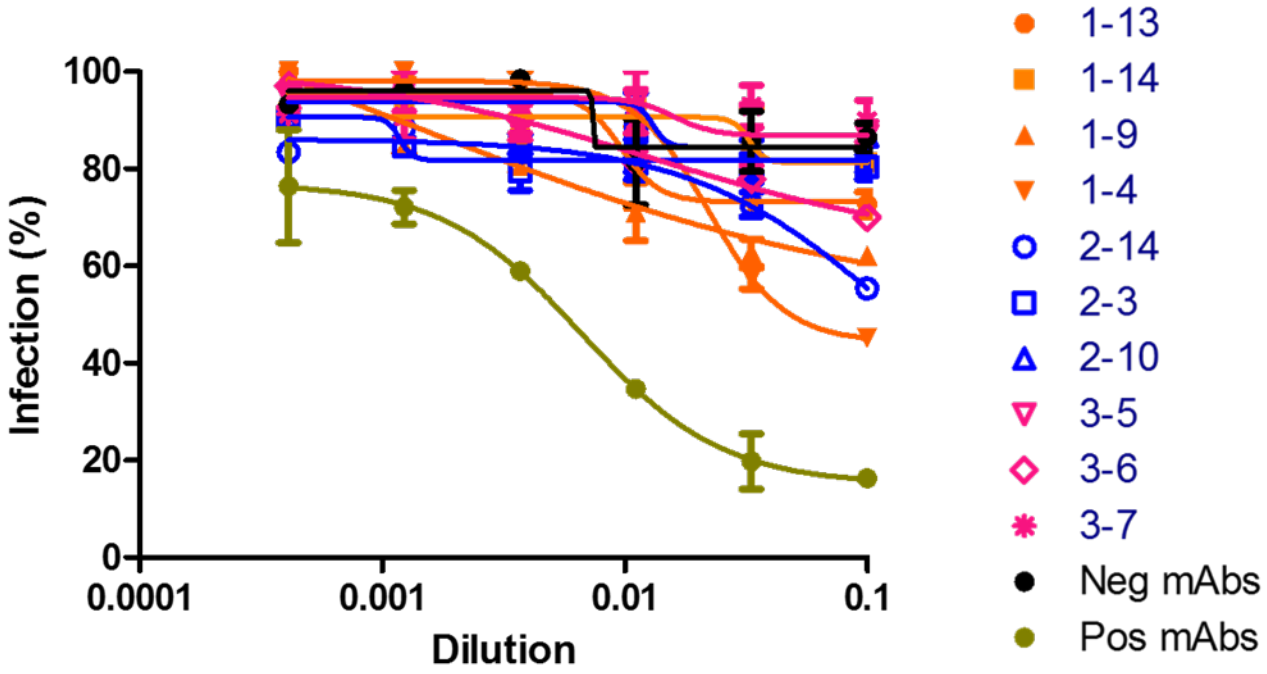

Figure 15. Neutralizing antibody in serum at 6 dpi. The VSV-MARV-GP group was marked as group 1 with the color of yellow; the VSV-MARV-ΔMuc GP group was group 2 in the color of blue; group 3 was VSV-WT group with pink; the Pos mAbs was in green and the Neg mAbs was in the color of black. The mouse number was marked as "group number-mouse number".

3.2 Development of monoclonal antibodies

3.2.1 Immunization of BALB/c mice

To develop mAbs against MARV, BALB/c mice were immunized with VSV-MARV-GP and VSV-MARV-ΔMuc GP every three weeks until the IgG response was high enough. In this study, three fusions were performed for each vaccine.

3.2.1.1 The first hybridoma development

Eight mice per group were used to develop mAbs. The vaccination schedule was shown in Figure 16A. On the vaccination day, around 2 x 10^5 pfu (100 μl) vaccine were injected by i.p., For each serum collection point, 10~30 μl of sera of each mouse were collected to detect the IgG response. Three weeks after the fourth vaccination, the IgG titer in serum was analyzed to choose two mice in each group to do the final boost. The 100 μg of purified MARV GP was injected once the mice with the highest IgG response were selected. Three to five days after the final boost, the spleens were collected to the next step.

Figure 16B showed the results of the IgG response of mice in the VSV-MARV-GP group. All the sera were diluted with 2% Skim Milk in the ratio of 1:400. The OB_{650} was used to measure the IgG level. Week 1 was the results of pre-vaccination serum, which were also used as the baseline of the serum IgG detection. Most of the mice contained a continued increase of IgG titer from week 1 to week 13. Five out of eight mice in this group showed a high antibody response in serum, but another three animals only contained a middle level of IgG response. At week 13, Mouse #1 and #4 were selected to boost with purified GP.

The IgG responses of VSV-MARV-ΔMuc GP were described in Figure 16C. Same with another group, the week 1 pre-serum was measured as a baseline. The antibody response of all the mice increased from beginning to the end. Among these mice, mouse #1 was detected an extreme high IgG response, which was much higher than any other mice. At the 13 weeks, mouse #1 and #5 were chosen for the final boost.

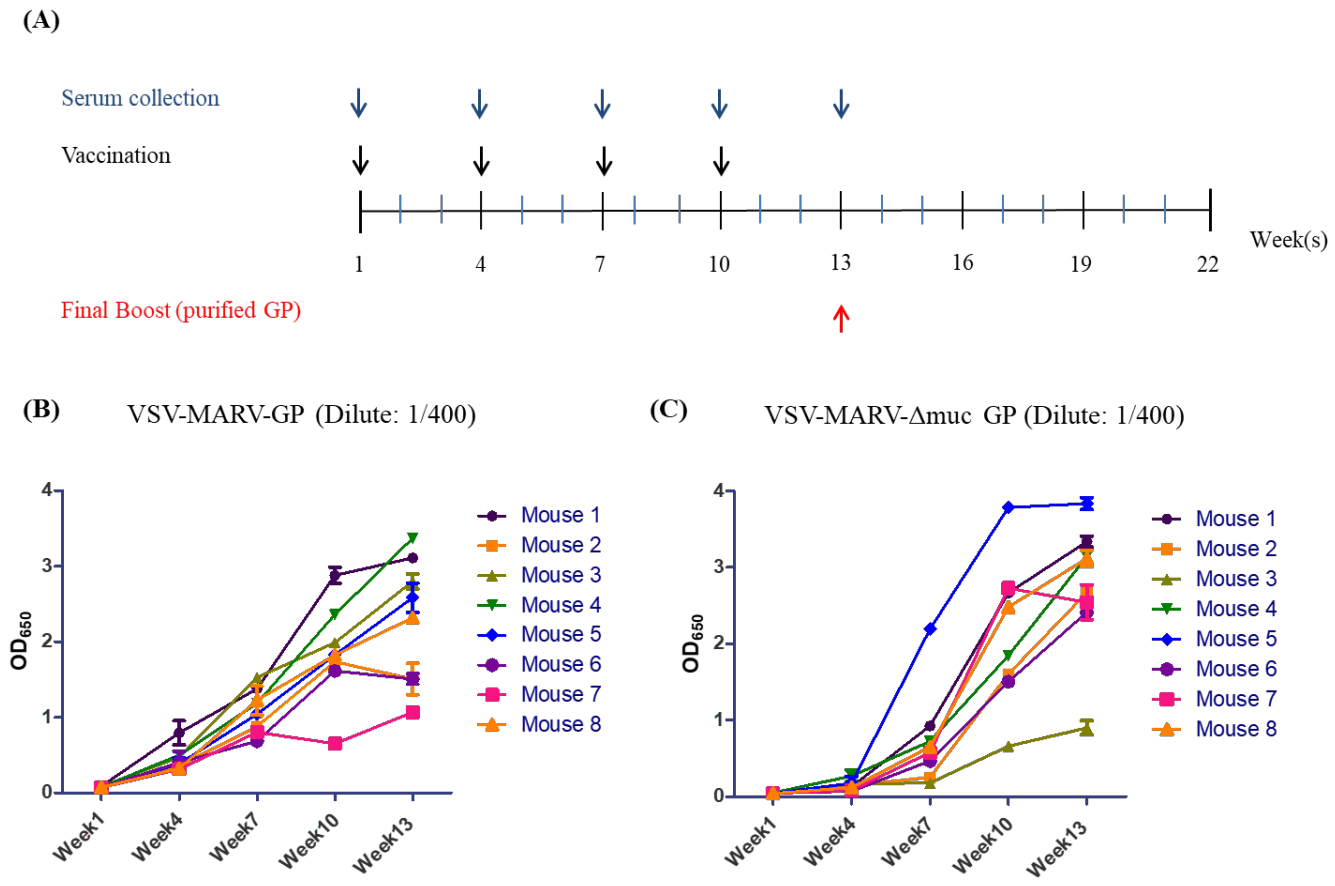

Figure 16. Timeline and IgG responds of first hybridoma developments. (A) The time schedule of the vaccination, serum collection and Final boost. The Anti-MARV GP IgG response in serum of each mouse in (B) VSV-MARV-GP group and (C) VSV-MARV-ΔMuc GP group.

3.2.1.2 The second hybridoma development

After the first hybridoma development, the over left mice were used to prepare the second hybridoma development. The left 6 mice in each group were vaccinated two more times. The vaccination and serum collection timeline was shown in Figure 17A. All the sera were collected before vaccination. Based on the antibody response, two animals in each group were selected to do the final boost at 25 weeks.

The IgG titer of the VSV-MARV-GP group was shown in Figure 17B. After 9 weeks of the last vaccination, the IgG response of four out of six mice showed a drop, but the other two contained a mild increase. At week 25, mouse #2 and #6 were selected to boost with purified MARV GP and then collected the spleen.

Figure 17C described the IgG titer of VSV-MARV-ΔMuc GP group. All the mice in this group detected a lower IgG response compared with the Week 13 data. After 2 more times of vaccinations, All the animals contained a higher level of antibody response. At week 25, two mice that contained the highest IgG responses were selected to do the final boost.

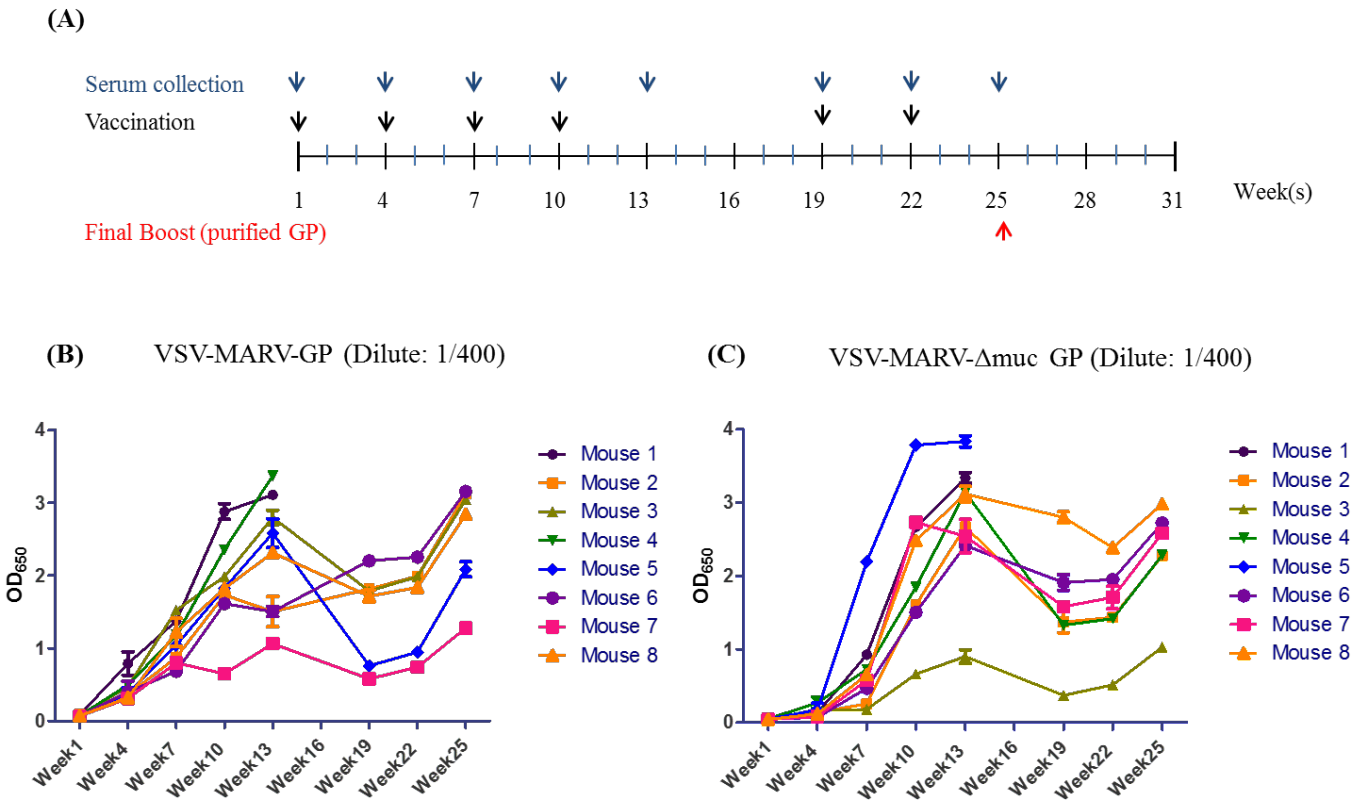

Figure 17. Timeline and IgG responds of second hybridoma development. (A) The time schedule of the vaccination, serum collection and Final boost. The Anti-MARV GP IgG response in serum of each mouse in (B) VSV-MARV-GP group and (C) VSV-MARV-ΔMuc GP group.

3.2.1.3 The third hybridoma development

Five mice were used in each group at the third mAbs development experiment. The immunization schedule was shown in Figure 18A. Similar to the previous two times, about 2 x 10^5 pfu VSV-MARV-GP or VSV-MARV-ΔMuc GP vaccines were injected by i.p.. Serum was collected before vaccinations. Because there were two mice in VSV-MARV-ΔMuc GP group that showed a high level of anti-MARV GP antibody titers, the final boost was performed after three immunizations for these two mice. As for the VSV-MARV-GP group, one more vaccination was given before the final boost.

The IgG response of VSV-MARV-GP group was shown in Figure 18B. Surprisingly, no detectable anti-MARV GP antibody was found in sera at week 4. After the second vaccination was given, the IgG response was increasing quickly until week 13. The IgG titer of Mouse #9 and #13 was high enough to do the final boost with 100 μg purified MARV GP Ang.

Figure 18C described IgG responses in the serum of the VSV-MARV-ΔMuc GP group at different time points. Similar to the VSV-MARV-GP group, no animals detected anti-MARV GP antibody in serum at week 4. However, two mice (#11 and #12) were observed a rapid increase after week 7. The antibody OD number of 1/400 diluted samples reached around three. Furthermore, high dilution sera from these two mice still resulted in a high OD value (data not showed). In this case, the final boost of VSV-MARV-ΔMuc GP group was performed after three vaccinations at week 10.

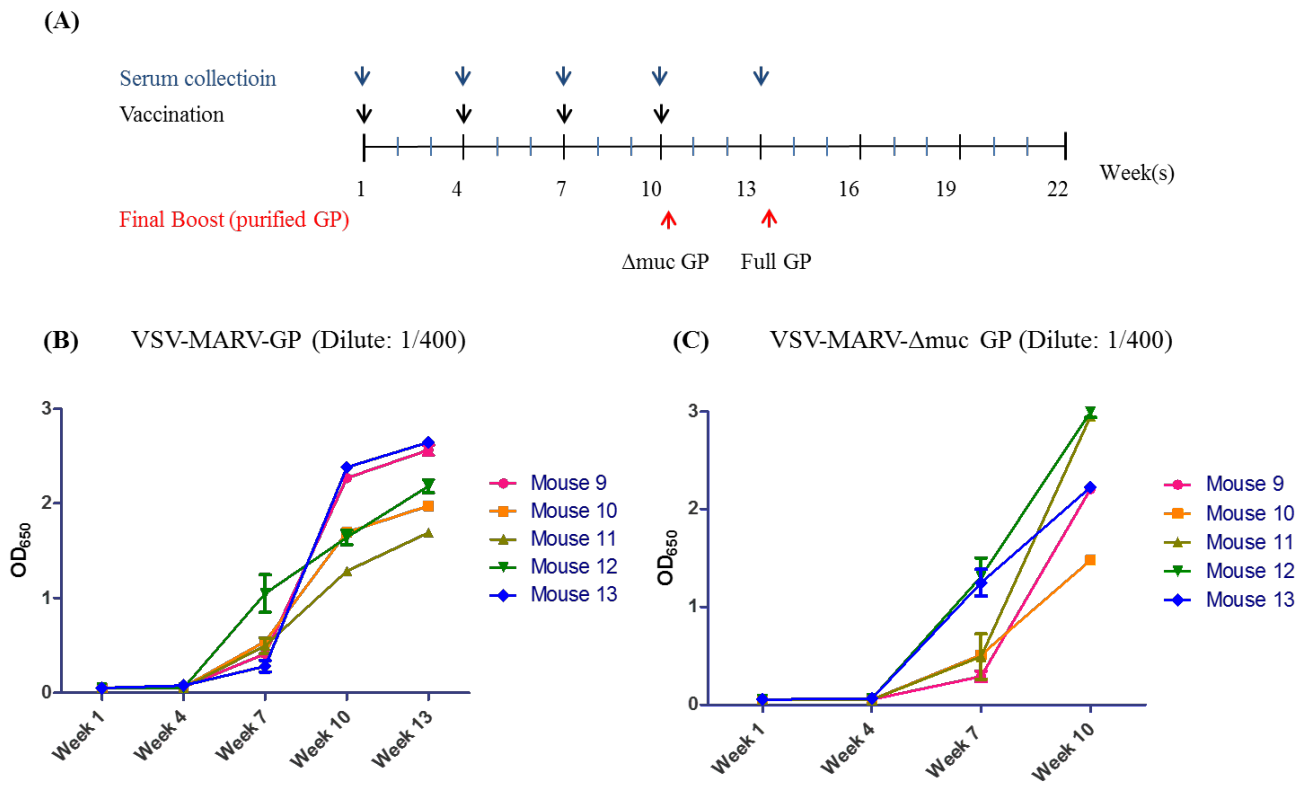

Figure 18. Timeline and IgG responds of third hybridoma development. (A) The time schedule of the vaccination, serum collection and Final boost. The Anti-MARV GP IgG response in serum of each mouse in (B) VSV-MARV-GP group and (C) VSV-MARV-ΔMuc GP group.

3.2.2 Development of hybridoma

To develop the monoclonal antibodies binding to MARV GP, hybridoma technology was used in this study. Following the methods described at 2.4.2 Monoclonal antibodies (mAbs) generation, three fusions for each vaccine groups were performed. The P3X were thawed two weeks in advance to confirm enough myeloma cells were adapted to Medium A. The antibody-forming cells were collected from the spleens of mice mentioned previously. Two spleens from the same group were used together to collect splenocytes.

Following the method mentioned at 2.4.2.3, the viability and number of both cell lines were measured. Figure 19 showed the viability of the myeloma cells and splenocytes for each fusion. Most of the cell viabilities were higher than 90%, only the splenocytes 1D showed an 85% viability. The highest cell activity was detected at splenocytes 2F, which reached almost 100%. A possible reason for the lower viability percentage of splenocytes 1D was the longer operation time of these cells collection. It was suggested that the collection of spleen cells should be done within 30 minutes after spleen collected. These viability results supported all the cells were ready for fusions.

Medium D was used to select and clone the fusion cells. The single fusion cell grew to a cell colony in the semi-solid selection media after 10-14 days growth. The colonies were picked carefully and then transferred to growth media for further experiments. For each fusion, 500-1000 colonies were picked.

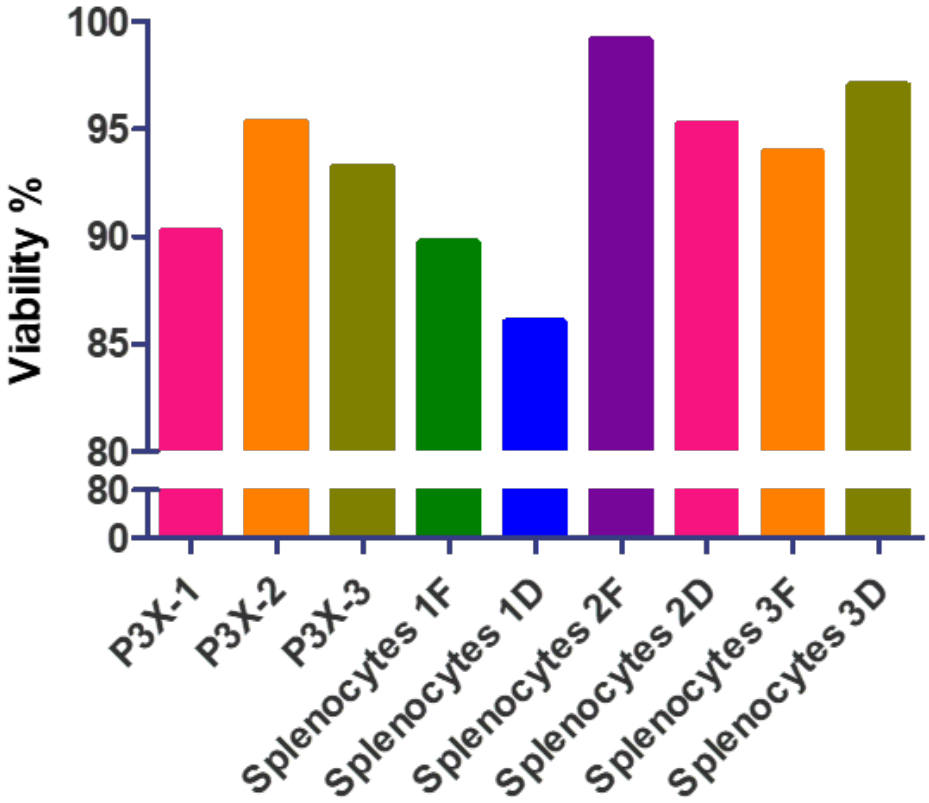

Figure 19. The viability of myeloma cells and splenocytes for each fusion. The number of times for each fusion were marked as 1, 2 or 3. For example, the myeloma cell used in first-time fusion was marked as P3X-1. The VSV-MARV-GP group was marked "F" (Full-length GP), the VSV-MARV-ΔMuc GP group was marked as "D" (Mucin deleted GP).

3.2.3 Characterization of mAbs-produced hybridoma

The method of ELISA was used to detect the anti-MARV GP antibody level in the supernatant of the hybridoma. There were two factors showed influence at OD value, which were the antibody titer and antibody binding strength. In this case, the hybridoma supernatant contained an OD_{650} value of more than 1.0 was selected as a good candidate for the further experiment. The value was lower than 1.0 when the antibodies in supernatant contained a low binding efficiency or the hybridoma could not produce a high titer of IgG in cell culture.

Following these rules, fifty in total hybridoma candidates were selected after (Table 4 and Table 5). The hybridoma candidates were named with the way of "group information - the times of hybridoma development, plate number of hybridoma screen – the well location". F2-1H10, for example, meant this hybridoma candidate was from VSV-MARV-GP group of the second time hybridoma development, the colony of this hybridoma grown in the H10 well of the first 96-well plate.

Table 4. Hybridoma generated from VSV-MARV-GP group

Name	OD_{650}	Neutralization	Name	OD_{650}	Neutralization
F2-1H10	3.2435	Negative	F2-5H7	2.4358	Negative
F2-1H11	3.0151	Negative	F2-5H10	1.6423	Negative
F2-1H12	2.8987	Negative	F3-1H1	2.0815	Negative
F2-2C9	2.9709	Negative	F3-1H3	2.8943	Negative
F2-2H3	3.29	Negative	F3-2H4	2.7783	Negative
F2-2H5	2.9812	Negative	F3-2H5	2.892	Negative
F2-2H6	3.3322	Negative	F3-3A8	1.3388	Negative

F2-3G10	2.0135	Negative	F3-4B3	1.1363	Negative
F2-3G12	1.4525	Negative	F3-4C1	1.2746	Negative
F2-3H11	2.5453	Negative	F3-4B12	1.0642	Negative
F2-4H11	2.4462	Negative	F3-6C5	2.6076	Negative
F2-5F2	1.7005	Negative			

Surprisingly, more than 2,000 colonies were picked in the first hybridoma development experiment from two groups, but none of them produced any anti-MARV GP antibodies. To confirm if the fusion of myeloma cells and splenocytes was successful, an ELISA experiment was performed. 30 μl supernatant of each hybridoma were used to coat plate, and the goat-anti-mouse HRP antibody was used as primary antibody after block. No secondary antibody was added, but TMB was used after the primary antibody. The plates were read after 30min RT incubation, and no positive signals were observed. These results suggested the hybridoma did not produce any mouse antibodies, which indicated the fusion of hybridoma and P3X cells failed. All the colonies were actually the colony of myeloma cells. It was unknown why the selection medium D did not work during the 14-days incubation.

Table 5. Hybridoma generated from VSV-MARV-ΔMuc GP group

Name	OD_{650}	Neutralization	Name	OD_{650}	Neutralization
D2-1H9	3.1778	Negative	D2-6H12	2.5718	Negative
D2-1H10	2.9199	Negative	D2-2H4	3.0359	Negative
D2-1H11	2.9066	Negative	D3-1E5	2.5769	Negative

D2-1H12	3.3327	Negative	D3-1H12	0.9654	Negative
D2-2H1	3.2534	Negative	D3-2G6	2.7784	Negative
D2-2H2	2.8641	Negative	D3-3A2	1.5226	Negative
D2-2H3	2.9205	Negative	D3-3G10	2.2776	Negative
D2-2H4	3.2848	Negative	D3-4C2	2.3822	Negative
D2-3H7	3.3195	Negative	D3-4C5	1.2181	Negative
D2-3H11	2.5965	Negative	D3-4H4	1.2003	Negative
D2-4H11	2.483	Negative	D3-4C8	1.4671	Negative
D2-5C1	1.5792	Negative	D3-5H3	2.8511	Negative
D2-5C8	2.4042	Negative	D3-5H11	2.6559	Negative
D2-5H12	2.8924	Negative			

After the selection of hybridoma candidates, a GFP-based neutralization assay was performed to detect the neutralizing antibody titer. Follow the method described at 2.3.3 GFP-based neutralization assay, all the supernatant samples were detected. However, none of the supernatant showed more than 20% neutralization (Figure 4 & Figure 5).

3.2.4 Neutralization in serum

The sera from spleen-collected mice detected the neutralization by using the method of GFP-based neutralization assay. As the animals were euthanized to collect spleens, the volume of serum was abundant. In this case, the start point of the serum dilution was 1/10. The ratio of MOI 0.1 VSV-MARV-GP GFP and Vero-E6 cells were used for this experiment. In Figure 20, VSV-MARV-GP group was marked as group 1 with the color of yellow, VSV-MARV-ΔMuc GP group was marked as group 2 with the color of blue.

Both positive mAbs and negative mAbs worked well in this experiment. The results showed all the serum only contain a limited or no neutralization. Only the serum from mouse #2-1 demonstrates neutralization around 22%, but the negative mAbs results suggested the baseline of the sensitivity was about 20%.

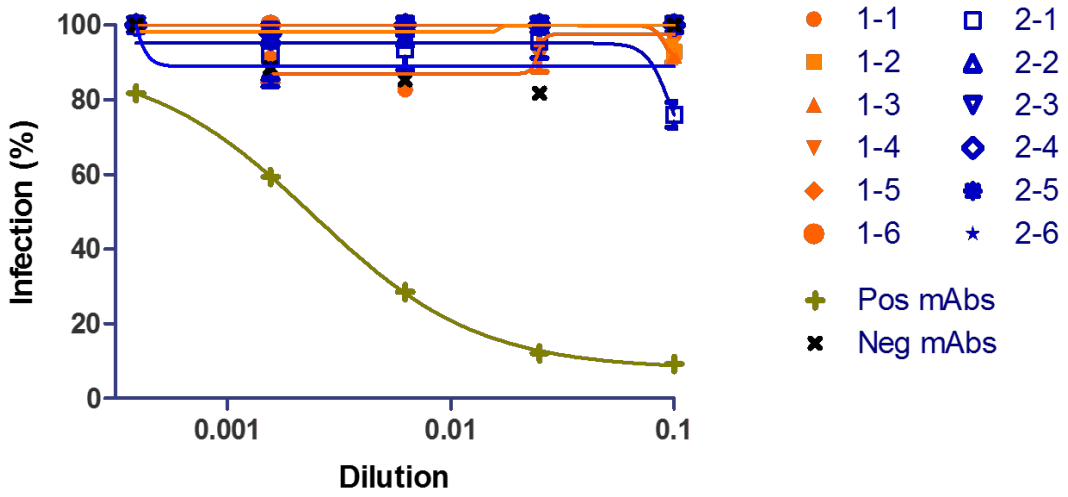

Figure 20. Neutralization of the serum from spleen-collected mice. The VSV-MARV-GP group was marked as group 1 with the color of yellow; the VSV-MARV-ΔMuc GP group was group 2 in the color of blue; the Pos mAbs was in green and the Neg mAbs was in the color of black. The mouse number was marked as "group number-mouse number".

CHAPTER: 4 DISCUSSION

4.1 Growth kinetics of VSV-based viruses

The hypothesis of this study was that A vaccine expressing the mucin-like domain deleted GP (ΔMucGP) of Marburg virus will yield more and better neutralizing mAbs than a vaccine expressing the full GP. In order to compare the difference between the two VSV vectored vaccines these viruses were characterized for viral replication determined. To evaluate the differences in viral growth, the growth kinetics of VSV-MARV-GP and VSV-MARV-ΔMuc GP were evaluated and compared to a VSV-MARV-GP GFP virus which was used in a GFP-based neutralization assay.

The results of the two vaccines showed no significant difference in growth over the duration of the experiment. This suggested these two vaccines had similar replication. The same dose of the two vaccines could be used in the *in vivo* vaccination assessment. On the other hand, the growth curve of VSV-MARV-GP GFP showed a decrease in the TCID50/ml at 72 hours after infection. A slight increase in titer was observed between the 48 and 72 h time points. Based on these results, the GFP-based neutralization assay data collection time point was set at 48 h. It is also possible to collect the data at 72 h, but the neutralization occurs only for the very first round of infection, after that the virus grows normally and can reach high levels despite some initial neutralization.

4.2 Mucin-like domain functions

4.2.1 Removing the MLD did not influence the infection efficiency in an *in vitro* assay

The growth kinetics of VSV-MARV-GP and VSV-MARV-ΔMuc GP also indicated that the MLD did not impact infection efficiency as no significant differences were seen. However, the biggest disadvantage of *in vitro* experiments was that it cannot simulate fully replicate the impact of the immune system. The domain might play some roles in the immune evasion to assist the infection by the viral particles.

To detect the functions of the MLD in the viral life cycle, further *in vivo* experiments about the viral infection efficiency were necessary.

4.2.2 Removing the MLD induced an earlier IgG response

The results of the IgG responses following vaccination showed the antibody titers in the serum of VSV-MARV-ΔMuc GP (Group 2) vaccinated mice were significantly higher than the VSV-MARV-GP (Group 1) vaccinated mice at 14 dpv. At 28 dpv; antibody titers of mice between the vaccines were not statically different. These results suggest the humoral response caused by VSV-MARV-ΔMuc GP appeared earlier than the antibody response produced by VSV-MARV-GP. At 28 dpv, the antibody response of Group 2 mice may have already been at the stage of decline. However, the antibody titers of Group 1 were probably around the peak.

These results suggest that removing the MLD could improve primary antibody responses. A possible function of the MLD is that it inhibits the recognition of MARV GP by the humoral immune response. Because the size of the MLD is even bigger than the sum of GP1 (without the MLD) and GP2, the antigen recognition efficiency of B cells might be impacted.

However, to confirm the MLD functions, further experiments are required. For example, the difference of T cell responses and B cell responses between the VSV-MARV-GP and VSV-MARV-ΔMuc GP groups could be useful.

4.2.3 Removing the MLD reduced the vaccine protection

In the survival study, both the average percent weight loss and the survival rate of the VSV-MARV-ΔMuc GP group were non-significantly lower than those of the VSV-MARV-GP group. The clinical score also provides some circumstantial evidence about the difference in vaccine efficacy between the two vaccines. None of the survivors in the VSV-MARV-GP group had any clinical signs after infection, but four out of six surviving mice in the VSV-MARV-ΔMuc GP group showed clinical signs between 4 dpi to 8 dpi.

A possible reason for the lower protection efficacy of the VSV-MARV-ΔMuc GP group is the exposure of useless epitopes. Although removing this domain could expose more epitopes on the MARV GP, the antibodies that bind to these epitopes could not reach them during the MARV infection due to the shield of the MLD. The immunological memory will be active after the viral antigen is recognized, but the production of these antibodies will take some resources of the immune system. In other words, this reaction will reduce the generation of high binding anti-

MARV GP antibodies. Because the MLD and glycan cap will be removed in the endosome during the fusion of viral membrane and endosomal membrane, the epitopes under the protection of the MLD could be recognized as well.

Another possibility for the lower protection from the VSV-MARV-ΔMuc GP vaccine is the different immune state compared with the VSV-MARV-GP group. As mentioned previously, the humoral response of the ΔMuc GP group was earlier than the full-length group. At the challenge day, the immune response against the VSV-MARV-ΔMuc GP may have already been at the end stage, which required more time to reactivate. On the other hand, the antibody response against the VSV-MARV- GP was probably at the earlier stage before the peak of antibody titre.

To analyze the influence of the MLD on vaccine protection, a short-term vaccine protection experiment would be required. Vaccination of the animals at different time points would allow us to check the vaccine protection at different immune response stages.

4.2.4 The MLD is not the key to neutralizing antibody generation

In the vaccine evaluation study, although a limited neutralization was detected at 6 dpi and endpoint samples, there was no significant difference between the two vaccines. In the 6 dpi serum samples, the full-length GP vaccine even contained a higher neutralization than the mucin-deleted group. Furthermore, the results of the development of monoclonal antibodies showed no neutralizing antibodies were generated after three fusions. All the serum from spleen-collected mice did not show strong neutralization level, even though the antibody titer of each mouse was extremely high on the day of euthanasia. These results suggest the MLD is not the key to generating anti-MARV neutralizing antibodies.

Some studies about the EBOV MLD suggest a VLP vaccine made using the mucin-deleted GP produced more anti-EBOV GP antibodies in the serum than VLPs made using the full GP ones (Basler et al., 2011). A structural study also showed that the different positions of the MLDs of MARV and EBOV might lead to different functions (Hashiguchi et al., 2015). A lot of EBOV neutralizing antibodies bind to the base part of the GP, but this position of MARV is protected by the MLD. These studies supported the hypothesis that the MLD could be the reason for the failed generation of MARV neutralizing antibodies through vaccination. However, the results of this study suggest this is not the case.

4.3 Non-neutralizing IgG functions

All the antibodies elicited prior to challenge and following challenge only showed a limited level of neutralization. The dead animals in the survival study all had an antibody response similar to the survivors at 28 dpv, which suggested the protection of the vaccines might not depend on the antibody level at the challenge day.

However, one of the animals euthanized at 4 dpi in VSV-MARV-GP group showed a high level of anti-MARV GP antibodies, and no viral replications was found in the blood, liver, kidneys, and lungs. It suggested the antibody in the serum at challenge day was not high enough to induce protection in mice. The antibody titer from other mice decreased to an undetectable level at 4 dpi but jumped to an extremely high level just 2 days later, although the 4 dpi data and 6 dpi data were from different animals. A possible reason is the speed of antibody production was lower than the viral replications by 4 dpi. Because the viral loads were too high, all the antibodies produced by vaccination were bound to the virus. Then, the immunological memory could lead to the B cells proliferation and antibody production 5~7 days after the antigen re-exposure. In this case, the antibody titer showed dramatic increases at 6 dpi. Furthermore, the animals that showed high IgG at 6 dpi also had lower viremia and viral loads in tissues, lower weight loss and lower clinical score compared to the other mice, despite the fact there was only limited or no neutralizing antibody activity. This suggests that although the antibody titer at challenge day was not related to the survival, the antibodies in the serum might play an important role after infection.

Based on the studies on MARV and EBOV therapies, there is no doubt that neutralizing antibodies were a good treatment candidate. Post-exposure treatment suggested the neutralizing antibodies could clear the virus from blood efficiently. However, there is still a knowledge gap about non-neutralizing antibody functions. A publication by Froude reported several protective mAbs against MARV without neutralization (Froude et al., 2017). These antibodies showed some efficacy in the plaque size reduction assay and up to 100% protection in mouse post-exposure experiment against MA-MARV. In this case, some studies suggested some other antibody function, such as ADCC, complement-mediated toxicity (CMT) and ADCP, might also play some roles in mediated protection.

On the other hand, since macrophages are the early targets of MARV, ADCP might increase the viral infection efficiency. The Fc chain of the antibody will attract macrophages close to the infected cells. In this case, once the new viral particles are released, these macrophages will be infected. The antibody function of antibody-dependent enhancement (ADE) was also reported in some studies, which suggests a low or non-neutralizing antibody might enhance viral infections in some situations.

4.4 Neutralizing antibody generation

Neutralizing antibodies were detectable in some MA-MARV infected mice, which suggest that neutralizing antibodies against MARV could be developed from survived mice. Furthermore, there are reports showing some NHP survivors have a low level of neutralizing antibodies after MARV exposure (Mire et al., 2014). However, the immune responses against MARV infection were quite different between mice and NHPs. The results of this study showed only a limited neutralization activity in the serum of some mice. It suggests the mouse model, at least the BALB/c mouse model, develops a different immune response against MA-MARV infection compared with NHPs. A clinical trial suggested the human survivors have a Th1-dependent immune response with a low level of neutralizing IgG responses.

It is still unknown why anti-MARV neutralizing mAbs cannot be generated through vaccination, but the same method could develop anti-EBOV neutralizing mAbs. Recent publications suggested MARV VP35 may play an important role in the viral evasion (Hume & Mühlberger, 2018). The evasion pathway of MARV VP35 is different from EBOV VP35. This difference between MARV and EBOV might be the reason for the failure of anti-MARV neutralizing antibody generation. The pressure to the immune system may play some roles in the neutralizing antibody production. The neutralizing antibody titer in serum will be detectable after the challenge with real MARV, even though the neutralization titer was quite limited. And some other studies about VLP vaccines suggested that a VLP vaccine expressing MARV GP, VP40 and NP cannot lead to the generation of neutralizing antibodies (Warfield & Aman, 2011). In this case, a VSV based vaccine expressing both MARV GP on the surface and VP35 inside the viral particle might work in developing neutralizing antibodies.

Another possible way to generate neutralizing antibodies is developing neutralizing antibodies after MARV exposure. As mentioned previously, a limited neutralizing antibody titer could be detected in babl/c mice after MA-MARV challenge. Some studies suggested a higher neutralizing antibody titer was observed in NHPs after MARV exposure.

The hybridoma technology is hard to use due to the spleen being a target of MARV as well. The fusion could be performed after the viruses were totally cleared. But some studies suggested the EBOV and MARV viral RNA could be silent in the cells of survivors. It may cause MARV re-infecting during the hybridoma growth, although the B cells are not the targets of MARV. Another problem is the limited neutralizing antibody titer, which is linked to the limited number of neutralizing antibodies produced from splenocytes.

A possible method to develop neutralizing antibody is to build up an antibody library from the NHPs that have neutralizing antibodies. B cells will finish the differentiation in the spleen and then transfer to the bone marrow to produce antibodies. But the heavy chain and light chain genes of antibodies were already generated in B cells after the differentiation. Furthermore, the memory B cells are also located at bone marrow. In this case, collecting bone marrow of NHPs with neutralizing antibodies could collect most of the heavy chains and light chains genes in this animal. In theory, the neutralizing antibody heavy chain and light chain genes should be present. However, the problem of this method is that it is impossible to collect all the bone marrow, even though most of the antibody sequence could be collected.

CHAPTER: 5 CONCLUSIONS

VSV-based vaccines expressing MARV-GP and MARV-ΔMuc GP were used to try to generate neutralizing antibodies against MARV. The evaluation of two vaccines was performed to compare the vaccine efficacy. The virus growth kinetics showed there was no significant difference between the infection and replication of the two vaccines. It suggested the mucin-like domain in live MARV vaccines did not influence the infection efficiency *in vitro* assay. However, the results of pre-challenge IgG response detection suggested removing the mucin-like domain could significantly increase the primary IgG response in BALB/c mice.

The survival study indicated both vaccines could protect MA-MARV infected mice, but the VSV-MARV-GP vaccine provided 20% higher protection than VSV-MARV-ΔMuc GP vaccine. A lower clinical score and lower weight loss of full GP group mice were observed. Those initial results also provided some circumstantial evidence about the vaccine efficacy difference and vaccine protection. Furthermore, the detection of viral RNA levels suggested the VSV-MARV-GP vaccine could help to decrease the load of viral RNA in blood at 4 dpi. Both vaccines showed abilities to decrease the viral RNA replication in blood and several tissues at 6 dpi. However, the viral RNA level in the VSV-MARV-GP group was slightly lower than the VSV-MARV-ΔMuc GP group both at 4 dpi and 6 dpi. All these results suggest that removing the mucin-like domain reduced the vaccine protection. The vaccine efficacy study also showed that the mice contained high level of non-neutralizing IgG levels in sera were observed lower weight lose, clinical signs, and viral RNA replication than those of other mice. These results indicate the non-neutralizing antibodies probably play an important role in the protection against MA-MARV infection, a possible function of these antibodies is ADCC.

Both the results of monoclonal antibodies development and vaccine evaluations suggested the mucin-like domain of MARV is not the key for induction of neutralizing antibody generation in blab/c mice. VSV-MARV-ΔMuc GP cannot induce neutralizing antibodies in the immunized BALB/c mice. However, a limited neutralizing antibody response was detected in the serum of some infected mice. Furthermore, some publications also observed neutralizing antibodies in MARV-infected NHP survivors. In this case, some other mechanisms behind the MARV infection are the keys of anti-MARV neutralizing antibody generation.

Overall, based on the results presented in this study and the evidence from the literature, several conclusions are suggested. The mucin-like domain is not the key to developing neutralizing antibodies against MARV. On the other hand, removing the mucin-like domain on vaccine induced an earlier IgG response and lower protection, which suggested the mucin-like domain might contain some functions which affect immune evasion and viral life cycle. Non-neutralizing antibodies likely played an important role in MARV infection protection, a possible mechanism is the ADCC antibody function. And to get more treatment candidates against MARV, neutralizing antibodies against MARV might be generated from MARV-infected mouse or NHP survivors.

CHAPTER: 6 REFERENCES

Albariño, C. G., Shoemaker, T., Khristova, M. L., Wamala, J. F., Muyembe, J. J., Balinandi, S., … Ströher, U. (2013). Genomic analysis of filoviruses associated with four viral hemorrhagic fever outbreaks in Uganda and the Democratic Republic of the Congo in 2012. *Virology*, *442*(2), 97–100. https://doi.org/10.1016/J.VIROL.2013.04.014

Alimonti, J., Fernando, L., Melito, P., Qiu, X., Jones, S. M., Feldmann, H., … Klenk, H.-D. (2007). Assessment of a Vesicular Stomatitis Virus-Based Vaccine by Use of the Mouse Model of Ebola Virus Hemorrhagic Fever. *The Journal of Infectious Diseases*, *196*(Supplement_2), S404–S412. https://doi.org/10.1086/520591

Alves, D. A., Glynn, A. R., Steele, K. E., Lackemeyer, M. G., Garza, N. L., Buck, J. G., … Reed, D. S. (2010). Aerosol Exposure to the Angola Strain of Marburg Virus Causes Lethal Viral Hemorrhagic Fever in Cynomolgus Macaques. *Veterinary Pathology*, *47*(5), 831–851. https://doi.org/10.1177/0300985810378597

Amman, B. R., Nyakarahuka, L., McElroy, A. K., Dodd, K. A., Sealy, T. K., Schuh, A. J., … Towner, J. S. (2014). Marburgvirus resurgence in Kitaka Mine bat population after extermination attempts, Uganda. *Emerging Infectious Diseases*, *20*(10), 1761–1764. https://doi.org/10.3201/eid2010.140696

Amman, B., Swanepoel, R., T. Nichol, S., & Towner, J. S. (2017). Ecology of Filoviruses. In *Current topics in microbiology and immunology* (Vol. 411). https://doi.org/10.1007/82_2017_10

Bamberg, S., Kolesnikova, L., Möller, P., Klenk, H.-D., & Becker, S. (2005). VP24 of Marburg Virus Influences Formation of Infectious Particles. *Journal of Virology*, *79*(21), 13421 LP-13433. https://doi.org/10.1128/JVI.79.21.13421-13433.2005

Banadyga, L., He, S., Siragam, V., Zhu, W., Qiu, X., & Cheng, K. (2019). The Cytokine Response Profile of Ebola Virus Disease in a Large Cohort of Rhesus Macaques Treated with Monoclonal Antibodies. https://doi.org/10.1093/ofid/ofz046

Banadyga, L., Wong, G., & Qiu, X. (2018). Small Animal Models for Evaluating Filovirus Countermeasures. *ACS Infectious Diseases*, *4*(5), 673–685. https://doi.org/10.1021/acsinfecdis.7b00266

Barcelo, B., Dorion, C., Weatherill, D., Pou, D., Grovas, I., Rodriguez-Martinez, J., … Borchert, M. (2007). The Médecins Sans Frontières Intervention in the Marburg Hemorrhagic Fever Epidemic, Uige, Angola, 2005. I. Lessons Learned in the Hospital. *The Journal of Infectious Diseases*, *196*(Supplement_2), S154–S161. https://doi.org/10.1086/520548

Basler, C. F., Chandran, K., Tantral, L., Mulherkar, N., & Martinez, O. (2011). Impact of Ebola Mucin-Like Domain on Antiglycoprotein Antibody Responses Induced by Ebola Virus-

Like Particles. *The Journal of Infectious Diseases*, *204*(suppl_3), S825–S832. https://doi.org/10.1093/infdis/jir295

Bausch, D. G., Borchert, M., Grein, T., Roth, C., Swanepoel, R., Libande, M. L., … Rollin, P. E. (2003). Risk Factors for Marburg Hemorrhagic Fever, Democratic Republic of the Congo. *Emerging Infectious Disease Journal*, *9*(12), 1531. https://doi.org/10.3201/eid0912.030355

Bausch, D. G., Nichol, S. T., Muyembe-Tamfum, J. J., Borchert, M., Rollin, P. E., Sleurs, H., … Swanepoel, R. (2006). Marburg Hemorrhagic Fever Associated with Multiple Genetic Lineages of Virus. *New England Journal of Medicine*, *355*(9), 909–919. https://doi.org/10.1056/NEJMoa051465

Becker, S., & Mühlberger, E. (1999). Co- and posttranslational modifications and functions of Marburg virus proteins. *Current Topics in Microbiology and Immunology*, *235*, 23–34. Retrieved from http://europepmc.org/abstract/MED/9893376

Becker, S., Rinne, C., Hofsäß, U., Klenk, H.-D., & Mühlberger, E. (1998). Interactions of Marburg Virus Nucleocapsid Proteins. *Virology*, *249*(2), 406–417. https://doi.org/https://doi.org/10.1006/viro.1998.9328

Beer, B., Kurth, R., & Bukreyev, A. (1999). Characteristics of Filoviridae: Marburg and Ebola Viruses. *Naturwissenschaften*, *86*(1), 8–17. https://doi.org/10.1007/s001140050562

Bertherat, E., Talarmin, A., & Zeller, H. (1999). [Democratic Republic of the Congo: between civil war and the Marburg virus. International Committee of Technical and Scientific Coordination of the Durba Epidemic]. *Medecine tropicale : revue du Corps de sante colonial*, *59*(2), 201–204. Retrieved from http://europepmc.org/abstract/MED/10546197

Bharat, T. A. M., Riches, J. D., Kolesnikova, L., Welsch, S., Krähling, V., Davey, N., … Briggs, J. A. G. (2011). Cryo-Electron Tomography of Marburg Virus Particles and Their Morphogenesis within Infected Cells. *PLOS Biology*, *9*(11), e1001196. Retrieved from https://doi.org/10.1371/journal.pbio.1001196

Bhattacharyya, S., Hope, T. J., & Young, J. A. T. (2011). Differential requirements for clathrin endocytic pathway components in cellular entry by Ebola and Marburg glycoprotein pseudovirions. *Virology*, *419*(1), 1–9. https://doi.org/https://doi.org/10.1016/j.virol.2011.07.018

Blinov, V. M., Feldmann, H., Volchkova, V. A., Dolnik, O., Chepurnov, A. A., Volchkov, V. E., & Netesov, S. V. (1999). Characterization of the L gene and 5’ trailer region of Ebola virus. *Journal of General Virology*, *80*(2), 355–362. https://doi.org/10.1099/0022-1317-80-2-355

Bornholdt, Z. A., Herbert, A. S., Mire, C. E., He, S., Cross, R. W., Wec, A. Z., … Dye, J. M. (2019). A Two-Antibody Pan-Ebolavirus Cocktail Confers Broad Therapeutic Protection in Ferrets and Nonhuman Primates. *Cell Host & Microbe*, *25*(1), 49–58.e5. https://doi.org/https://doi.org/10.1016/j.chom.2018.12.005

Bornholdt, Z. A., Turner, H. L., Murin, C. D., Li, W., Sok, D., Souders, C. A., … Walker, L. M. (2016). Isolation of potent neutralizing antibodies from a survivor of the 2014 Ebola virus outbreak. *Science*, *351*(6277), 1078 LP-1083. https://doi.org/10.1126/science.aad5788

Brannan, J. M., He, S., Howell, K. A., Prugar, L. I., Zhu, W., Vu, H., … Aman, M. J. (2019). Post-exposure immunotherapy for two ebolaviruses and Marburg virus in nonhuman primates. *Nature Communications*, *10*(1), 105. https://doi.org/10.1038/s41467-018-08040-w

Brauburger, K., Hume, A. J., Mühlberger, E., Olejnik, J., Brauburger, K., Hume, A. J., … Olejnik, J. (2012). Forty-Five Years of Marburg Virus Research. *Viruses*, *4*(10), 1878–1927. https://doi.org/10.3390/v4101878

Bukreyev, A. A., Volchkov, V. E., Blinov, V. M., & Netesov, S. V. (1993). The GP-protein of Marburg virus contains the region similar to the 'immunosuppressive domain' of oncogenic retrovirus P15E proteins. *FEBS Letters*, *323*(1–2), 183–187. https://doi.org/10.1016/0014-5793(93)81476-G

Carette, J. E., Raaben, M., Wong, A. C., Herbert, A. S., Obernosterer, G., Mulherkar, N., … Brummelkamp, T. R. (2011). Ebola virus entry requires the cholesterol transporter Niemann–Pick C1. *Nature*, *477*, 340. Retrieved from https://doi.org/10.1038/nature10348

Chan, S. Y., Speck, R. F., Ma, M. C., & Goldsmith, M. A. (2000). Distinct Mechanisms of Entry by Envelope Glycoproteins of Marburg and Ebola (Zaire) Viruses. *Journal of Virology*, *74*(10), 4933 LP-4937. https://doi.org/10.1128/JVI.74.10.4933-4937.2000

Chandran, K., Sullivan, N. J., Felbor, U., Whelan, S. P., & Cunningham, J. M. (2005). Endosomal Proteolysis of the Ebola Virus Glycoprotein Is Necessary for Infection. *Science*, *308*(5728), 1643 LP-1645. https://doi.org/10.1126/science.1110656

Commission, R. of an I. (1978). Ebola haemorrhagic fever in Zaire, 1976. *Bulletin of the World Health Organization*, *56*(2), 271–293. Retrieved from https://www.ncbi.nlm.nih.gov/pubmed/307456

Corti, D., Misasi, J., Mulangu, S., Stanley, D. A., Kanekiyo, M., Wollen, S., … Sullivan, N. J. (2016). Protective monotherapy against lethal Ebola virus infection by a potently neutralizing antibody. *Science*, *351*(6279), 1339 LP-1342. https://doi.org/10.1126/science.aad5224

Côté, M., Misasi, J., Ren, T., Bruchez, A., Lee, K., Filone, C. M., … Cunningham, J. (2011). Small molecule inhibitors reveal Niemann–Pick C1 is essential for Ebola virus infection. *Nature*, *477*, 344. Retrieved from https://doi.org/10.1038/nature10380

Crary, S. M., Towner, J. S., Honig, J. E., Shoemaker, T. R., & Nichol, S. T. (2003). Analysis of the role of predicted RNA secondary structures in Ebola virus replication. *Virology*, *306*(2), 210–218. https://doi.org/https://doi.org/10.1016/S0042-6822(02)00014-4

Cross, R. W., Mire, C. E., Feldmann, H., & Geisbert, T. W. (2018). Post-exposure treatments for Ebola and Marburg virus infections. *Nature Reviews Drug Discovery*, *17*, 413. Retrieved from https://doi.org/10.1038/nrd.2017.251

Daddario-DiCaprio, K. M., Geisbert, T. W., Geisbert, J. B., Ströher, U., Hensley, L. E., Grolla, A., … Jones, S. M. (2006). Cross-Protection against Marburg Virus Strains by Using a Live, Attenuated Recombinant Vaccine. *Journal of Virology*, *80*(19), 9659 LP-9666. https://doi.org/10.1128/JVI.00959-06

DiCarlo, A., Klußmeier, A., Hartlieb, B., Biedenkopf, N., & Becker, S. (2011). Phosphorylation of Marburg Virus NP Region II Modulates Viral RNA Synthesis. *The Journal of Infectious Diseases*, *204*(suppl_3), S927–S933. https://doi.org/10.1093/infdis/jir319

Dolnik, O., Kolesnikova, L., & Becker, S. (2007). Filoviruses: Interactions with the host cell. *Cellular and Molecular Life Sciences*, *65*(5), 756. https://doi.org/10.1007/s00018-007-7406-2

Dolnik, O., Kolesnikova, L., Stevermann, L., & Becker, S. (2010). Tsg101 Is Recruited by a Late Domain of the Nucleocapsid Protein To Support Budding of Marburg Virus-Like Particles. *Journal of Virology*, *84*(15), 7847 LP-7856. https://doi.org/10.1128/JVI.00476-10

Dominguez-Soto, A., Aragoneses-Fenoll, L., Martin-Gayo, E., Martinez-Prats, L., Colmenares, M., Naranjo-Gomez, M., … Corbi, A. L. (2007). The DC-SIGN–related lectin LSECtin mediates antigen capture and pathogen binding by human myeloid cells. *Blood*, *109*(12), 5337 LP-5345. https://doi.org/10.1182/blood-2006-09-048058

Druar, C., Saini, S. S., Cossitt, M. A., Yu, F., Qiu, X., Geisbert, T. W., … Wiersma, E. J. (2005). Analysis of the expressed heavy chain variable-region genes of Macaca fascicularis and isolation of monoclonal antibodies specific for the Ebola virus' soluble glycoprotein. *Immunogenetics*, *57*(10), 730–738. https://doi.org/10.1007/s00251-005-0047-4

Dunning, J., Sahr, F., Rojek, A., Gannon, F., Carson, G., Idriss, B., … team, for the R.-T. trial. (2016). Experimental Treatment of Ebola Virus Disease with TKM-130803: A Single-Arm Phase 2 Clinical Trial. *PLOS Medicine*, *13*(4), e1001997. Retrieved from https://doi.org/10.1371/journal.pmed.1001997

Empig, C. J., & Goldsmith, M. A. (2002). Association of the Caveola Vesicular System with Cellular Entry by Filoviruses. *Journal of Virology*, *76*(10), 5266 LP-5270. https://doi.org/10.1128/JVI.76.10.5266-5270.2002

Enterlein, S., Schmidt, K. M., Schümann, M., Conrad, D., Krähling, V., Olejnik, J., & Mühlberger, E. (2009). The Marburg Virus 3′ Noncoding Region Structurally and Functionally Differs from That of Ebola Virus. Journal of Virology, 83(9), 4508 LP-4519. https://doi.org/10.1128/JVI.02429-08

Escudero-Pérez, B., & Muñoz-Fontela, C. (2019). Role of Type I Interferons on Filovirus Pathogenesis. Vaccines . https://doi.org/10.3390/vaccines7010022

Feldmann, H., Will, C., Schikore, M., Slenczka, W., & Klenk, H.-D. (1991). Glycosylation and oligomerization of the spike protein of marburg virus. *Virology*, *182*(1), 353–356. https://doi.org/https://doi.org/10.1016/0042-6822(91)90680-A

Feldmann, H., & Geisbert, T. W. (2011). Recombinant Vesicular Stomatitis Virus–Based Vaccines Against Ebola and Marburg Virus Infections. *The Journal of Infectious Diseases*, *204*(suppl_3), S1075–S1081. https://doi.org/10.1093/infdis/jir349

Feldmann, H., Mühlberger, E., Randolf, A., Will, C., Kiley, M. P., Sanchez, A., & Klenk, H.-D. (1992). Marburg virus, a filovirus: méssenger RNAs, gene order, and regulatory elements of the replication cycle. *Virus Research*, *24*(1), 1–19. https://doi.org/https://doi.org/10.1016/0168-1702(92)90027-7

Feldmann, H., Nichol, S. T., Klenk, H.-D., Peters, C. J., & Sanchez, A. (1994). Characterization of Filoviruses Based on Differences in Structure and Antigenicity of the Virion Glycoprotein. *Virology*, *199*(2), 469–473. https://doi.org/https://doi.org/10.1006/viro.1994.1147

Flyak, A. I., Shen, X., Murin, C. D., Turner, H. L., David, J. A., Fusco, M. L., … Crowe, J. E. (2016). Cross-Reactive and Potent Neutralizing Antibody Responses in Human Survivors of Natural Ebolavirus Infection. *Cell*, *164*(3), 392–405. https://doi.org/https://doi.org/10.1016/j.cell.2015.12.022

Fowler, T., Bamberg, S., Möller, P., Klenk, H.-D., Meyer, T. F., Becker, S., & Rudel, T. (2005). Inhibition of Marburg virus protein expression and viral release by RNA interference. *Journal of General Virology*, *86*(4), 1181–1188. https://doi.org/10.1099/vir.0.80622-0

Fritz, E. A., Geisbert, J. B., Geisbert, T. W., Hensley, L. E., & Reed, D. S. (2008). Cellular Immune Response to Marburg Virus Infection in Cynomolgus Macaques. *Viral Immunology*, *21*(3), 355–364. https://doi.org/10.1089/vim.2008.0023

Froude, J. W., Pelat, T., Miethe, S., Zak, S. E., Wec, A. Z., Chandran, K., … Dye, J. M. (2017). Generation and characterization of protective antibodies to Marburg virus. *MAbs*. https://doi.org/10.1080/19420862.2017.1299848

Gear, J. S., Cassel, G. A., Gear, A. J., Trappler, B., Clausen, L., Meyers, A. M., … Gear, J. H. (1975). Outbreake of Marburg virus disease in Johannesburg. *British Medical Journal*, *4*(5995), 489 LP-493. https://doi.org/10.1136/bmj.4.5995.489

Geisbert, T. W., & Jahrling, P. B. (1995). Differentiation of filoviruses by electron microscopy. *Virus Research*, *39*(2), 129–150. https://doi.org/https://doi.org/10.1016/0168-1702(95)00080-1

Geisbert, T. W., Bailey, M., Geisbert, J. B., Asiedu, C., Roederer, M., Grazia-Pau, M., … Sullivan, N. J. (2010). Vector Choice Determines Immunogenicity and Potency of Genetic Vaccines against Angola Marburg Virus in Nonhuman Primates. *Journal of Virology*, *84*(19), 10386 LP-10394. https://doi.org/10.1128/JVI.00594-10

Geisbert, T. W., Bausch, D. G., & Feldmann, H. (2010). Prospects for immunisation against Marburg and Ebola viruses. *Reviews in Medical Virology*, *20*(6), 344–357. https://doi.org/10.1002/rmv.661

Geisbert, T. W., Daddario-DiCaprio, K. M., Geisbert, J. B., Reed, D. S., Feldmann, F., Grolla, A., … Feldmann, H. (2008). Vesicular stomatitis virus-based vaccines protect nonhuman primates against aerosol challenge with Ebola and Marburg viruses. *Vaccine*, *26*(52), 6894–6900. https://doi.org/https://doi.org/10.1016/j.vaccine.2008.09.082

Geisbert, T. W., Fritz, E. A., Geisbert, J. B., Hensley, L. E., Daddario-DiCaprio, K. M., Larsen, T., … Formenty, P. (2007). Marburg Virus Angola Infection of Rhesus Macaques: Pathogenesis and Treatment with Recombinant Nematode Anticoagulant Protein c2. *The Journal of Infectious Diseases*, *196*(Supplement_2), S372–S381. https://doi.org/10.1086/520608

Geisbert, T. W., Hensley, L. E., Geisbert, J. B., Leung, A., Johnson, J. C., Grolla, A., & Feldmann, H. (2010). Postexposure treatment of Marburg virus infection. *Emerging Infectious Diseases*, *16*(7), 1119–1122. https://doi.org/10.3201/eid1607.100159

Geisbert, T. W., Hensley, L. E., Gibb, T. R., Steele, K. E., Jaax, N. K., & Jahrling, P. B. (2000). Apoptosis Induced In Vitro and In Vivo During Infection by Ebola and Marburg Viruses. *Laboratory Investigation*, *80*, 171. Retrieved from https://doi.org/10.1038/labinvest.3780021

Geyer, H., Geyer, R., Will, C., Klenk, H.-D., & Feldmann, H. (1992). Carbohydrate structure of Marburg virus glycoprotein. *Glycobiology*, *2*(4), 299–312. https://doi.org/10.1093/glycob/2.4.299

Gnirß, K., Kühl, A., Karsten, C., Glowacka, I., Bertram, S., Kaup, F., … Pöhlmann, S. (2012). Cathepsins B and L activate Ebola but not Marburg virus glycoproteins for efficient entry into cell lines and macrophages independent of TMPRSS2 expression. *Virology*, *424*(1), 3–10. https://doi.org/https://doi.org/10.1016/j.virol.2011.11.031

Goldstein, T., Anthony, S. J., Gbakima, A., Bird, B. H., Bangura, J., Tremeau-Bravard, A., … Mazet, J. A. K. (2018). The discovery of Bombali virus adds further support for bats as hosts of ebolaviruses. *Nature Microbiology*, *3*(10), 1084–1089. https://doi.org/10.1038/s41564-018-0227-2

Gordon Smith, C. E., Simpson, D. I. H., Bowen, E. T. W., & Zlotnik, I. (1967). FATAL HUMAN DISEASE FROM VERVET MONKEYS. *The Lancet*, *290*(7526), 1119–1121. https://doi.org/10.1016/S0140-6736(67)90621-6

Grant-Klein, R. J., Altamura, L. A., & Schmaljohn, C. S. (2011). Progress in recombinant DNA-derived vaccines for Lassa virus and filoviruses. *Virus Research*, *162*(1), 148–161. https://doi.org/https://doi.org/10.1016/j.virusres.2011.09.005

Grant-Klein, R. J., Van Deusen, N. M., Badger, C. V, Hannaman, D., Dupuy, L. C., & Schmaljohn, C. S. (2012). A multiagent filovirus DNA vaccine delivered by intramuscular electroporation completely protects mice from ebola and Marburg virus challenge. *Human Vaccines & Immunotherapeutics*, *8*(11), 1703–1706. https://doi.org/10.4161/hv.21873

Group, P. I. I. W., Team, M.-N. P. I. I. S., Davey Jr, R. T., Dodd, L., Proschan, M. A., Neaton, J., … Malvy, D. (2016). A Randomized, Controlled Trial of ZMapp for Ebola Virus Infection. *The New England Journal of Medicine*, *375*(15), 1448–1456. https://doi.org/10.1056/NEJMoa1604330

Han, B.-S., Jang, H.-Y., Racine, T., Qiu, X., & Sin, J.-I. (2018). Purification and characterization of monoclonal IgG antibodies recognizing Ebola virus glycoprotein. *Clin Exp Vaccine Res*, *7*(2), 119–128. Retrieved from http://synapse.koreamed.org/DOIx.php?id=10.7774%2Fcevr.2018.7.2.119

Harty, R. N., Stone, S., & Liu, Y. (2011). Characterization of Filovirus Protein–Protein Interactions in Mammalian Cells Using Bimolecular Complementation. *The Journal of Infectious Diseases*, *204*(suppl_3), S817–S824. https://doi.org/10.1093/infdis/jir293

Hashiguchi, T., Fusco, M. L., Bornholdt, Z. A., Lee, J. E., Flyak, A. I., Matsuoka, R., … Saphire, E. O. (2015). Structural Basis for Marburg Virus Neutralization by a Cross-Reactive Human Antibody. *Cell*, *160*(5), 904–912. https://doi.org/https://doi.org/10.1016/j.cell.2015.01.041

Hashiguchi, T., Fusco, M. L., Bornholdt, Z. A., Lee, J. E., Flyak, A. I., Matsuoka, R., … Saphire, E. O. (2015). Structural Basis for Marburg Virus Neutralization by a Cross-Reactive Human Antibody. *Cell*, *160*(5), 904–912. https://doi.org/https://doi.org/10.1016/j.cell.2015.01.041

He, S., Safronetz, D., Banadyga, L., Rahim, M. N., Zhu, W., Zhang, Z., & Qiu, X. (2018). Postexposure Protective Efficacy of T-705 (Favipiravir) Against Sudan Virus Infection in Guinea Pigs. *The Journal of Infectious Diseases*, *218*(suppl_5), S649–S657. https://doi.org/10.1093/infdis/jiy303

Hevey, M., Negley, D., VanderZanden, L., Tammariello, R. F., Geisbert, J., Schmaljohn, C., … Schmaljohn, A. L. (2001). Marburg virus vaccines: comparing classical and new approaches. *Vaccine*, *20*(3), 586–593. https://doi.org/https://doi.org/10.1016/S0264-410X(01)00353-X

Hevey, M., Negley, D., Geisbert, J., Jahrling, P., & Schmaljohn, A. (1997). Antigenicity and Vaccine Potential of Marburg Virus Glycoprotein Expressed by Baculovirus Recombinants. *Virology*, *239*(1), 206–216. https://doi.org/https://doi.org/10.1006/viro.1997.8883

Hevey, M., Negley, D., Pushko, P., Smith, J., & Schmaljohn, A. (1998). Marburg Virus Vaccines Based upon Alphavirus Replicons Protect Guinea Pigs and Nonhuman Primates. *Virology*, *251*(1), 28–37. https://doi.org/https://doi.org/10.1006/viro.1998.9367

Hoenen, T., Jung, S., Herwig, A., Groseth, A., & Becker, S. (2010). Both matrix proteins of Ebola virus contribute to the regulation of viral genome replication and transcription. *Virology*, *403*(1), 56–66. https://doi.org/https://doi.org/10.1016/j.virol.2010.04.002

Hume, A., & Mühlberger, E. (2018). Marburg Virus Viral Protein 35 Inhibits Protein Kinase R Activation in a Cell Type–Specific Manner. *The Journal of Infectious Diseases*, *218*(suppl_5), S403–S408. https://doi.org/10.1093/infdis/jiy473

Ignatyev, G. M., Agafonov, A. P., Streltsova, M. A., & Kashentseva, E. A. (1996). Inactivated Marburg virus elicits a nonprotective immune response in Rhesus monkeys. *Journal of Biotechnology*, *44*(1), 111–118. https://doi.org/https://doi.org/10.1016/0168-1656(95)00104-2

Jacob, H., & Solcher, H. (1968). Über eine durch grüne Meerkatzen (Cercopithecus aethiops) übertragene, zu Gliaknötchenencephalitis führende Infektionskrankheit ("Marburger Krankheit"). *Acta Neuropathologica*, *11*(1), 29–44. https://doi.org/10.1007/BF00692793

Jeffers, S. A., Sanders, D. A., & Sanchez, A. (2002). Covalent Modifications of the Ebola Virus Glycoprotein. *Journal of Virology*, *76*(24), 12463 LP-12472. https://doi.org/10.1128/JVI.76.24.12463-12472.2002

Jeffs, B., Villa, L., Bernal, O., Palma, P. P., Roddy, P., Borchert, M., … Jones, S. M. (2010). Factors Associated with Marburg Hemorrhagic Fever: Analysis of Patient Data from Uige, Angola. *The Journal of Infectious Diseases*, *201*(12), 1909–1918. https://doi.org/10.1086/652748

Johnson, E. D., Johnson, B. K., Silverstein, D., Tukei, P., Geisbert, T. W., Sanchez, A. N., & Jahrling, P. B. (1996). Characterization of a new Marburg virus isolated from a 1987 fatal case in Kenya BT - Imported Virus Infections. In T. F. Schwarz & G. Siegl (Eds.) (pp. 101–114). Vienna: Springer Vienna.

Johnston, J., Geldenhuys, P., Crees, M., Wulff, H., Conrad, J. L., Smith, E. B., & Isaacson, M. (1978). Epidemiologic Investigation of Marburg Virus Disease, Southern Africa, 1975 *. *The American Journal of Tropical Medicine and Hygiene*, *27*(6), 1210–1215. https://doi.org/10.4269/ajtmh.1978.27.1210

Jones, S. M., Feldmann, H., Ströher, U., Geisbert, J. B., Fernando, L., Grolla, A., … Geisbert, T. W. (2005). Live attenuated recombinant vaccine protects nonhuman primates against Ebola and Marburg viruses. *Nature Medicine*, *11*, 786. Retrieved from https://doi.org/10.1038/nm1258

Jouvenet, N., Neil, S. J. D., Zhadina, M., Zang, T., Kratovac, Z., Lee, Y., … Bieniasz, P. D. (2009). Broad-Spectrum Inhibition of Retroviral and Filoviral Particle Release by Tetherin. *Journal of Virology*, *83*(4), 1837 LP-1844. https://doi.org/10.1128/JVI.02211-08

Kagirita, A., Jeffs, B., Amman, B., Manning, C., Kansiime, E., Farnon, E. C., … Nichol, S. T. (2011). Outbreak of Marburg Hemorrhagic Fever Among Miners in Kamwenge and Ibanda Districts, Uganda, 2007. *The Journal of Infectious Diseases*, *204*(suppl_3), S796–S799. https://doi.org/10.1093/infdis/jir312

Kaletsky, R. L., Francica, J. R., Agrawal-Gamse, C., & Bates, P. (2009). Tetherin-mediated restriction of filovirus budding is antagonized by the Ebola glycoprotein. *Proceedings of the National Academy of Sciences*, *106*(8), 2886 LP-2891. https://doi.org/10.1073/pnas.0811014106

Keck, Z.-Y., Enterlein, S. G., Howell, K. A., Vu, H., Shulenin, S., Warfield, K. L., … Aman, M. J. (2016). Macaque Monoclonal Antibodies Targeting Novel Conserved Epitopes within Filovirus Glycoprotein. *Journal of Virology*, *90*(1), 279 LP-291. https://doi.org/10.1128/JVI.02172-15

Keshwara, R., Hagen, K. R., Abreu-Mota, T., Papaneri, A. B., Liu, D., Wirblich, C., … Schnell, M. J. (2018). A Recombinant Rabies Virus Expressing the Marburg Virus Glycoprotein is Dependent Upon ADCC for Protection Against Marburg Virus Disease in a Murine Model. *Journal of Virology*, JVI.01865-18. https://doi.org/10.1128/JVI.01865-18

King, L. B., Fusco, M. L., Flyak, A. I., Ilinykh, P. A., Huang, K., Gunn, B., … Saphire, E. O. (2018). The Marburgvirus-Neutralizing Human Monoclonal Antibody MR191 Targets a Conserved Site to Block Virus Receptor Binding. *Cell Host & Microbe*, *23*(1), 101–109.e4. https://doi.org/https://doi.org/10.1016/j.chom.2017.12.003

King, L. B., Fusco, M. L., Flyak, A. I., Ilinykh, P. A., Huang, K., Gunn, B., … Saphire, E. O. (2018). The Marburgvirus-Neutralizing Human Monoclonal Antibody MR191 Targets a Conserved Site to Block Virus Receptor Binding. *Cell Host & Microbe*, *23*(1), 101–109.e4. https://doi.org/https://doi.org/10.1016/j.chom.2017.12.003

Kissling, R. E., Robinson, R. Q., Murphy, F. A., & Whitfield, S. G. (1968). Agent of Disease Contracted from Green Monkeys. *Science*, *160*(3830), 888 LP-890. https://doi.org/10.1126/science.160.3830.888

Koellhoffer, J. F., Malashkevich, V. N., Harrison, J. S., Toro, R., Bhosle, R. C., Chandran, K., … Lai, J. R. (2012). Crystal Structure of the Marburg Virus GP2 Core Domain in Its Postfusion Conformation. *Biochemistry*, *51*(39), 7665–7675. https://doi.org/10.1021/bi300976m

Kolesnikova, L., Berghöfer, B., Bamberg, S., & Becker, S. (2004). Multivesicular Bodies as a Platform for Formation of the Marburg Virus Envelope. *Journal of Virology*, *78*(22), 12277 LP-12287. https://doi.org/10.1128/JVI.78.22.12277-12287.2004

Kolesnikova, L., Bohil, A. B., Cheney, R. E., & Becker, S. (2007). Budding of Marburgvirus is associated with filopodia. *Cellular Microbiology*, *9*(4), 939–951. https://doi.org/10.1111/j.1462-5822.2006.00842.x

Kolesnikova, L., Bugany, H., Klenk, H.-D., & Becker, S. (2002). VP40, the Matrix Protein of Marburg Virus, Is Associated with Membranes of the Late Endosomal Compartment. *Journal of Virology*, *76*(4), 1825 LP-1838. https://doi.org/10.1128/JVI.76.4.1825-1838.2002

Kolesnikova, L., Mittler, E., Schudt, G., Shams-Eldin, H., & Becker, S. (2012). Phosphorylation of Marburg virus matrix protein VP40 triggers assembly of nucleocapsids with the viral envelope at the plasma membrane. *Cellular Microbiology*, *14*(2), 182–197. https://doi.org/10.1111/j.1462-5822.2011.01709.x

Kolesnikova, L., Mühlberger, E., Ryabchikova, E., & Becker, S. (2000). Ultrastructural Organization of Recombinant Marburg Virus Nucleoprotein: Comparison with Marburg Virus Inclusions. *Journal of Virology*, *74*(8), 3899 LP-3904. https://doi.org/10.1128/JVI.74.8.3899-3904.2000

Kolesnikova, L., Strecker, T., Morita, E., Zielecki, F., Mittler, E., Crump, C., & Becker, S. (2009). Vacuolar Protein Sorting Pathway Contributes to the Release of Marburg Virus. *Journal of Virology*, *83*(5), 2327 LP-2337. https://doi.org/10.1128/JVI.02184-08

Konde, M. K., Baker, D. P., Traore, F. A., Sow, M. S., Camara, A., Barry, A. A., … Fish, E. N. (2017). Interferon β-1a for the treatment of Ebola virus disease: A historically controlled, single-arm proof-of-concept trial. *PLOS ONE*, *12*(2), e0169255. Retrieved from https://doi.org/10.1371/journal.pone.0169255

Kondratowicz, A. S., Lennemann, N. J., Sinn, P. L., Davey, R. A., Hunt, C. L., Moller-Tank, S., … Maury, W. (2011). T-cell immunoglobulin and mucin domain 1 (TIM-1) is a receptor for Zaire Ebolavirus and Lake Victoria Marburgvirus. *Proceedings of the National Academy of Sciences*, *108*(20), 8426–8431. https://doi.org/10.1073/pnas.1019030108

Kuhn, J. H., Becker, S., Ebihara, H., Geisbert, T. W., Johnson, K. M., Kawaoka, Y., … Jahrling, P. B. (2010). Proposal for a revised taxonomy of the family Filoviridae: classification, names of taxa and viruses, and virus abbreviations. *Archives of Virology*, *155*(12), 2083–2103. https://doi.org/10.1007/s00705-010-0814-x

Liu, G., Wong, G., Su, S., Bi, Y., Plummer, F., Gao, G. F., … Qiu, X. (2017). Clinical Evaluation of Ebola Virus Disease Therapeutics. *Trends in Molecular Medicine*, *23*(9), 820–830. https://doi.org/https://doi.org/10.1016/j.molmed.2017.07.002

Makino, A., Shinya, K., Yamayoshi, S., Noda, T., & Kawaoka, Y. (2011). Identification of Amino Acids in Marburg Virus VP40 That Are Important for Virus-Like Particle Budding. *The Journal of Infectious Diseases*, *204*(suppl_3), S871–S877. https://doi.org/10.1093/infdis/jir309

Manicassamy, B., Wang, J., Jiang, H., & Rong, L. (2005). Comprehensive Analysis of Ebola Virus GP1 in Viral Entry. *Journal of Virology*, *79*(8), 4793 LP-4805. https://doi.org/10.1128/JVI.79.8.4793-4805.2005

Manicassamy, B., Wang, J., Rumschlag, E., Tymen, S., Volchkova, V., Volchkov, V., & Rong, L. (2007). Characterization of Marburg virus glycoprotein in viral entry. *Virology*, *358*(1), 79–88. https://doi.org/https://doi.org/10.1016/j.virol.2006.06.041

Martini, G. A., & Siegert, R. (1971). *Marburg virus disease*. Springer-Verlag. Retrieved from https://books.google.ca/books?id=SoFrAAAAMAAJ

Marzi, A., Gramberg, T., Simmons, G., Möller, P., Rennekamp, A. J., Krumbiegel, M., … Pöhlmann, S. (2004). DC-SIGN and DC-SIGNR interact with the glycoprotein of Marburg virus and the S protein of severe acute respiratory syndrome coronavirus. *Journal of Virology*, *78*(21), 12090–12095. https://doi.org/10.1128/JVI.78.21.12090-12095.2004

Marzi, A., Konrad, A., Kühl, A., Banning, C., Behrens, G., Feldmann, H., … Schubert, U. (2011). The Ebola Virus Glycoprotein and HIV-1 Vpu Employ Different Strategies to Counteract the Antiviral Factor Tetherin. *The Journal of Infectious Diseases*, *204*(suppl_3), S850–S860. https://doi.org/10.1093/infdis/jir378

Marzi, A., Schnittler, H.-J., Feldmann, H., Beimforde, N., Biedenkopf, N., Aleksandrowicz, P., … Hoenen, T. (2011). Ebola Virus Enters Host Cells by Macropinocytosis and Clathrin-Mediated Endocytosis. *The Journal of Infectious Diseases*, *204*(suppl_3), S957–S967. https://doi.org/10.1093/infdis/jir326

Matsuno, K., Kishida, N., Usami, K., Igarashi, M., Yoshida, R., Nakayama, E., … Takada, A. (2010). Different Potential of C-Type Lectin-Mediated Entry between Marburg Virus Strains. *Journal of Virology*, *84*(10), 5140 LP-5147. https://doi.org/10.1128/JVI.02021-09

Mavrakis, M., Kolesnikova, L., Schoehn, G., Becker, S., & Ruigrok, R. W. H. (2002). Morphology of Marburg Virus NP–RNA. *Virology*, *296*(2), 300–307. https://doi.org/https://doi.org/10.1006/viro.2002.1433

Mehedi, M., Groseth, A., Feldmann, H., & Ebihara, H. (2011). Clinical aspects of Marburg hemorrhagic fever. *Future Virology*, *6*(9), 1091–1106. https://doi.org/10.2217/fvl.11.79

Misasi, J., Chandran, K., Yang, J.-Y., Considine, B., Filone, C. M., Côté, M., … Cunningham, J. (2012). Filoviruses Require Endosomal Cysteine Proteases for Entry but Exhibit Distinct Protease Preferences. *Journal of Virology*, *86*(6), 3284 LP-3292. https://doi.org/10.1128/JVI.06346-11

Mittler, E., Kolesnikova, L., Hartlieb, B., Davey, R., & Becker, S. (2011). The Cytoplasmic Domain of Marburg Virus GP Modulates Early Steps of Viral Infection. *Journal of Virology*, *85*(16), 8188 LP-8196. https://doi.org/10.1128/JVI.00453-11

Mittler, E., Kolesnikova, L., Strecker, T., Garten, W., & Becker, S. (2007). Role of the Transmembrane Domain of Marburg Virus Surface Protein GP in Assembly of the Viral Envelope. *Journal of Virology*, *81*(8), 3942 LP-3948. https://doi.org/10.1128/JVI.02263-06

Modrof, J., Mühlberger, E., Klenk, H.-D., & Becker, S. (2002). Phosphorylation of VP30 impairs ebola virus transcription. *The Journal of Biological Chemistry*, *277*(36), 33099–104. https://doi.org/10.1074/jbc.M203775200

Mühlberger, E. (2007). Filovirus replication and transcription. *Future Virology*, *2*(2), 205–215. https://doi.org/10.2217/17460794.2.2.205

Mühlberger, E., Lötfering, B., Klenk, H.-D., & Becker, S. (1998). Three of the Four Nucleocapsid Proteins of Marburg Virus, NP, VP35, and L, Are Sufficient To Mediate Replication and Transcription of Marburg Virus-Specific Monocistronic Minigenomes. *Journal of Virology*, *72*(11), 8756 LP-8764. Retrieved from http://jvi.asm.org/content/72/11/8756.abstract

Mühlberger, E., Olejnik, J., Schmidt, K. M., Schümann, M., & Krähling, V. (2011). Recombinant Marburg Virus Expressing EGFP Allows Rapid Screening of Virus Growth and Real-time Visualization of Virus Spread. *The Journal of Infectious Diseases*, *204*(suppl_3), S861–S870. https://doi.org/10.1093/infdis/jir308

Mühlberger, E., Sanchez, A., Randolf, A., Will, C., Kiley, M. P., Klenk, H.-D., & Feldmann, H. (1992). The nucleotide sequence of the L gene of marburg virus, a filovirus: Homologies with paramyxoviruses and rhabdoviruses. *Virology*, *187*(2), 534–547. https://doi.org/https://doi.org/10.1016/0042-6822(92)90456-Y

Negredo, A., Palacios, G., Vázquez-Morón, S., González, F., Dopazo, H., Molero, F., … Tenorio, A. (2011). Discovery of an Ebolavirus-Like Filovirus in Europe. *PLOS Pathogens*, *7*(10), e1002304. Retrieved from https://doi.org/10.1371/journal.ppat.1002304

Neil, S. J. D., Sandrin, V., Sundquist, W. I., & Bieniasz, P. D. (2007). An Interferon-α-Induced Tethering Mechanism Inhibits HIV-1 and Ebola Virus Particle Release but Is Counteracted by the HIV-1 Vpu Protein. *Cell Host & Microbe*, *2*(3), 193–203. https://doi.org/https://doi.org/10.1016/j.chom.2007.08.001

Okware, S. I., Omaswa, F. G., Zaramba, S., Opio, A., Lutwama, J. J., Kamugisha, J., … Lamunu, M. (2002). An outbreak of Ebola in Uganda. *Tropical Medicine & International Health*, *7*(12), 1068–1075. https://doi.org/10.1046/j.1365-3156.2002.00944.x

Patel, A., Park, D. H., Davis, C. W., Smith, T. R. F., Leung, A., Tierney, K., … Weiner, D. B. (2018). In Vivo Delivery of Synthetic Human DNA-Encoded Monoclonal Antibodies Protect against Ebolavirus Infection in a Mouse Model. *Cell Reports*, *25*(7), 1982–1993.e4. https://doi.org/https://doi.org/10.1016/j.celrep.2018.10.062

Pettitt, J., Zeitlin, L., Kim, D. H., Working, C., Johnson, J. C., Bohorov, O., … Olinger, G. G. (2013). Therapeutic Intervention of Ebola Virus Infection in Rhesus Macaques with the MB-003 Monoclonal Antibody Cocktail. *Science Translational Medicine*, *5*(199), 199ra113 LP-199ra113. https://doi.org/10.1126/scitranslmed.3006608

Poch, O., Blumberg, B. M., Bougueleret, L., & Tordo, N. (1990). Sequence Comparison of Five Polymerases (L proteins) of Unsegmented Negative-strand RNA Viruses: Theoretical Assignment of Functional Domains. *Journal of General Virology*, *71*(5), 1153–1162. Retrieved from https://jgv.microbiologyresearch.org/content/journal/jgv/10.1099/0022-1317-71-5-1153

Qiu, X., Alimonti, J. B., Melito, P. L., Fernando, L., Ströher, U., & Jones, S. M. (2011). Characterization of Zaire ebolavirus glycoprotein-specific monoclonal antibodies. *Clinical Immunology*, *141*(2), 218–227. https://doi.org/https://doi.org/10.1016/j.clim.2011.08.008

Qiu, X., Audet, J., Wong, G., Pillet, S., Bello, A., Cabral, T., … Kobinger, G. P. (2012). Successful Treatment of Ebola Virus–Infected Cynomolgus Macaques with Monoclonal Antibodies. *Science Translational Medicine*, *4*(138), 138ra81 LP-138ra81. https://doi.org/10.1126/scitranslmed.3003876

Qiu, X., Fernando, L., Alimonti, J. B., Melito, P. L., Feldmann, F., Dick, D., … Jones, S. M. (2009). Mucosal Immunization of Cynomolgus Macaques with the VSVΔG/ZEBOVGP Vaccine Stimulates Strong Ebola GP-Specific Immune Responses. *PLOS ONE*, *4*(5), e5547. Retrieved from https://doi.org/10.1371/journal.pone.0005547

Qiu, X., Wong, G., Audet, J., Bello, A., Fernando, L., Alimonti, J. B., … Kobinger, G. P. (2014). Reversion of advanced Ebola virus disease in nonhuman primates with ZMapp. *Nature*, *514*, 47. Retrieved from https://doi.org/10.1038/nature13777

Qiu, X., Wong, G., Fernando, L., Audet, J., Bello, A., Strong, J., … Kobinger, G. P. (2013). mAbs and Ad-Vectored IFN-α Therapy Rescue Ebola-Infected Nonhuman Primates When Administered After the Detection of Viremia and Symptoms. *Science Translational Medicine*, *5*(207), 207ra143 LP-207ra143. https://doi.org/10.1126/scitranslmed.3006605

Ramanan, P., Shabman, R. S., Brown, C. S., Amarasinghe, G. K., Basler, C. F., & Leung, D. W. (2011). Filoviral Immune Evasion Mechanisms. *Viruses* . https://doi.org/10.3390/v3091634

Reed, C., Alves, D. A., Fritz, E. A., Geisbert, J. B., Hensley, L. E., Geisbert, T. W., & Larsen, T. (2011). Pathogenesis of Marburg Hemorrhagic Fever in Cynomolgus Macaques. *The Journal of Infectious Diseases*, *204*(suppl_3), S1021–S1031. https://doi.org/10.1093/infdis/jir339

Riemenschneider, J., Garrison, A., Geisbert, J., Jahrling, P., Hevey, M., Negley, D., … Schmaljohn, C. (2003). Comparison of individual and combination DNA vaccines for B. anthracis, Ebola virus, Marburg virus and Venezuelan equine encephalitis virus. *Vaccine*, *21*(25), 4071–4080. https://doi.org/https://doi.org/10.1016/S0264-410X(03)00362-1

Rollin, P. (2009). Filoviruses: A Compendium of 40 Years of Epidemiological, Clinical, and Laboratory Studies. *Emerging Infectious Diseases*, *15*(12), 2079. https://doi.org/10.3201/eid1512.091044

Ryabchikova, E. I., & Price, B. B. S. (2004). *Ebola and Marburg viruses: a view of infection using electron microscopy.* USA: Battelle Press.

Sanchez, A. (2007). Analysis of Filovirus Entry into Vero E6 Cells, Using Inhibitors of Endocytosis, Endosomal Acidification, Structural Integrity, and Cathepsin (B and L) Activity. *The Journal of Infectious Diseases*, *196*(Supplement_2), S251–S258. https://doi.org/10.1086/520597

Sanchez, A., Kiley, M. P., Holloway, B. P., & Auperin, D. D. (1993). Sequence analysis of the Ebola virus genome: organization, genetic elements, and comparison with the genome of Marburg virus. *Virus Research*, *29*(3), 215–240. https://doi.org/https://doi.org/10.1016/0168-1702(93)90063-S

Schmaljohn, A., Grogan, C., Bosio, C. M., Negley, D., Ruthel, G., Aman, M. J., … Mohamadzadeh, M. (2003). Ebola and Marburg Viruses Replicate in Monocyte-Derived Dendritic Cells without Inducing the Production of Cytokines and Full Maturation. *The Journal of Infectious Diseases*, *188*(11), 1630–1638. https://doi.org/10.1086/379199

Schnittler, H. J., Mahner, F., Drenckhahn, D., Klenk, H. D., & Feldmann, H. (1993). Replication of Marburg virus in human endothelial cells. A possible mechanism for the development of viral hemorrhagic disease. *The Journal of Clinical Investigation*, *91*(4), 1301–1309. https://doi.org/10.1172/JCI116329

Schnittler, H. J., & Feldmann, H. (2003). Viral hemorrhagic fever – a vascular disease? *Thromb Haemost*, *89*(06), 967–972. https://doi.org/10.1055/s-0037-1613397

Schornberg, K., Matsuyama, S., Kabsch, K., Delos, S., Bouton, A., & White, J. (2006). Role of Endosomal Cathepsins in Entry Mediated by the Ebola Virus Glycoprotein. *Journal of Virology*, *80*(8), 4174 LP-4178. https://doi.org/10.1128/JVI.80.8.4174-4178.2006

Seebach, J., Böckeler, M., Afanasieva, T., Schnittler, H.-J., Suttorp, N., Ströher, U., & Feldmann, H. (2007). Breakdown of Paraendothelial Barrier Function during Marburg Virus Infection Is Associated with Early Tyrosine Phosphorylation of Platelet Endothelial Cell Adhesion Molecule—1. *The Journal of Infectious Diseases*, *196*(Supplement_2), S337–S346. https://doi.org/10.1086/520606

Shahhosseini, S., Das, D., Qiu, X., Feldmann, H., Jones, S. M., & Suresh, M. R. (2007). Production and characterization of monoclonal antibodies against different epitopes of Ebola virus antigens. *Journal of Virological Methods*, *143*(1), 29–37. https://doi.org/https://doi.org/10.1016/j.jviromet.2007.02.004

Sinn, P. L., Hickey, M. A., Staber, P. D., Dylla, D. E., Jeffers, S. A., Davidson, B. L., … McCray, P. B. (2003). Lentivirus Vectors Pseudotyped with Filoviral Envelope Glycoproteins Transduce Airway Epithelia from the Apical Surface Independently of Folate Receptor Alpha. *Journal of Virology*, *77*(10), 5902 LP-5910. https://doi.org/10.1128/JVI.77.10.5902-5910.2003

Sissoko, D., Laouenan, C., Folkesson, E., M'Lebing, A.-B., Beavogui, A.-H., Baize, S., … Group, J. S. (2016). Experimental Treatment with Favipiravir for Ebola Virus Disease (the JIKI Trial): A Historically Controlled, Single-Arm Proof-of-Concept Trial in Guinea. *PLOS Medicine*, *13*(3), e1001967. Retrieved from https://doi.org/10.1371/journal.pmed.1001967

Slenczka, W., & Klenk, H. D. (2007). Forty Years of Marburg Virus. *The Journal of Infectious Diseases*, *196*(Supplement_2), S131–S135. https://doi.org/10.1086/520551

Smith, D. H., Isaacson, M., Johnson, K. M., Bagshawe, A., Johnson, B. K., Swanapoel, R., … Koinange Keruga, W. (1982). MARBURG-VIRUS DISEASE IN KENYA. *The Lancet*, *319*(8276), 816–820. https://doi.org/10.1016/S0140-6736(82)91871-2

Soule, G., Tran, K., Tierney, K., Fernando, L., He, S., Wong, G., … de La Vega, M.-A. (2018). Marburg and Ravn Virus Infections Do Not Cause Observable Disease in Ferrets. *The Journal of Infectious Diseases*, *218*(suppl_5), S471–S474. https://doi.org/10.1093/infdis/jiy245

Spiegelberg, L., Wahl-Jensen, V., Kolesnikova, L., Feldmann, H., Becker, S., & Hoenen, T. (2011). Genus-specific recruitment of filovirus ribonucleoprotein complexes into budding particles. *The Journal of General Virology*, *92*(Pt 12), 2900–2905. https://doi.org/10.1099/vir.0.036863-0

Sprecher, A., Shoemaker, T., Polonsky, J. A., Wamala, J. F., de Clerck, H., Porten, K., & Van Herp, M. (2014). Emerging Filoviral Disease in Uganda: Proposed Explanations and Research Directions. *The American Journal of Tropical Medicine and Hygiene*, *90*(5), 790–793. https://doi.org/10.4269/ajtmh.13-0374

Ströher, U., West, E., Bugany, H., Klenk, H.-D., Schnittler, H.-J., & Feldmann, H. (2001). Infection and Activation of Monocytes by Marburg and Ebola Viruses. *Journal of Virology*, *75*(22), 11025 LP-11033. https://doi.org/10.1128/JVI.75.22.11025-11033.2001

Swenson, D. L., Warfield, K. L., Larsen, T., Alves, D. A., Coberley, S. S., & Bavari, S. (2008). Monovalent virus-like particle vaccine protects guinea pigs and nonhuman primates against infection with multiple Marburg viruses. *Expert Review of Vaccines*, *7*(4), 417–429. https://doi.org/10.1586/14760584.7.4.417

Swenson, D. L., Warfield, K. L., Negley, D. L., Schmaljohn, A., Aman, M. J., & Bavari, S. (2005). Virus-like particles exhibit potential as a pan-filovirus vaccine for both Ebola and Marburg viral infections. *Vaccine*, *23*(23), 3033–3042. https://doi.org/https://doi.org/10.1016/j.vaccine.2004.11.070

Takada, A., Feldmann, H., Stroeher, U., Bray, M., Watanabe, S., Ito, H., … Kawaoka, Y. (2003). Identification of Protective Epitopes on Ebola Virus Glycoprotein at the Single Amino Acid Level by Using Recombinant Vesicular Stomatitis Viruses. *Journal of Virology*, *77*(2), 1069 LP-1074. https://doi.org/10.1128/JVI.77.2.1069-1074.2003

Tapparel, C., Maurice, D., & Roux, L. (1998). The Activity of Sendai Virus Genomic and Antigenomic Promoters Requires a Second Element Past the Leader Template Regions: a Motif (GNNNNN)₃ Is Essential for Replication. *Journal of Virology*, *72*(4), 3117 LP-3128. Retrieved from http://jvi.asm.org/content/72/4/3117.abstract

Teams, E. V. S., Teams, E. V. S., Teams, E. V. S., Teams, E. V. S., Teams, E. V. S., Teams, E. V. S., … Breman, J. G. (1999). A Search for Ebola Virus in Animals in the Democratic Republic of the Congo and Cameroon: Ecologic, Virologic, and Serologic Surveys, 1979–1980. *The Journal of Infectious Diseases*, *179*(Supplement_1), S139–S147. https://doi.org/10.1086/514278

Timen, A., Koopmans, M. P. G., Vossen, A. C. T. M., Doornum, G. J. J. van, Günther, S., Berkmortel, F. van den, … Coutinho, R. A. (2009). Response to Imported Case of Marburg Hemorrhagic Fever, the Netherlands. *Emerging Infectious Disease Journal*, *15*(8), 1171. https://doi.org/10.3201/eid1508.090015

Timmins, J., Schoehn, G., Kohlhaas, C., Klenk, H.-D., Ruigrok, R. W. H., & Weissenhorn, W. (2003). Oligomerization and polymerization of the filovirus matrix protein VP40. *Virology*, *312*(2), 359–368. https://doi.org/https://doi.org/10.1016/S0042-6822(03)00260-5

Towner, J. S., Amman, B. R., Sealy, T. K., Carroll, S. A. R., Comer, J. A., Kemp, A., … Rollin, P. E. (2009). Isolation of Genetically Diverse Marburg Viruses from Egyptian Fruit Bats. *PLOS Pathogens*, *5*(7), e1000536. Retrieved from https://doi.org/10.1371/journal.ppat.1000536

Valmas, C., & Basler, C. F. (2011). Marburg Virus VP40 Antagonizes Interferon Signaling in a Species-Specific Manner. *Journal of Virology*, *85*(9), 4309 LP-4317. https://doi.org/10.1128/JVI.02575-10

Valmas, C., Grosch, M. N., Schümann, M., Olejnik, J., Martinez, O., Best, S. M., … Mühlberger, E. (2010). Marburg Virus Evades Interferon Responses by a Mechanism Distinct from Ebola Virus. *PLOS Pathogens*, *6*(1), e1000721. Retrieved from https://doi.org/10.1371/journal.ppat.1000721

van Griensven, J., Edwards, T., de Lamballerie, X., Semple, M. G., Gallian, P., Baize, S., … Haba, N. (2016). Evaluation of Convalescent Plasma for Ebola Virus Disease in Guinea. *New England Journal of Medicine*, *374*(1), 33–42. https://doi.org/10.1056/NEJMoa1511812

Volchkov, V. E., Volchkova, V. A., Ströher, U., Becker, S., Dolnik, O., Cieplik, M., … Feldmann, H. (2000). Proteolytic Processing of Marburg Virus Glycoprotein. *Virology*, *268*(1), 1–6. https://doi.org/https://doi.org/10.1006/viro.1999.0110

Wang, D., Schmaljohn, A. L., Raja, N. U., Trubey, C. M., Juompan, L. Y., Luo, M., … Dong, J. Y. (2006). De novo syntheses of Marburg virus antigens from adenovirus vectors induce potent humoral and cellular immune responses. *Vaccine*, *24*(15), 2975–2986. https://doi.org/https://doi.org/10.1016/j.vaccine.2005.11.046

Wang, J., Manicassamy, B., Caffrey, M., & Rong, L. (2011). Characterization of the receptor-binding domain of Ebola glycoprotein in viral entry. *Virologica Sinica*, *26*(3), 156. https://doi.org/10.1007/s12250-011-3194-9

Wang, Q., Yang, H., Liu, X., Dai, L., Ma, T., Qi, J., … Gao, G. F. (2016). Molecular determinants of human neutralizing antibodies isolated from a patient infected with Zika virus. *Science Translational Medicine*, *8*(369), 369ra179 LP-369ra179. https://doi.org/10.1126/scitranslmed.aai8336

Warfield, K. L., Alves, D. A., Bradfute, S. B., Reed, D. K., VanTongeren, S., Kalina, W. V, … Bavari, S. (2007). Development of a model for marburgvirus based on severe-combined immunodeficiency mice. *Virology Journal*, *4*(1), 108. https://doi.org/10.1186/1743-422X-4-108

Warfield, K. L., & Aman, M. J. (2011). Advances in Virus-Like Particle Vaccines for Filoviruses. *The Journal of Infectious Diseases*, *204*(suppl_3), S1053–S1059. https://doi.org/10.1093/infdis/jir346

Warfield, K. L., Bradfute, S. B., Wells, J., Lofts, L., Cooper, M. T., Alves, D. A., … Bavari, S. (2009). Development and Characterization of a Mouse Model for Marburg Hemorrhagic Fever. *Journal of Virology*, *83*(13), 6404 LP-6415. https://doi.org/10.1128/JVI.00126-09

Warfield, K. L., Swenson, D. L., Negley, D. L., Schmaljohn, A. L., Aman, M. J., & Bavari, S. (2004). Marburg virus-like particles protect guinea pigs from lethal Marburg virus infection. *Vaccine*, *22*(25), 3495–3502. https://doi.org/https://doi.org/10.1016/j.vaccine.2004.01.063

Wec, A. Z., Bornholdt, Z. A., He, S., Herbert, A. S., Goodwin, E., Wirchnianski, A. S., … Chandran, K. (2019). Development of a Human Antibody Cocktail that Deploys Multiple Functions to Confer Pan-Ebolavirus Protection. *Cell Host & Microbe*, *25*(1), 39–48.e5. https://doi.org/https://doi.org/10.1016/j.chom.2018.12.004

Weik, M., Enterlein, S., Schlenz, K., & Mühlberger, E. (2005). The Ebola Virus Genomic Replication Promoter Is Bipartite and Follows the Rule of Six. *Journal of Virology*, *79*(16), 10660 LP-10671. https://doi.org/10.1128/JVI.79.16.10660-10671.2005

Weissenhorn W., Dessen A., Calder L. J., Harrison S. C., Skehel J. J., & Wiley, D. C. (1999). Structural basis for membrane fusion by enveloped viruses. *Molecular Membrane Biology*, *16*(1), 3–9. https://doi.org/10.1080/096876899294706

Weissenhorn, W., Carfí, A., Lee, K.-H., Skehel, J. J., & Wiley, D. C. (1998). Crystal Structure of the Ebola Virus Membrane Fusion Subunit, GP2, from the Envelope Glycoprotein Ectodomain. *Molecular Cell*, *2*(5), 605–616. https://doi.org/https://doi.org/10.1016/S1097-2765(00)80159-8

Welsch, S., Kolesnikova, L., Krähling, V., Riches, J. D., Becker, S., & Briggs, J. A. G. (2010). Electron Tomography Reveals the Steps in Filovirus Budding. *PLOS Pathogens*, *6*(4), e1000875. Retrieved from https://doi.org/10.1371/journal.ppat.1000875

Wenigenrath, J., Kolesnikova, L., Hoenen, T., Mittler, E., & Becker, S. (2010). Establishment and application of an infectious virus-like particle system for Marburg virus. *Journal of General Virology*, *91*(5), 1325–1334. Retrieved from https://jgv.microbiologyresearch.org/content/journal/jgv/10.1099/vir.0.018226-0

Whelan, S. P. J., Barr, J. N., & Wertz, G. W. (2004). Transcription and Replication of Nonsegmented Negative-Strand RNA Viruses BT - Biology of Negative Strand RNA Viruses: The Power of Reverse Genetics. In Y. Kawaoka (Ed.) (pp. 61–119). Berlin, Heidelberg: Springer Berlin Heidelberg. https://doi.org/10.1007/978-3-662-06099-5_3

Will, C., Mühlberger, E., Linder, D., Slenczka, W., Klenk, H. D., & Feldmann, H. (1993). Marburg virus gene 4 encodes the virion membrane protein, a type I transmembrane glycoprotein. *Journal of Virology*, *67*(3), 1203 LP-1210. Retrieved from http://jvi.asm.org/content/67/3/1203.abstract

Wilson, J. A., Hevey, M., Bakken, R., Guest, S., Bray, M., Schmaljohn, A. L., & Hart, M. K. (2000). Epitopes Involved in Antibody-Mediated Protection from Ebola Virus. *Science*, *287*(5458), 1664 LP-1666. https://doi.org/10.1126/science.287.5458.1664

Wong, G., Richardson, J. S., Pillet, S., Patel, A., Qiu, X., Alimonti, J., … Kobinger, G. P. (2012). Immune Parameters Correlate with Protection Against Ebola Virus Infection in Rodents and Nonhuman Primates. *Science Translational Medicine*, *4*(158), 158ra146 LP-158ra146. https://doi.org/10.1126/scitranslmed.3004582

World Health Organisation. (2010). WHO | Ebola Reston in pigs and humans in the Philippines. *WHO*. Retrieved from https://www.who.int/csr/don/2009_02_03/en/

World Health Organization. (2017). WHO | Marburg virus disease. Retrieved March 11, 2019, from https://www.who.int/csr/disease/marburg/en/

World Health Organization. (2018). WHO | Ebola outbreak 2014-2015. Retrieved March 11, 2019, from https://www.who.int/csr/disease/ebola/en/

World Health Organization. (2008). WHO | End of Ebola outbreak in Uganda. Retrieved March 11, 2019, from https://www.who.int/csr/don/2007_02_20b/en/

Yaddanapudi, K., Palacios, G., Towner, J. S., Chen, I., Sariol, C. A., Nichol, S. T., & Lipkin, W. I. (2006). Implication of a retrovirus-like glycoprotein peptide in the immunopathogenesis of Ebola and Marburg viruses. *The FASEB Journal*, *20*(14), 2519–2530. https://doi.org/10.1096/fj.06-6151com

Yamayoshi, S., Noda, T., Ebihara, H., Goto, H., Morikawa, Y., Lukashevich, I. S., … Kawaoka, Y. (2008). Ebola Virus Matrix Protein VP40 Uses the COPII Transport System for Its Intracellular Transport. *Cell Host & Microbe*, *3*(3), 168–177. https://doi.org/https://doi.org/10.1016/j.chom.2008.02.001

Yang, X.-L., Tan, C. W., Anderson, D. E., Jiang, R.-D., Li, B., Zhang, W., … Shi, Z.-L. (2019). Characterization of a filovirus (Měnglà virus) from Rousettus bats in China. *Nature Microbiology*, *4*(3), 390–395. https://doi.org/10.1038/s41564-018-0328-y

Zhao, D., Wang, W., Zong, W., Xiong, S., Zhang, Q., Ji, F., & Xu, X. (2017). Synthesis of Bi2S3/BiVO4 Heterojunction with a One-Step Hydrothermal Method Based on pH Control and the Evaluation of Visible-Light Photocatalytic Performance. *Materials* . https://doi.org/10.3390/ma10080891

Zhu, W., Zhang, Z., He, S., Wong, G., Banadyga, L., & Qiu, X. (2018). Successful treatment of Marburg virus with orally administrated T-705 (Favipiravir) in a mouse model. *Antiviral Research*, *151*, 39–49. https://doi.org/https://doi.org/10.1016/j.antiviral.2018.01.011